# HARDWARE DESIGN OF PORTABLE POTENTIOSTAT FOR ON-SITE COVID-19 DETECTION

BY

MUHAMMAD AFIQ BIN ABDUL GHANI

INTERNATIONAL ISLAMIC UNIVERSITY MALAYSIA

2024

# HARDWARE DESIGN OF PORTABLE POTENTIOSTAT FOR ON-SITE COVID-19 DETECTION

BY

MUHAMMAD AFIQ BIN ABDUL GHANI

A dissertation submitted in fulfillment of the requirement for the degree of Master of Science in Engineering

Kulliyyah Of Engineering
International Islamic University Malaysia

MARCH 2024

# ABSTRACT

Global pandemic COVID-19 was a massive issue in the early part of the decade and made worse with the emergence of various mutations. There are various testing methods to detect the COVID-19. Antigen test kits have low sensitivity in detecting asymptomatic patients. Although PCR test kits are very accurate, it needs to be performed in the laboratory by trained laboratory workers. Alternative detection techniques are electrochemical detection which have high accuracy comparable to PCR. Portable potentiostat was proposed as a point-of-care device for on-site screening of COVID-19, which would improve accessibility, accuracy, and reduce the overall cost of virus detection. The developed portable potentiostat, NACOTS, had been designed with cyclic voltammetry, differential pulse voltammetry, and electrochemical impedance spectroscopy capabilities. NACOTS had been benchmarked against commercialized potentiostat. The on-site diagnosis of COVID-19 had been done using the designed NACOTS hardware. NACOTS printed circuit board development from early Alpha development until the final revision had been shown. Comparison of NACOTS Beta revision was done against PGSTAT302N Autolab and μStat-i 400 DropSens to evaluate the reliability and stability. The result showed similar results across three potentiostats. The final version of NACOTS was benchmarked against Sensit and Pico Development Kit and showed similar results across all potentiostats. On-site testing has been conducted on two occasions. The first on-site test managed to differentiate between the positive and negative samples. The UITM team has performed clinical testing on 148 COVID-19 samples on RT-PCR and NACOTS. Developed potentiostats with COVID-19 detection capabilities have been benchmarked against NACOTS. NACOTS have the edge in terms of having an incubation chamber for the LAMP process, fast detection time, which is less than a minute, as well as the number of samples that were being tested through the clinical test. NACOTS have been tested on 148 samples, when compared to the benchmarked papers which were tested on less than 14 samples.

# ملخص البحث

مثل الوباء العالمي فيروس كورونا مشكلة كبيرة في أوائل هذا العقد، وتفاقمت هذه المشكلة مع ظهور طفرات مختلفة من الفيروس، وقد تم اكتشاف طرق اختبار مختلفة للكشف عن الشخص المصاب بالفيروس. تتسم مجموعة اختبار المستضد بحساسية منخفضة في الكشف عن مرضى فيروس كورونا الذين لا تظهر عليهم الأعراض، أمّا مجموعة اختبار (PCR)، فبالرغم من دقتها العالية، إلا إنّ إجراءها يحتاج إلى مختبر حيث يتم تنفيذها من قبل عمال مختبر مدربين. وقد ظهرت تقنيات جديدة كهروكيميائية، حيث تصل دقتها إلى 100% مقارنة باختبار (PCR). وفي هذه الدراسة، تم تطوير جهاز قياس الجهد المحمول للتشخيص والفحص الموقعي، الأمر الذي من شأنه أيضاً أن يزيد من إمكانية الوصول إلى الاختبار، إضافة إلى خفض تكلفته. وقد تم تصميم جهاز قياس الجهد المحمول (NACOTS) بحيث يمكنه قياس الجهد الدوري، وقياس جهد النبض التفاضلي، والقيام بالتحليل الطيفي للمقاومة الكهروكيميائية. وقد تم مقارنة جهاز (NACOTS) مع البدائل التجارية المتوفرة. كما تم إجراء التشخيص الموقعي لفيروس كورونا باستخدام جهاز (NACOTS) الذي تم تطويره. تم عرض تطوير لوحة الدوائر المطبوعة لجهاز (NACOTS) من النموذج البدائي (Alpha) حتى النموذج النهائي. وقد تمت مقارنة نموذج (NACOTS Beta) مع (PGSTAT302N Autolab) و (µStat-i 400 DropSens) من أجل تقييم الموثوقية والاستقرار، فكانت النتائج متماثلة في أجهزة قياس الجهد الثلاثة. كما تمت مقارنة النموذج النهائي لـ (NACOTS) مع كل من (Sensit) و (Pico Development Kit)، حيث أظهرت المقارنة نتائج متماثلة في جميع الأجهزة. وقد أجري الاختبار

الموقعي في حالتين، حيث تمكن الاختبار الموقعي الأول من التمييز بين العينات الإيجابية والسلبية. كما أجرى فريق (UITM) اختبارات سريرية على 148 عينة من فيروس كورونا باستخدام كل من (RT-PCR) و (NACOTS)، وتمت مقارنة جهاز (NACOTS) الذي تم تطويره مع أجهزة قياس الجهد بقدرات الكشف عن فيروس كورونا، حيث أظهرت النتائج تميّز (NACOTS) من حيث وجود غرفة حضانة لعملية (LAMP)، ووقت الكشف السريع الذي يقل عن دقيقة، بالإضافة إلى عدد العينات التي يتم اختبارها من خلال الاختبار السريري. وقد تم اختبار (NACOTS) على 148 عينة مقارنة بالأبحاث المرجعية التي اقتصر فيها الاختبار 14 عينة فقط.

# APPROVAL PAGE

I certify that I have supervised and read this study and that, in my opinion, it conforms to acceptable standards of scholarly presentation and is fully adequate, in scope and quality, as a dissertation for the degree of Master of Science in Engineering.

Anis Nurashikin Nordin
Supervisor

Rosminazuin Bt. Ab. Rahim
Co-Supervisor

……..
Teddy Surya Gunawan
Co-Supervisor

……..
Zainiharyati Mohd Zain
Co-Supervisor

I certify that I have read this study and that, in my opinion it conforms to acceptable standards of scholarly presentation and is fully adequate, in scope and quality, as a dissertation for the degree of Master of Science in Engineering.

……..
Aliza Aini Md Ralib @ Md Raghib
Examiner

……..
Muhammad Ibn Ibrahimy
Examiner

This dissertation was submitted to the Department of Electrical and Computer Engineering and is accepted as a fulfilment of the requirement for the degree of Master of Science in Engineering.

……..
Othman Omran Khalifa
Head, Department of Electrical and Computer Engineering

This dissertation was submitted to the Kulliyyah of Engineering and is accepted as a fulfillment of the requirement for the degree of Master of Science in Engineering.

……..
Khairul Azami Sidek
Covering Dean, Kulliyyah of Engineering

# DECLARATION

I hereby declare that this dissertation is the result of my own investigations, except where otherwise stated. I also declare that it has not been previously or concurrently submitted as a whole for any other degrees at IIUM or other institutions.

Muhammad Afiq bin Abdul Ghani

Signature…… Date…7th March 2024…

**INTERNATIONAL ISLAMIC UNIVERSITY MALAYSIA**

**DECLARATION OF COPYRIGHT AND AFFIRMATION OF FAIR USE OF UNPUBLISHED RESEARCH**

**HARDWARE DESIGN OF PORTABLE POTENTIOSTAT FOR ON-SITE DIAGNOSIS AND SCREENING FOR COVID-19**

I declare that the copyright holder of this thesis/dissertation is jointly owned by the student International Islamic University Malaysia.





By signing this form, I acknowledged that I have read and understand the IIUM Intellectual Property Right and Commercialization policy.

Affirmed by Muhammad Afiq bin Abdul Ghani

…… 7th March 2024

Signature Date

*This thesis is dedicated to my parents for patiently watching me grow and supporting me while I was at my lowest.*

*Dedicated to my beloved brother, Anis. You are always in my heart.*

# ACKNOWLEDGEMENT

All glory is due to Allah, the Almighty, whose Grace and Mercies have been with me throughout my program. Although it has been tasking, His Mercies and Blessings on me ease the herculean task of completing this dissertation.

I am most indebted to my supervisor, Prof. Dr. Anis Nurashikin, kindness, thoroughness, and patience has facilitated the successful completion of my work. Despite her commitments, she took time to guide and give feedback on this research. I am also grateful to my co-supervisor, Dr. Rosminazuin, and Prof Teddy Surya Gunawan, whose support and cooperation contributed to the outcome of this work.

Not forgetting, the whole NACOTS teams from both IIUM and UITM, who cooperate and collaborate well during the whole project.

Lastly, my gratitude goes to my whole family especially my parents for understanding and supporting my journey.

Once again, we glorify Allah for His endless mercy on us one of which is enabling us to successfully round off the efforts of writing this thesis. Alhamdulillah

# TABLE OF CONTENTS

# LIST OF TABLES

# LIST OF FIGURES

# LIST OF ABBREVIATIONS

| | |
|---|---|
| CV | Cyclic Voltammetry |
| DNA | Deoxyribonucleic Acid |
| DPV | Differential Pulse Voltammetry |
| EIS | Electrochemical Impedance Spectroscopy |
| PCB | Printed Circuit Board |
| PCR | Polymerase Chain Reaction |
| RNA | Ribonucleic Acid |

# CHAPTER 1

# INTRODUCTION

## 1.1 Background

In early 2020, the world was hit by the global pandemic from the virus known as COVID-19. COVID-19 comes from a group of related RNA viruses known as coronaviruses that cause diseases in mammals and birds (Platto, Xue, & Carafoli, 2020). COVID-19 cases are still increasing with several mutations of different variants (Roy, Dhillon, Habib, & Pugazhandhi, 2021). Therefore, COVID-19 cases need to be identified quickly and accurately.

Currently, there are multiple methods approved by the FDA that can be used to identify or detect COVID-19 viruses, which are molecular, antigen, and serology tests (Chau, Strope, & Figg, 2020 ). Molecular test results turnaround time can take from one day to a week, antigen test results are rapid where results are ready within 15 minutes. Serology tests can take from the same day or up to three days. Antigen tests are the most widely used, but compared to PCR tests, the antigen test is accurate when tested on a symptomatic patient (Pilarowski et al., 2021) and became less accurate when the individual is asymptomatic (Smith et al., 2021). In the early stage, the PCR test is the most accurate since most asymptomatic cases were tested to be negative through antigen and serology tests (Miller et al., 2020).

Current widely used methods of COVID-19 tests are PCR, antigen, and serology tests. Antigen test is a cheap testing method widely used worldwide due to its fast turnaround time, around 10-15 minutes. However, with the emerging variants, such as Omicron, the test could not detect the variant for several days due to the nature of the variant being infectious. The median time of positive PCR to the first antigen test to be positive was three days, unlike other variants (Adamson, Sikka, Wyllie, & Premsrirut, 2022). The test also have low sensitivity when tested on asymptomatic patients which is at 58.7% for Veritor and 59.4% for Biosensor brand (Schuit et al., 2021). It is vital for a test method to have a fast turnaround time, but pairing with accuracy is also essential, especially with the emergence of new variants.

Another method, the PCR testing method, has been the golden standard of COVID-19 detection. However, the price range of the kits are more expensive, and the cost to setup testing facilities which can be up to $15000 (Ramdas, Darzi, & Jain, 2020), limits the accessibility of comprehensive test in poorer regions. The laboratory equipment for PCR test analysis is not portable and requires specific technical expertise. If done on-site, turnaround test time for PCR can take around 4-6 hours and can increase to at least 3-7 days due to logistics (Ramdas et al., 2020). Therefore, comprehensive tests need to have a short turnaround time as well as high portability of detection.

The serology test, or ELISA, is ineffective in capturing early-stage infection due to the nature of the test in which the detection of IgM, IgA, or IgG. These antibody productions only increase after a few days of infection, which is only at 45% clinical sensitivity after seven days (Miller et al., 2020).

Other than a current molecular test, which depends on quantitative reverse transcription PCR (qRT-PCR), which consumes time and needs expensive instrumentation, another alternative method is electrochemical detection of the virus. The method was tested by Chaibun et al., 2021. They used voltammetry and managed to detect viral genes as low as 1 copy/μL in less than 2 hours. (Mahari, Roberts, Shahdeo, & Gandhi, 2020) also have developed an electrochemical device for rapid detection of COVID-19 antigen, which can provide fast, precise, and ultra-sensitive results within 10s-30s. The technique shows great potential for electrochemical detection as one of the main COVID-19 testing methods.

## 1.2 Problem Statements and Its Significance

COVID-19 was a huge global issue, especially with the emergence of variances and mutations every few months. Therefore, there is a need for testing methods that are accessible, accurate, and efficient.

Current COVID test-kit especially antigen test kits, have low sensitivity when tested on asymptomatic patients and might not be able to detect new variant of viruses. Another type of detection method is PCR which is the golden standard but needs to be performed in the processing lab by trained laboratory workers thus making it expensive and costly.

A new alternative method of COVID-19 testing is electrochemical detection. Previous research has shown that the method is highly sensitive and comparable to the PCR test. The test comes with a faster processing time compared to PCR which is only around 10 to 30 seconds per sample. Electrochemical detections need to be performed using a device called potentiostat.

Lab grade potentiostats are very accurate, however, the large size makes it lack portability. The cost of lab grade potentiostats are very high. Due to these limitations, lab grade potentiostats are not portable to bring into the remote areas, thus limiting access to the device. An alternative to these potentiostats are portable potentiostats. However, portable potentiostats came with a stigma that it is not as accurate.

With portable potentiostat, the device can be developed into a point of care device for virus detection. For the device to qualify as a point-of-care testing device, it must be portable, small, lightweight, easy to use, and accessible. In this research, the potentiostat needs to be able to perform electrochemical technique called differential pulse voltammetry (DPV) to detect COVID-19 viruses. The research aims to design point of care devices that can be used on-site to screen COVID-19 cases.

## 1.3 Research Objectives

1. To design and develop portable potentiostat with differential pulse voltammetry capabilities.
2. To benchmark and compare the performance of the designed potentiostat with existing devices (research-based and commercial)
3. To perform on-site diagnosis of COVID-19 using the designed hardware.

## 1.4 Research Scope

The study focuses on the hardware design of portable potentiostat, which will only cover cyclic voltammetry measurement and impedance spectroscopy. The research scope will not cover software design, graphical user interface (GUI), package design, and electrode optimization.

## 1.5 Research Methodology

Figure 1.1 shows the research methodology which involves the portable potentiostat design and fabrication flow. First, literature review needs to be done before proceeding with prototyping and research on potentiostat. Then, user specification needs to be determined. Important user specifications are portability, connectivity, and electrochemical testing. These specifications will be done using the portable potentiostat. After selecting the specifications, prototyping and research on the potentiostat was done. This phase includes experimenting on various potentiostats and determining the model of the potentiostat chip that will be used. The next phase was determining components to make sure the components were available before designing or fabricating the printed circuit board, PCB. After assembling the PCB, the benchmarking test was done to see if the device worked as intended. Troubleshoot and failure analysis would be done if the benchmarking test failed. Then the whole process of determining which components are available will start again. After benchmarking passed, the board was sent to the user for testing. If there is any new feedback on improvement from the users, then user specifications need to be determined again. The

design and fabrication flow are completed after the benchmarking and user tests are passed.

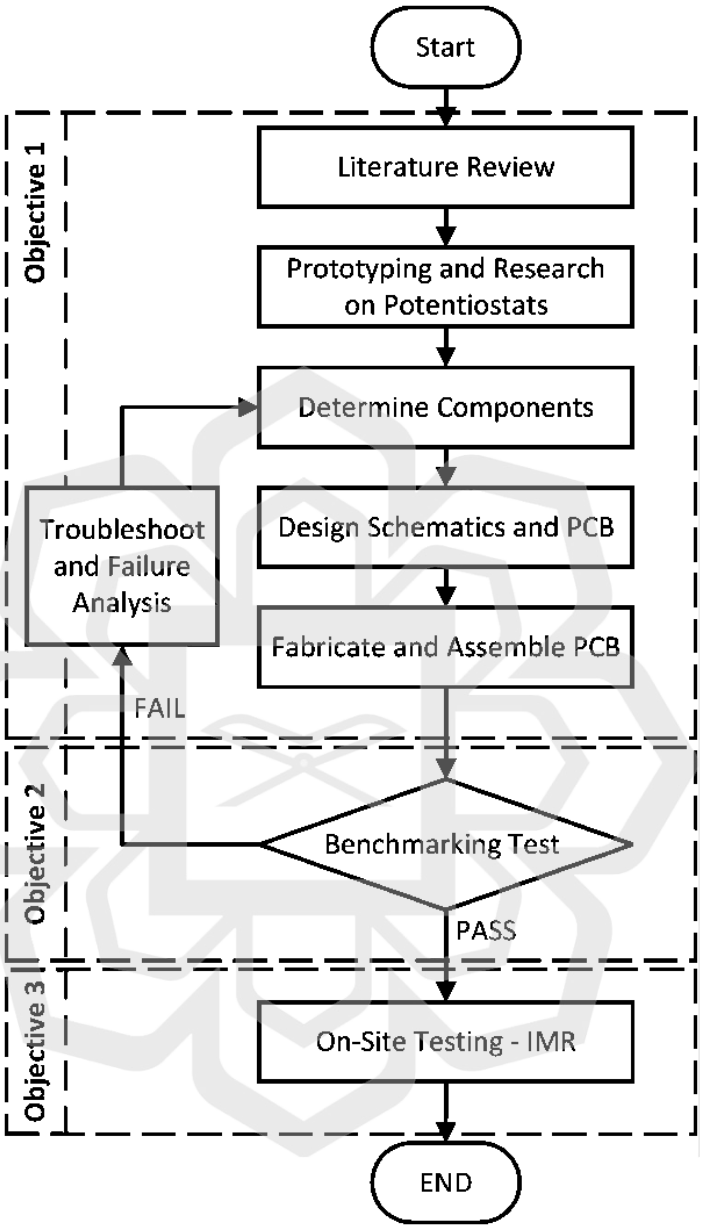


Figure 1.1 Overall research methodology flowchart.

## 1.6 Organization of Dissertation

The following are the organization of this dissertation. Chapter 2 focuses on the literature review of COVID-19 testing methods, electrochemical techniques, as well as comparison of portable potentiostats. In Chapter 3, the design and development of NACOTS potentiostat are shown, with how the potentiostat is developed from alpha to final revision, and the tests methodologies that will be conducted in Chapter 4. Chapter 4 will cover the results and discussions of the research. Chapter 5 covers the conclusion of the dissertation, significance to the field, as well as limitations and future work.

# CHAPTER 2

# LITERATURE REVIEW

## 2.1 Overview

In this chapter, the literature review covers the common COVID-19 testing methods. Then, electrochemical techniques are highlighted as one of the new methods to detect COVID-19. Electrochemical techniques are discussed in detail since the technique will be used and implemented on the potentiostat for COVID-19 detection. Related works from researchers have been evaluated to find advantages and disadvantages of the potentiostats to leverage the knowledge to design a better potentiostat that will fit the current usage.

## 2.2 COVID-19 Testing Methods

There are various testing methods for COVID-19 such as Antigen test (Albert et al., 2021), PCR test (Brandal et al., 2021) and serology test (Miller et al., 2020). Various testing methods came in with different methods of testing accuracies. Clinical sensitivity is being used to evaluate the accuracy for the test below. According to Lalkhen & McCluskey, 2008 clinical sensitivity is the ability for the test to correctly identify patients that are infected. For example, a test that has sensitivity of 70% means, the test can detect patients that are infected (true positives) but 30% other infected patients are not detected (false negatives).

New emerging variants and mutation of COVID-19 also provide more challenges in terms of detections. Virus mutations can impair the ability of the oligonucleotides to stick to the virus's genetic material properly. As a result, the PCR test may become less sensitive and may not detect the mutated virus as effectively (Lippi, Simundic, & Plebani, 2020). In the latest COVID-19 variant, Omicron, the antigen test pose may not be fit to detect the variant (Adamson et al., 2022).

### 2.2.1 Rapid Antigen Test

Rapid antigen test is one of the common tests in detecting COVID-19, and it is very fast and portable with fast turnaround test time (Albert et al., 2021). It only needs around 15-30 minutes to obtain the result. As of the time of this proposal being written, from 30 person across US that were infected with omicron variants had been tested with positive PCR, but two rapid antigen tests for the same individual are reported to be negative (Lanese, 2022), in which raises questions on reliability of antigen test to detect newer variant of COVID-19 (Ramdas, Darzi, & Jain, 2020. The cheap cost of the test makes it widely used everywhere in the world. Figure 2.1 shows how the basic antigen testing works. The saliva samples are dropped on the sample pad and will flow laterally on the membrane. The sample will pass through two lines, which are the test line which will turn into different color if positive and the control line which determines the validity of the result.

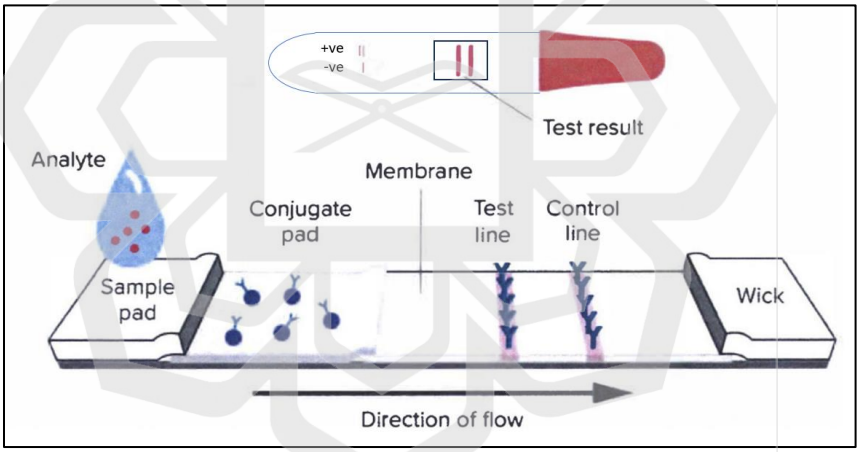


Figure 2.1 Antigen testing principles and how a result is determined through detection of target antigen. (Pavia & Plummer, 2021)

Study conducted by Adamson et al., 2022 showed that patients tested positive with PCR test but still showed negative on antigen test two times. Due to ever-changing mutations or variants, the antigen test is not as reliable unless a new antigen test kit is produced specific to the current variants.

According to Pilarowski et al., 2021, the test depends highly on whether the infected patients are symptomatic or asymptomatic. The test needs to be more accurate

on asymptomatic patients in which the sensitivity is only at 58.7% (Schuit et al., 2021). According to the other test that being done by Albert et al., 2021, antigen tests show 79.6% positive by using RT-PCR positive test as reference.

### 2.2.2 PCR Test

PCR or polymerase chain reaction test is one of the gold standards that are currently used all around. PCR is a diagnostic technique used to detect and identify genetic material, such as DNA or RNA, in a biological sample.

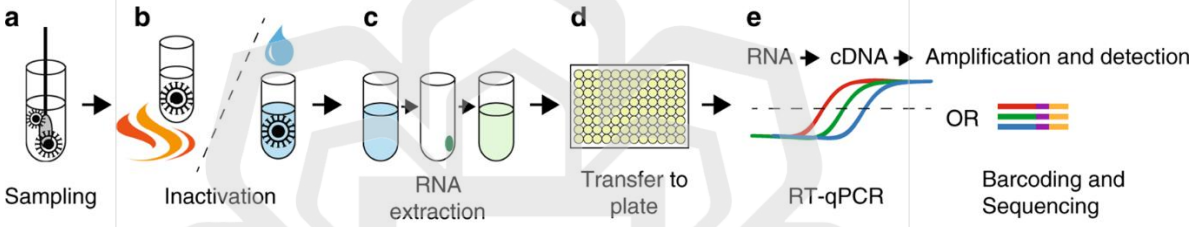


Figure 2.2 Overview of COVID-19 RT-PCR Test procedure. (a) Sample collection from patient (b) Inactivation of virus by heating or reagents (c) RNA extraction (d) Transfer to PCR plate before performing RT-PCR reading(Smyrlaki et al., n.d.)

According to Miller et al., 2020, the PCR test for COVID-19 is being done to detect virus-specific nucleic acid which is normally found inside infected patients' nasal cavity. The turnaround time for a PCR test can range from 4-6 hours to up to 2.4 days to process the samples (Ramdas, Darzi, & Jain, 2020). PCR tests however are highly sensitive and can even detect the latest Omicron variants (Brandal et al., 2021). Figure 2.2 shows an overview of RT-PCR test procedure.

The high sensitivities of the PCR kit come with high infrastructure and consumable costs Ramdas et al., 2020. The price of a single PCR kit is more expensive than rapid antigen test and need to be ran in a certified processing lab. This makes it unsuitable for mass deployment in developing countries.

This test has the highest clinical sensitivity accuracy and detection for first few days of infection with accuracy of >90% positive on the first 5 days. However, the test

requires equipment in the lab which is lack portability causing the test turnaround time to be increased.

### 2.2.3 Serology Test

Serology is a test that measuring IgA, IgG, and IgM antibodies in the blood (Miller et al., 2020). This method is normally used to detect whether an individual have been infected in the past. The weakness of the test is that it is hard to test patient that are infected before 7$^{th}$ day of infection The clinical sensitivity accuracy of serology test that been done by Miller et al., 2020 shown that the tests are >50% seropositive after 7$^{th}$ day, >80% after 12$^{th}$ day and 100% by 21$^{st}$ day of infection. Figure 2.3 shows the serology test flow by using the serology kit.


Figure 2.3 Serology Test Kit flow (1) Blood sample is collected (2) Sample is dropped on the sensor (3) Buffer dropped on the sensor (4) Result can be seen after 10 minutes (BioMedomics Inc., 2023)

Table 2-1 Comparison on current COVID-19 detection test

| **Testing Method** | **Strength** | **Working Principles** | **Limitation** | **Clinical Sensitivity** |
|---|---|---|---|---|
| Rapid Antigen Detection | Faster test time. Only need around 15-30 minutes | Saliva sample dropped on the test kit, the color will change when antigen bind with the marker, showing positive. | less accurate based on whether the individual is symptomatic | 79.6% positive by using RT-PCR positive test as reference (Albert et al., 2021) |
| PCR | Highest accuracy and detection for first few days of infection | RNA from virus is extracted, then amplified. Detection happens after amplification | Longer turnaround time due to equipment needed | >90% positive on the first 5 days (Ramdas et al., 2020) |
| Serology | Able to detect the individual have been infected in the past | Detecting antibody from blood samples | Hard to detect infected individual before seventh day of the infection | >50% seropositive after $7^{th}$ day, >80% after $12^{th}$ day and 100% by $21^{st}$ day of infection |

These tests have strength and limitations. To bridge the gap of portability, as well as test time, electrochemical methods will be used. Electrochemical method is a new method which is still under research. It is more portable than PCR method, but it tested more than the antigen test. The test that will be conducted involved the breaking of DNA or antibodies, before being tested through electrochemical test by using voltammetry and impedance spectroscopy.

## 2.3 Electrochemical Techniques

Electrochemistry is very useful method to view reactions that involve electron transfers (Elgrishi et al., 2018). It relates to the electron flow when there are chemical changes happening between substances during chemical reactions. It also explores the fundamental principles and processes behind redox reaction. A basic electrochemical cell is shown in Figure 2.4. The electrochemical cell consists of three electrodes: working, counter and reference. Working electrodes, is where most of the electrochemical reaction would happen. Reference electrode (RE) which will be the reference points when being compared to the other electrodes potentials. Counter

electrode (CE) is used to complete the electrical circuit (Elgrishi et al., 2018). The current flow in a three-electrode electrochemical cell is initiated by applying an external potential or voltage between the working electrode and the reference electrode. This potential difference drives the electrochemical reaction at the working electrode. The resulting current flows from the working electrode to the counter electrode through the external circuit, completing the electrical circuit(Chaudhary & Khanuja, 2022).

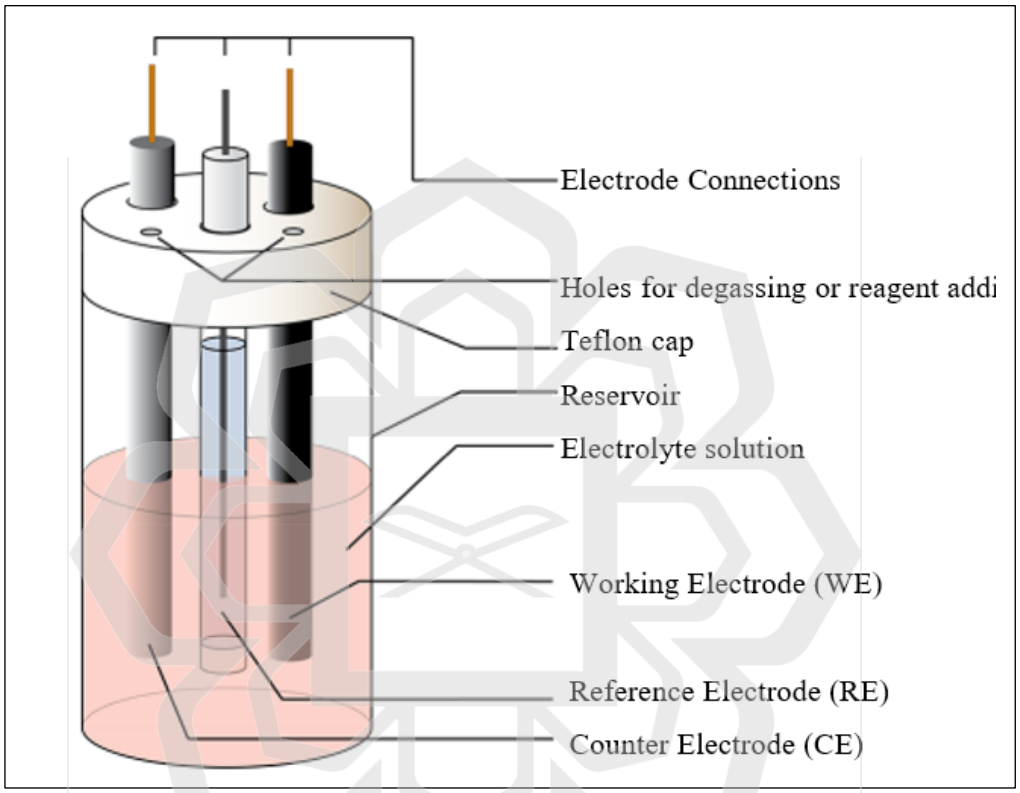


Figure 2.4 Example of representation of an electrochemical cell (Elgrishi et al., 2018)

There are various electrochemical techniques, such as voltammetry, impedance spectroscopy, amperometry, chronopotentiometry, etc. The details of three methods are cyclic voltammetry (CV), differential pulse voltammetry (DPV) and electrochemical impedance spectroscopy (EIS) are elaborated in the next sections.

### 2.3.1 Cyclic Voltammetry

Cyclic voltammetry (CV) is one of the techniques of voltammetry. Voltammetry technique is performed when different potentials are applied to the electrochemical cell and the current response was recorded to study the redox reaction. By performing voltammetry, voltage and current characteristics of medium can be known as well as mechanistic and kinetic details of electron transfer (Batchelor-Mcauley et al., 2015). CV are usually used to investigate molecular species' reduction and oxidation processes, thus making CV important to study the chemical reactions that involve electron transfer (Elgrishi et al., 2018).

Figure 2.5 (a) shows the input of cyclic voltammetry through the working electrode of electrochemical cell. The potential is applied as a triangular waveform, and is increased linearly versus time until it reaches the desired peak potential. In the second sweep, the voltage is reduced linearly versus time, till the baseline (Venton & DiScenza, 2020). This process is repeated based on the number of cycles specified by the user. Figure 2.5 (b) shown the voltammogram (current against potential). The first peak is the cathodic peak, and the second is anodic peak. Ideally separation peak in between anodic and cathodic peak (ΔEp), is 57 mV at 25 °C (2.22 RT/F) (Elgrishi et al., 2018).

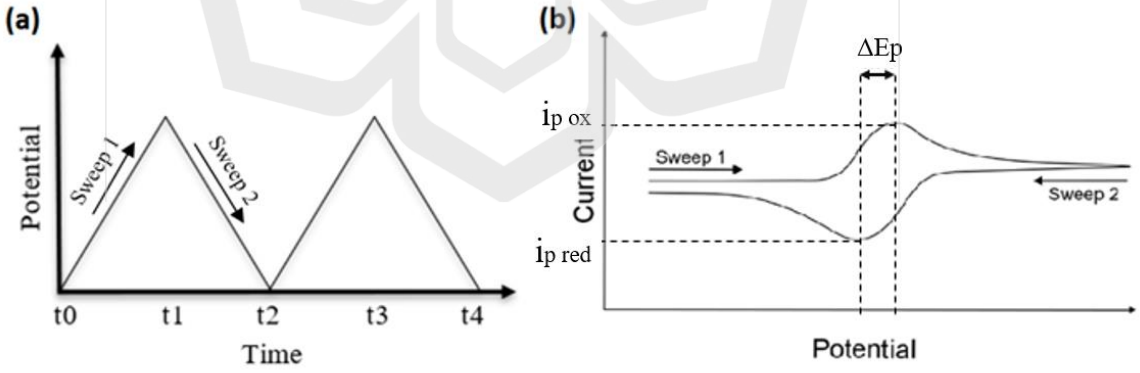


Figure 2.5 (a) Cyclic voltammetry input waveform (Elgrishi et al., 2018) (b) Cyclic voltammetry output waveform (Batchelor-Mcauley et al., 2015)

Basic electrochemical cell for cyclic voltammetry can be achieved by connecting potentiostat to the 3 electrodes of electrochemical cell. The schematic of the

electrochemical cell can be seen in Figure 2.6. $E_A$ is the applied potential; A is the ammeter to measure the current. C, R and W are counter electrode, reference electrode and working electrode. When potential is applied, reduction and oxidation process will occur in which involved the diffusion of electrons (Kissinger & Heineman, 1996), therefore it is crucial that the solution not to be stirred during the process.

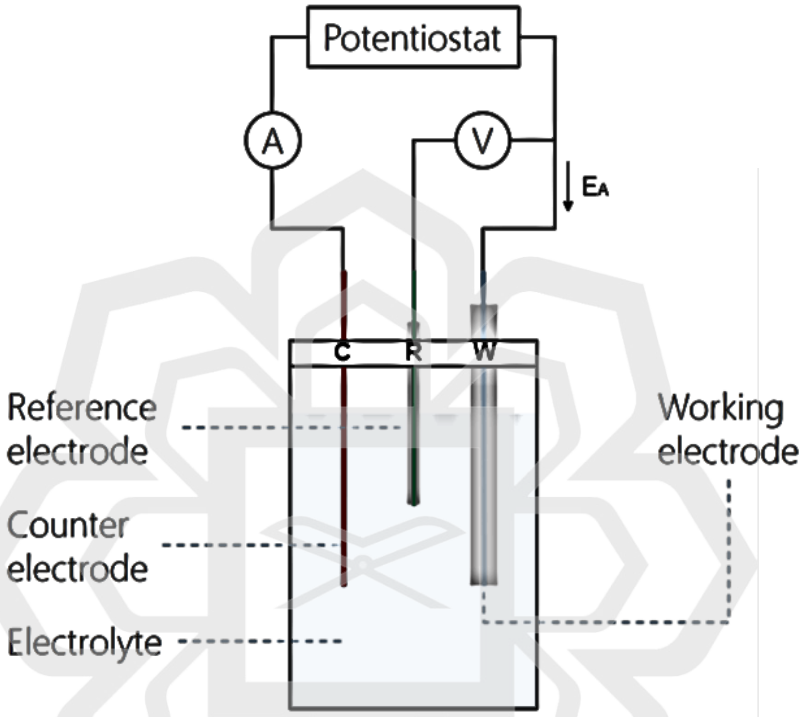


Figure 2.6 Cyclic voltammetry Electrochemical Cell (Forrister, 2018)

Another important factor of cyclic voltammetry is the scan rate. This is important since it can influence the data collection. Faster scan rates would lead to the decrement in the diffusion layer's size which will cause the increment of currents (Elgrishi et al., 2018). In Figure 2.6, the cyclic voltammogram are from the same analytes but at different scan rates. Figure 2.7(a) shown data at faster scan rate while Figure 2.7(b) shown data collected at slower scan rate. Two peaks are observed on faster scan rate but, cathodic peak disappeared due to slow scan rate allows sufficient time for the reduction on the forward scan to perform chemical reaction in which the product from the reaction is non electroactive.

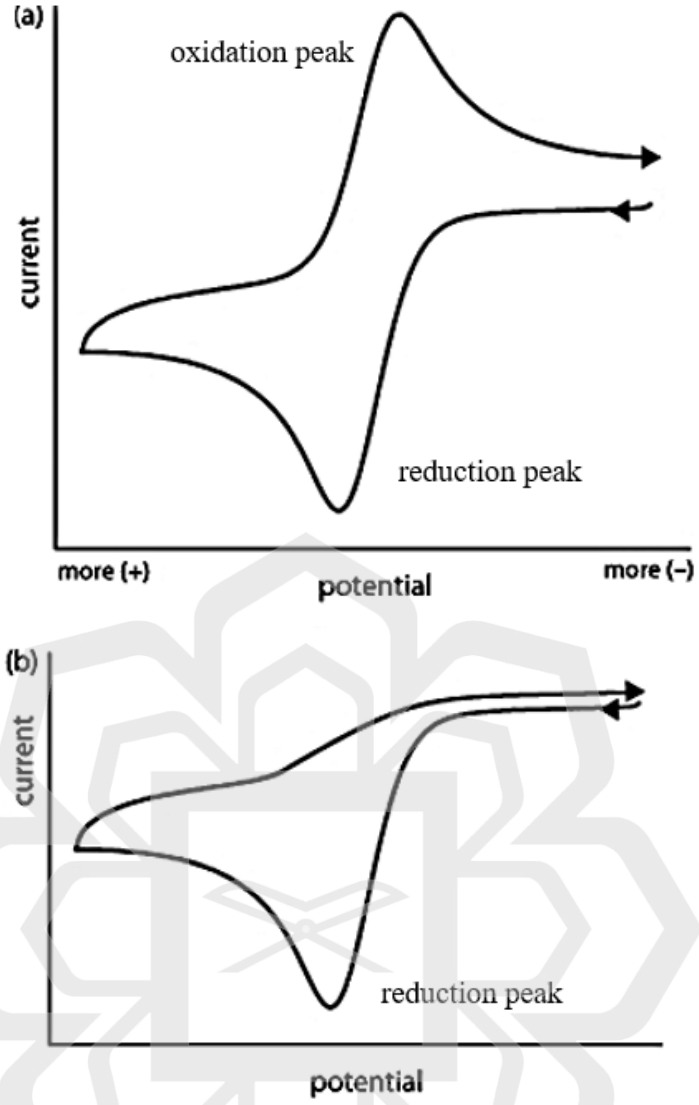


Figure 2.7 Impact of scan rate on CV curve (a) Faster scan rate (b) slower scan rate (Harvey, 2013)

### 2.3.2 Differential Pulse Voltammetry

Differential pulse voltammetry (DPV) is a technique in which linear ramp potential are being applied with the amplitude potential pulses(Simões & Xavier, 2017) The technique is used to study the redox properties of chemicals or biological elements with extremely low concentrations (Laborda, González, & Molina, 2014), which makes it great to detect pesticide (Zia et al., 2022) as well as used for medical biosensors (Brazaca, Ribovski, Janegitz, & Zucolotto, 2017).

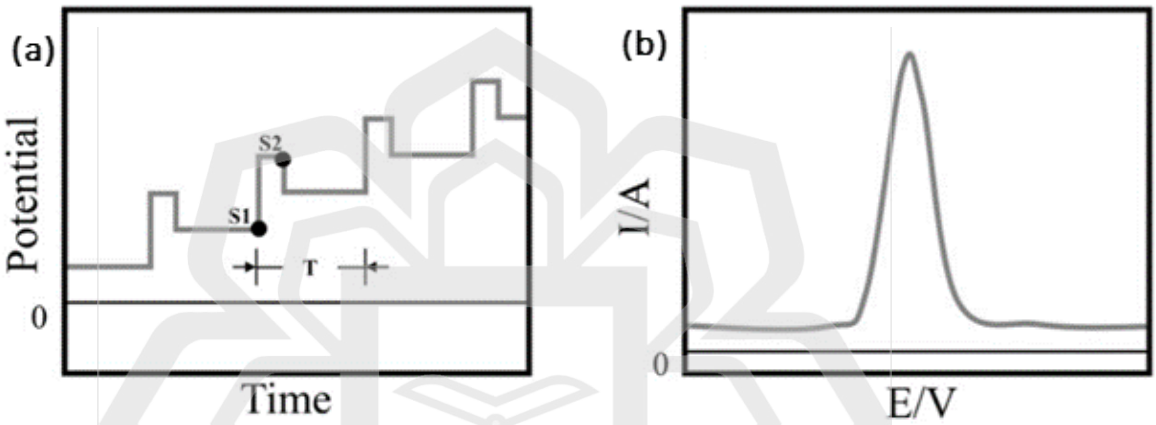


Figure 2.8 (a) Differential pulse voltammetry input waveform (b) Output waveform of differential pulse voltammetry (Liu et al., 2022)

Figure 2.8 (a) shown input waveform of DPV in which at specific intervals, voltage pulse at specific intervals. These pulses are increased in steps over time, T as shown. Before each pulse is applied and at the end of the step, current is sampled at points S1 and S2. The pure faradaic current is then calculated from the differences between S1 and S2. The value is then plotted against current which can be seen in Figure 2.8(b). (Liu et al., 2022). Oxidation reaction that takes place in the solution can be seen from the peak in the graph. Important value which are evaluated are the output are the value of the peak faradaic current.

### 2.3.3 Impedance Spectroscopy

According to Nossol et al., 2021 electrochemical impedance spectroscopy (EIS) is a technique to investigate electrical properties of various matters by measuring the current response after applying sinusoidal voltage. From the result of current response, the data can be represented in three forms, Fourier transform, to decompose the result for assessing the magnitude and frequency, in the form of bode plot to measure frequency response of the systems as well as in Nyquist plot. The results from Nyquist plot can determine double layer capacitance, electrolyte solution's ohmic resistance, Warburg impedance as well as electron transfer resistance.

Figure 2.9 (a) represents EIS electrochemical cell which is called Randle's equivalent circuit. $R_\Omega$ is the solution resistance, $C_d$ is double layer capacitance in which happened due to electron flow, Rct is charge-transfer resistance that happened due to reduction or oxidation of some chemical substance at an electrode, W is Warburg impedance which caused by the diffusion(Macdonald & Johnson, 2018). Figure 2.9 (b) shows the expected result of the Nyquist plot of impedance model of Randle's equivalent circuit. The semi-circle in the graph is when at higher frequencies, and at lower frequencies, Warburg impedance shown, and it became straight line at an angle of 45°.

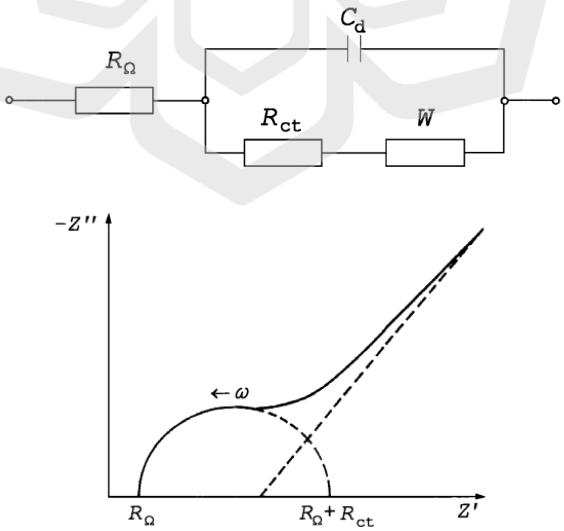


Figure 2.9 (a) Randle's equivalent circuit of EIS cell (Macdonald & Johnson, 2018)
(b) Nyquist plot of the EIS cell (Macdonald & Johnson, 2018)

## 2.4 Related Works of Portable Potentiostat

### 2.4.1 A low-cost and miniaturized potentiostat for sensing of biomolecular species such as TNF-α by electrochemical impedance spectroscopy (Pruna et al., 2018)

This work combines an analogue circuit which can be seen in Figure 2.10 with powerful microcontrollers to perform Digital to Analog Converter (DAC) and Analog to Digital Converter (ADC) separately. This work tries to tackle the incomplete and complex architectures of other designs by using two microcontrollers. PIC32 is used as main controller for the potentiostat while another PIC24 is used as 16-bit ADC as well as 10-bit DAC. The gap between PIC24 and PIC32 is filled by taking advantage of specific features of both microcontrollers. PIC24 is used as 16-bit ADC advantage compared to 10-bit ADC of PIC32, while PIC32 comes with 32-bit core which allows better processing performance.

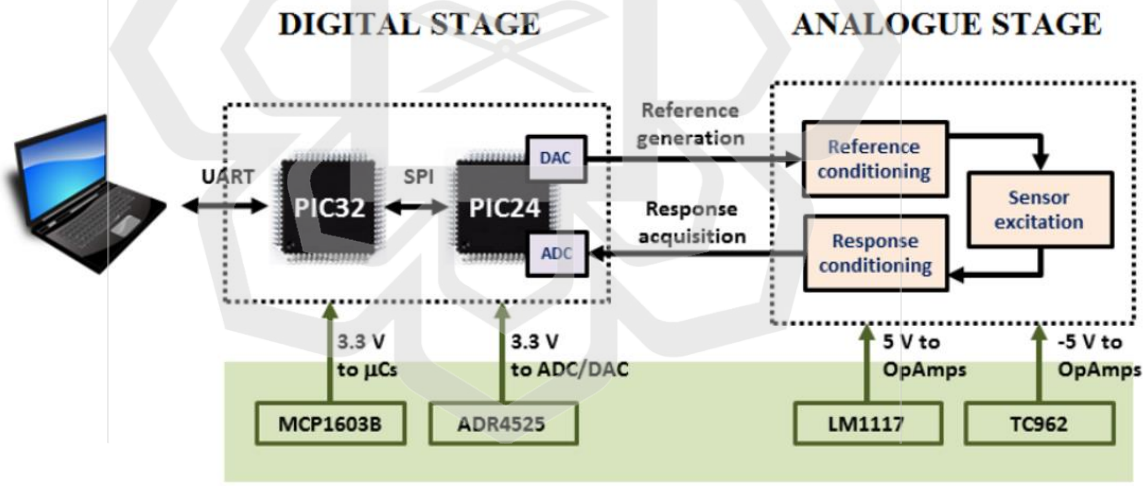


Figure 2.10 Block diagram of potentiostat that been designed by Pruna et al., 2018

Even though the system comes with great design, it also has issues with response signal not being clean enough to deduce sensor's impedance features properly. This is due to instabilities of electronic components, coupling of the electrical noise as well as instabilities during the data acquisition. The system was validated with EIS and CV. EIS was able to run from 10mHZ up to 10kHz. The resolution for the ADC is 16 bits

and the DAC is 10 bits. Figure 2.11 shows the circuit board of the potentiostat that Pruna et al., developed.

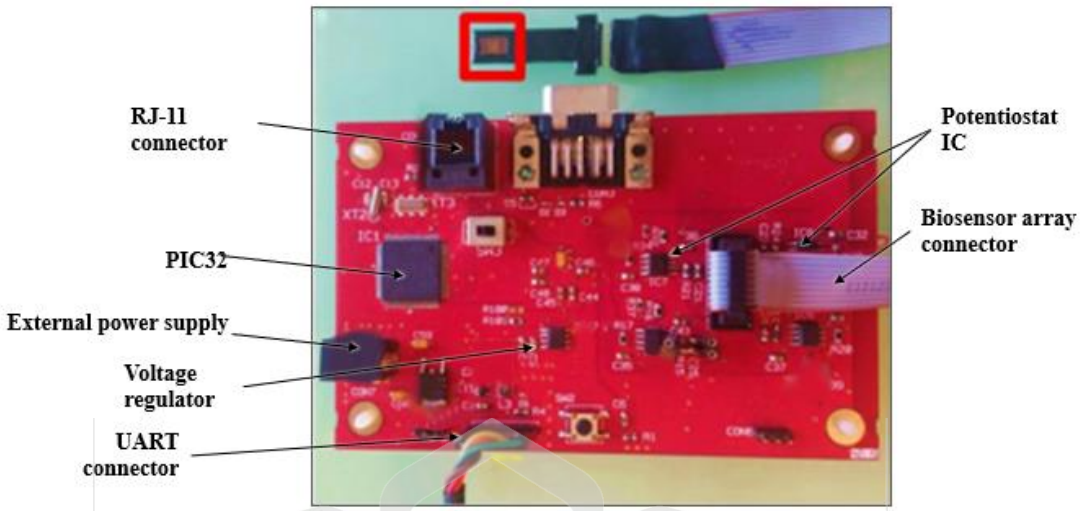


Figure 2.11 Potentiostat that been designed by Pruna et al., 2018

### 2.4.2 ABE-Stat, a Fully Open-Source and Versatile Wireless Potentiostat Project Including Electrochemical Impedance Spectroscopy (Jenkins et al., 2019)

ABE-Stat is a potentiostat system that is portable potentiostat with wireless and battery capabilities. Android interface can be connected wirelessly to collect measurement data. The device also has WIFI features. The electrochemical analyses that can be conducted with ABE-Stat are high impedance potentiometric measurements, cyclic voltammetry, and electrochemical impedance potentiometric measurements. It is one of the first fully open-sourced potentiostat, coming with electrochemical impedance spectroscopy (EIS) measurement capability across large frequency spectrum. The system comes with 24-bit ADC resolution and 16-bit DAC resolution which can be seen in the schematic in Figure 2.12. The lithium battery that came with the system can also run straight for 18 hours continuously. Figure 2.13 shows the packaging of the ABE-stat. The weakness of the system is even though it came with high resolution, the output noise is over an order magnitude larger.

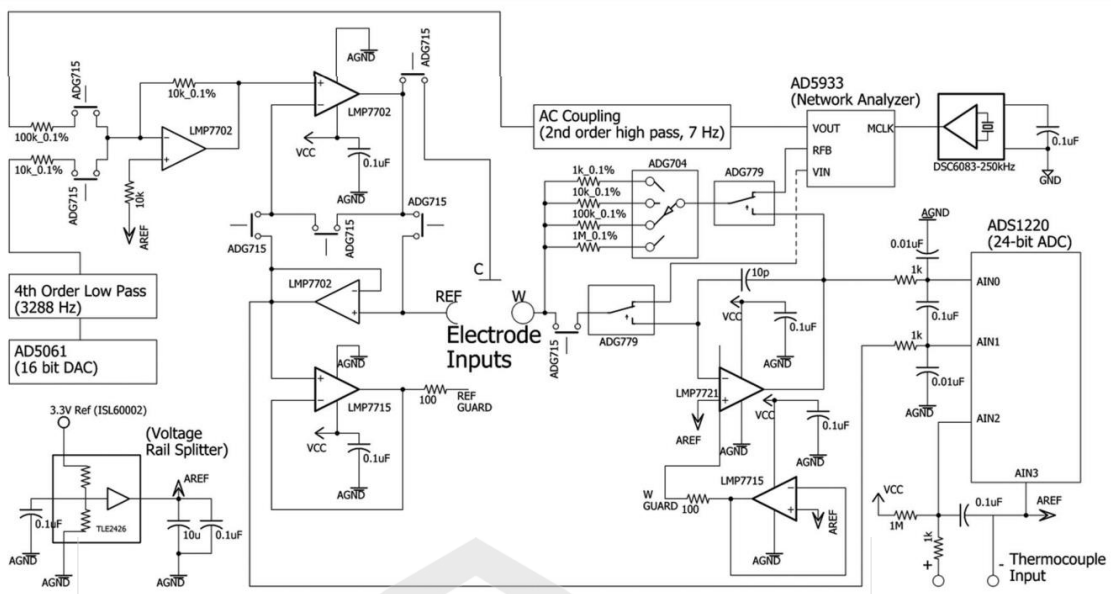


Figure 2.12 ABE-stat schematics (Jenkins et al., 2019)

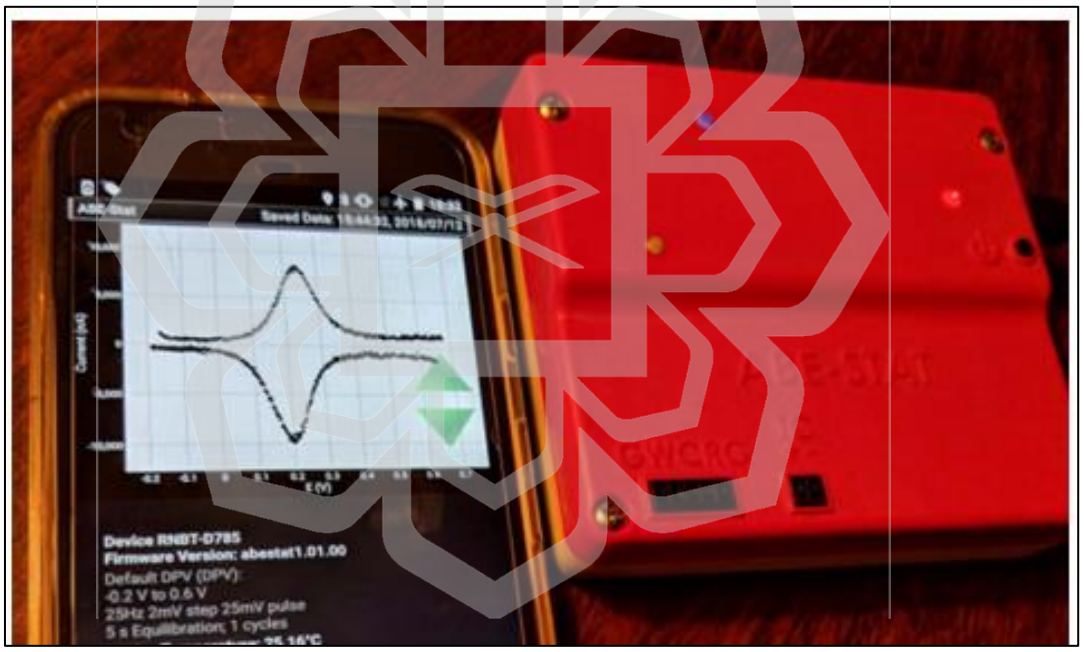


Figure 2.13 ABE-stat module in packaging which could be run with android (Jenkins et al., 2019)

### 2.4.3 SIMstat: Hardware Design Considerations for Implementing a Low-Cost, Portable Potentiostat (Cook, 2020)

This paper is a design concept of low cost and high precision potentiostat design with up to 14-bit ADC. Only simulation had been done. However, the circuit board design had also been completed but due to limited time frame, the circuit board wasn't able to be fabricated. The design took inspiration form ABE-stat, but ATmega1284 is used in the paper to improve the accuracy. However, the design is not coming with EIS measurement capability.

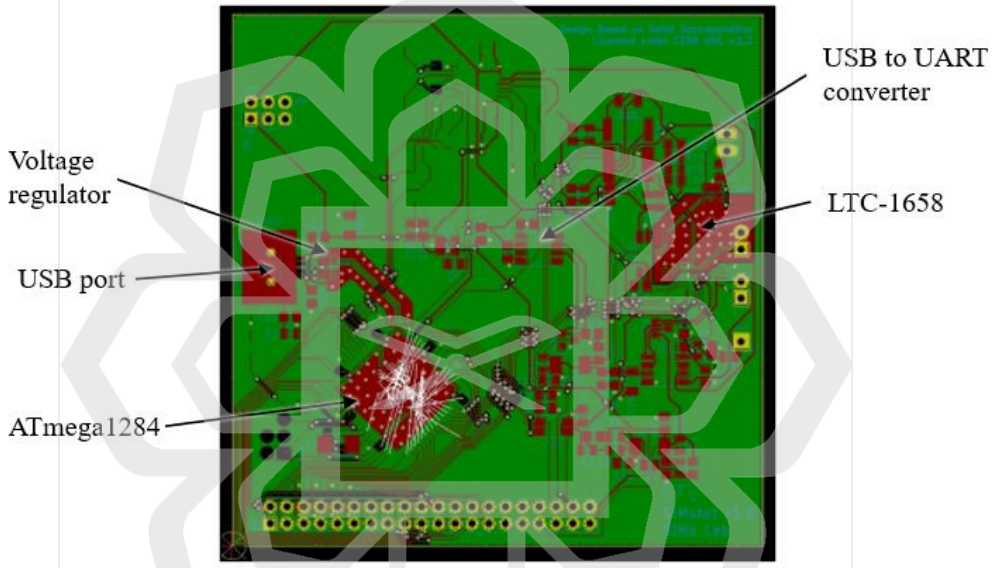


Figure 2.14 SIMstat board design by Cook, 2020

### 2.4.4 Kickstat: A coin-sized potentiostat for high-resolution electrochemical analysis (Hoilett et al., 2020)

KickStat is a one of the potentiostat with smallest form factors which can be seen in Figure 2.15 (a). It took advantage of the small sized LMP91000 potentiostat chip as well as small sized ARM Cortex-M0 + SAMD21 as the main controller. Even though SAMD21 has ADC capabilities, KickStat doesn't have impedance spectroscopy capability. The response of the device is within 0.6% compared to commercialized potentiostat. The design doesn't need any extensive circuitry to perform high-resolution electrochemical analysis such as linear sweep, cyclic and square wave voltammetry.

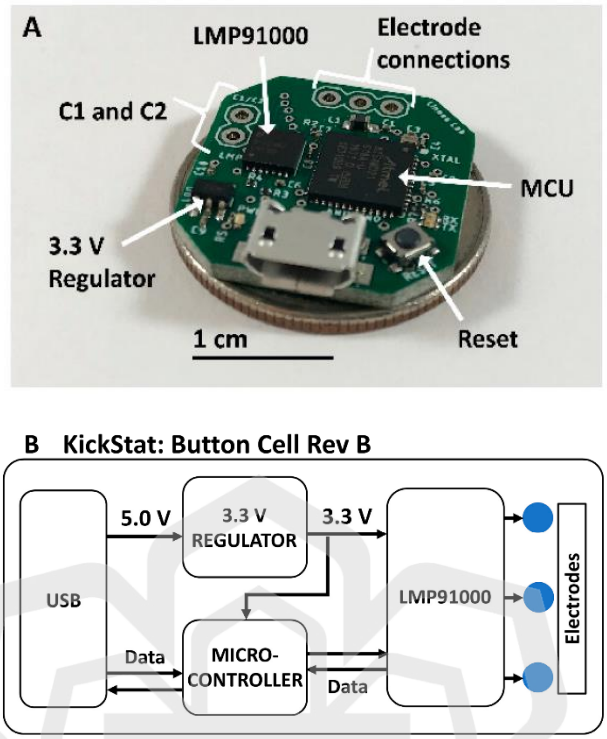


Figure 2.15 A) KickStat size comparison with coin B) KickStat block diagram (Hoilett et al., 2020)

### 2.4.5 MiniStat: Development and Evaluation of a Mini-Potentiostat for Electrochemical Measurements (Adams, Doeven, Quayle, & Kouzani, 2019)

Mini stat is a portable, flexible as well as low cost potentiostat which allows experiments to be ran simultaneously in parallel. The device in Figure 2.16 is with the size of 27 mm × 20 mm and comes with capability to perform square wave voltammetry, cyclic voltammetry as well as chronoamperometry. ATxmega32E5 microcontroller that being used also enabled the device to take high resolution reading with 12-bit DAC that present. The block diagram of the device can be seen in Figure 2.17. However, one of the features that are needed in this research, is not available with the device, which is impedance spectroscopy capability.

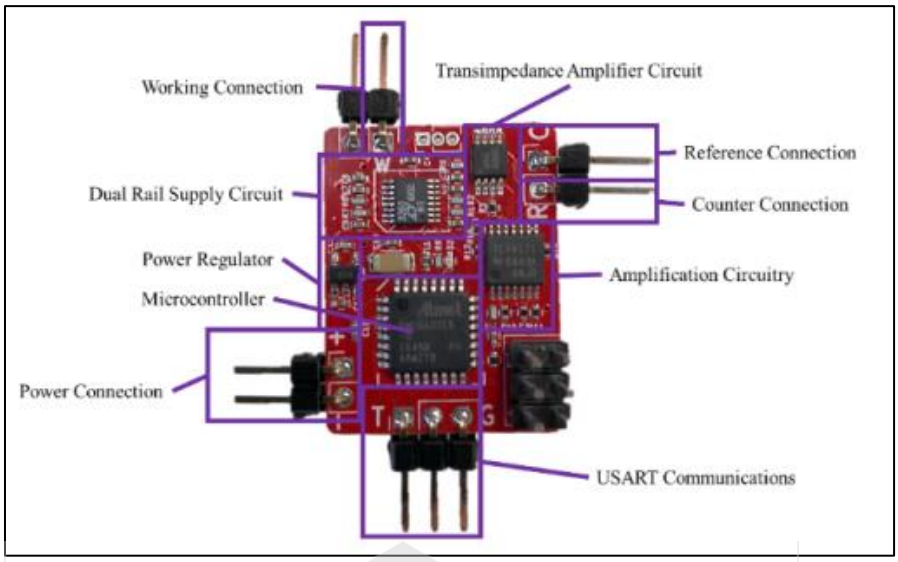


Figure 2.16 MiniStat potentiostat (Adams et al., 2019)

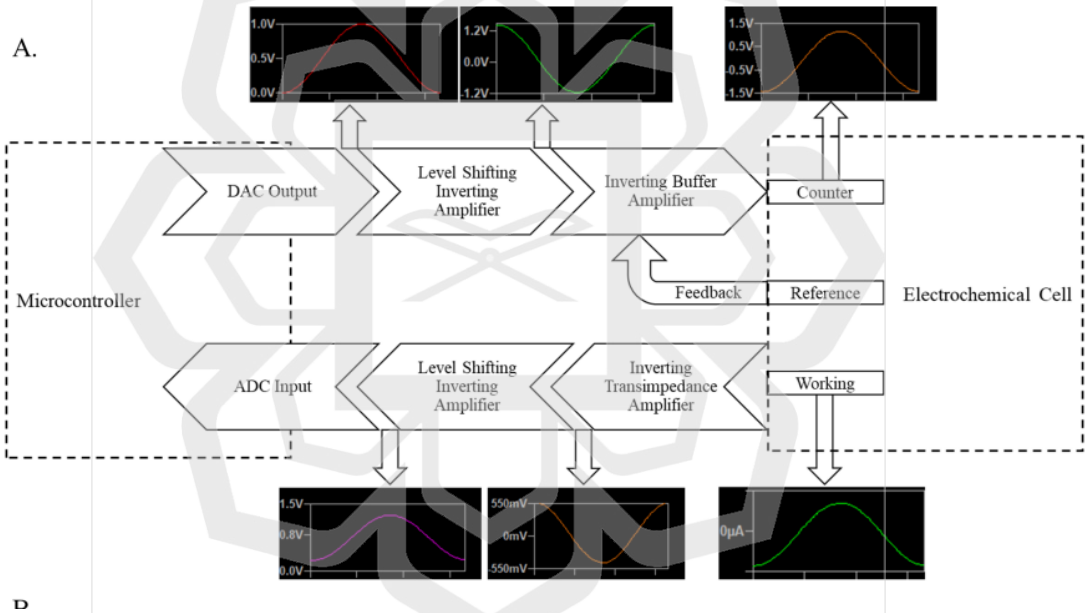


Figure 2.17 MiniStat block diagram for the potentiostat (Adams et al., 2019)

Table 2-2 Summary of Comparison of Portable Potentiostats

| **Reference** | **Available Measurements** | **Micro-controller** | **Description** | **Strength** | **Limitation** |
|---|---|---|---|---|---|
| Pruna et al., 2018 | Amperometry, CV, EIS | PIC32, PIC24, MCP1603B | Combining simple analogue circuitry with powerful microcontrollers, with low cost as well as small form factor | Versatility on impedance spectroscopy, can perform collect reading from as low as 10mHz | Only strong EIS correlation at 1-10Hz with commercialized potentiostat |
| Jenkins, Lee, Jun, Reyes-De-Corcuera, & McLamore, 2019 | CV, DPV, EIS | LMP7721, ADS1220 | **ABE-Stat** – open sourced and powered by battery potentiostat with wireless capabilities as well as Android interface | Can operate long time up to 18 hours continuous run time on battery | High noise on the ADC control amplifier. Test was not done with wireless enabled |
| Cook, 2020 | CV | ATmega1284, LTC-1658 | **SIMstat** – low cost and high precision potentiostat design | High reading precision with up to 14-bit ADC | No EIS capabilities, and no hardware or benchmark being done |
| Hoilett et al., 2020 | CV, SWV, NPV, Chronoamperometry | ARM Cortex-M0, SAMD21, LMP91000 | **KickStat** – coin sized potentiostat with high resolution electrochemical analysis | Small form factor, and response are within 0.6% compared to commercialized potentiostat | No EIS capabilities. Noisier compared to commercialized potentiostat |
| Adams, Doeven, Quayle, & Kouzani, 2019 | Linear sweep, CV, SWV | ATxmega32E5 | **MiniStat** - small form factor with accurate measurement compared to commercial's potentiostat. | High resolution with 12-bit DAC with low-cost design | No EIS capabilities. Larger footprint compared to other design |

## 2.5 Portable Potentiostat with COVID-19 Detection Capability

### 2.5.1 Electrochemical Biosensor Based on Laser-Induced Graphene for COVID-19 Diagnosing: Rapid and Low-Cost Detection of SARS-CoV-2 Biomarker Antibodies (Oliveira et al., 2022)

Oliveira et al., 2022 has developed a portable mini potentiostat which are able to detect the presence and absence of COVID-19 biomarkers. The biomarker can be detected with estimated processing time of 3 minutes. The developed potentiostat comes with the ability to perform cyclic voltammetry measurements and differential pulse voltammetry. It comprises of two main platforms, a micro-controlled platform and hardware connected to a computer which can be seen in Figure 2.18. The computer handles data processing, converting it into valuable information for comprehending the analyzed phenomenon using MATLAB R2016b software. The biosensor's current is derived from the measured voltage by the potentiostat through a mathematical equation representing the inverse modeling of the hardware(Oliveira et al., 2022).

The microcontroller platform comprises an Arduino UNO, primarily responsible for generating excitation signals and conducting data acquisition, both under the control of an ATmega328 microcontroller. This microcontroller can deliver positive voltage values ranging from 0 to 5 V, with an 8-bit resolution. Consequently, the digital output was configured to span from 2.1 V to 3.3 V, referencing the center value at 2.5 V. This configuration results in cyclic voltammetry ranging from −0.4 V to 0.8 V, employing a scan rate of 0.05 V·s−1 for two cycles, presented in a triangular waveform.

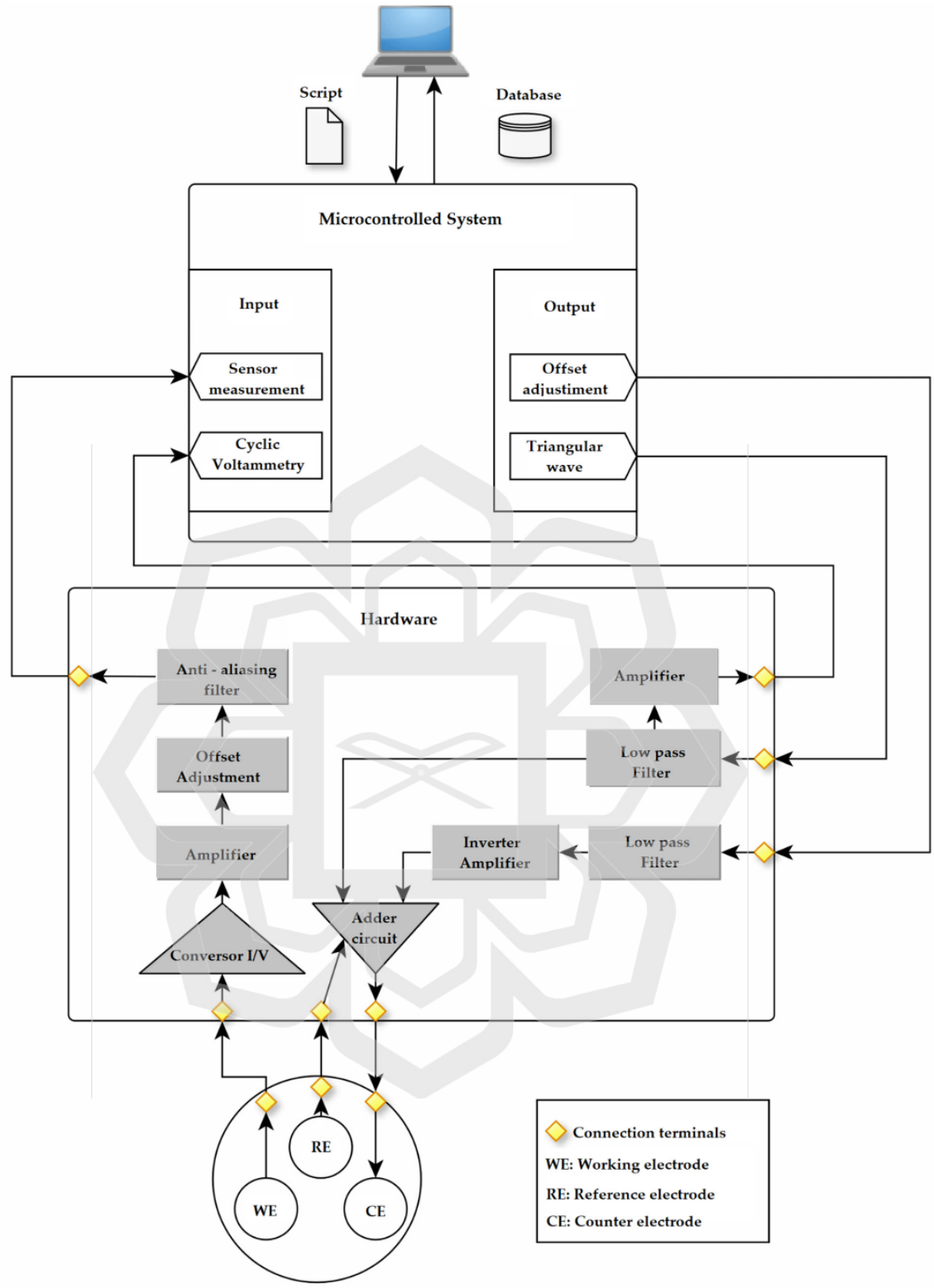


Figure 2.18 Block diagram of the portable potentiostat developed by Oliveira et al., to detect COVID-19 (Oliveira et al., 2022)

A second digital output was employed to provide a 2.5 V center voltage, serving as a reference for the hardware platform and to compensate the offset in CV. The microcontroller is also responsible for biosensor measurement data acquisition. Within

the Arduino UNO platform, there are six analog inputs, with two dedicated to gathering information from the biosensor measurement system. The microcontroller also features ADC with 10-bit resolution(Oliveira et al., 2022).

### 2.5.2 eCovSens-Ultrasensitive Novel In-House Built Printed Circuit Board Based Electrochemical Device for Rapid Detection of nCovid-19 antigen, a spike protein domain 1 of SARS-CoV-2 (Mahari, Roberts, Shahdeo, & Gandhi, 2020)

Mahari et. al, 2020 has developed PCB based potentiostat for COVID-19 detection. The developed eCovSens device as shown in Figure 2.19 identifies voltage changes through an SPCE electrode utilizing the principle of signal transduction. The modified biosensor consists of a bio-recognition element (nCovid-19 Ab), a transducer (carbon), and an electronic system comprising a display, processor, and amplifier (an in-house electrochemical instrument). The bio-recognition element, acting as a bio-receptor, engages with a specific analyte (nCovid-19 Ag) during the detection process. The transducer and Ag-Ab interactions interact to produce an output voltage signal. The signal output's intensity is directly correlated with the analyte's concentration (nCovid-19 Ag). The signal is then amplified and processed by the electronic system. Then, the output will be converted to digital reading by using ADC and displayed on the device screen. The data can also be Main detection technique for the device is differential pulse voltammetry .(Mahari et al., 2020).

A)

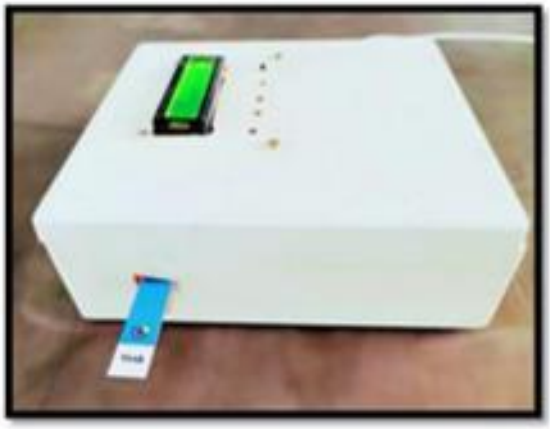

B)

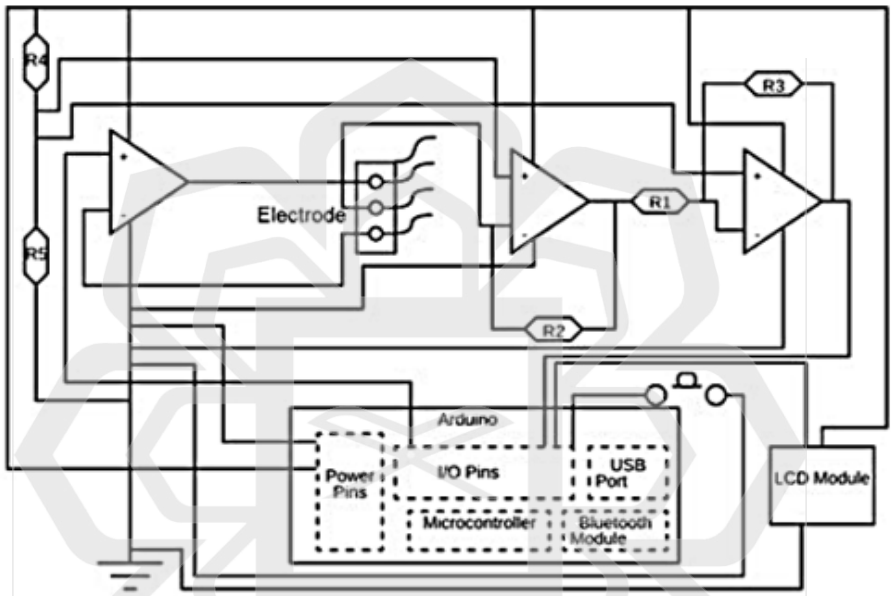


Figure 2.19 (A) eCovSens device (B) Circuit diagram of eCovSens (Mahari et al., 2020).

### 2.5.3 Bi-ECDAQ: An electrochemical dual-immuno-biosensor accompanied by a customized bi-potentiostat for clinical detection of SARS-CoV-2 Nucleocapsid proteins (Salahandish et al., 2022)

The Bi-ECDAQ's potentiostat module in Figure 2.20 is developed by Salahandish et al., is an advanced, programmable, and self-calibrating reading system featuring components like the Impedance converter (AD5933), Analog Front End, Memory, Programmable clock, and Microcontroller Unit breakout board (SparkFun Pro nRF52840). This innovative potentiostat accurately measures the impedance of two integrated yet independent immuno-biosensors. It then transmits the resulting digital

data to a computer or smartphone using wired (Universal Serial Bus - USB) or wireless (Bluetooth) communication protocols. Main technique of the device is Electrochemical Impedance Spectroscopy (Salahandish et al., 2022).

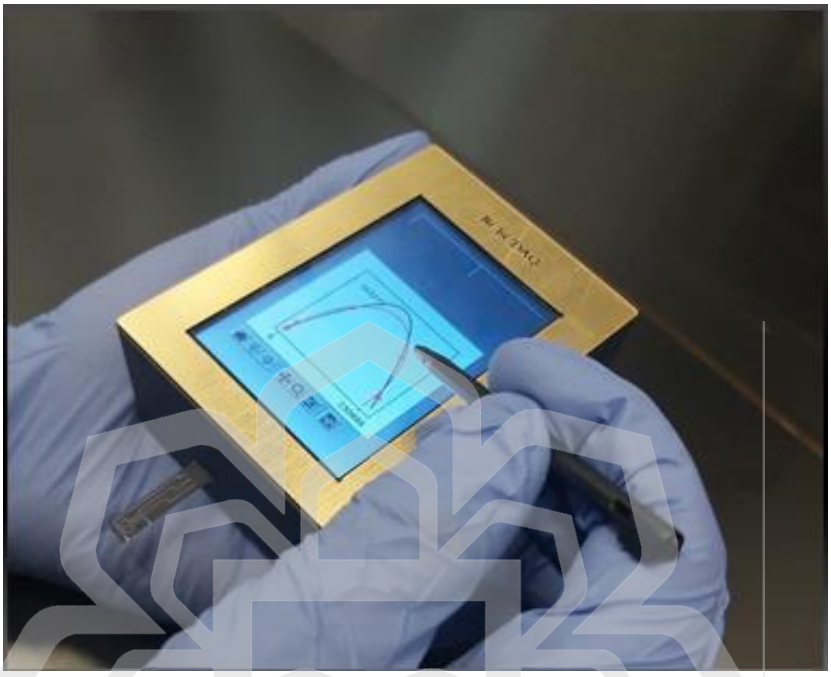

Figure 2.20 Bi-ECDAQ Potentiostat module (Salahandish et al., 2022)

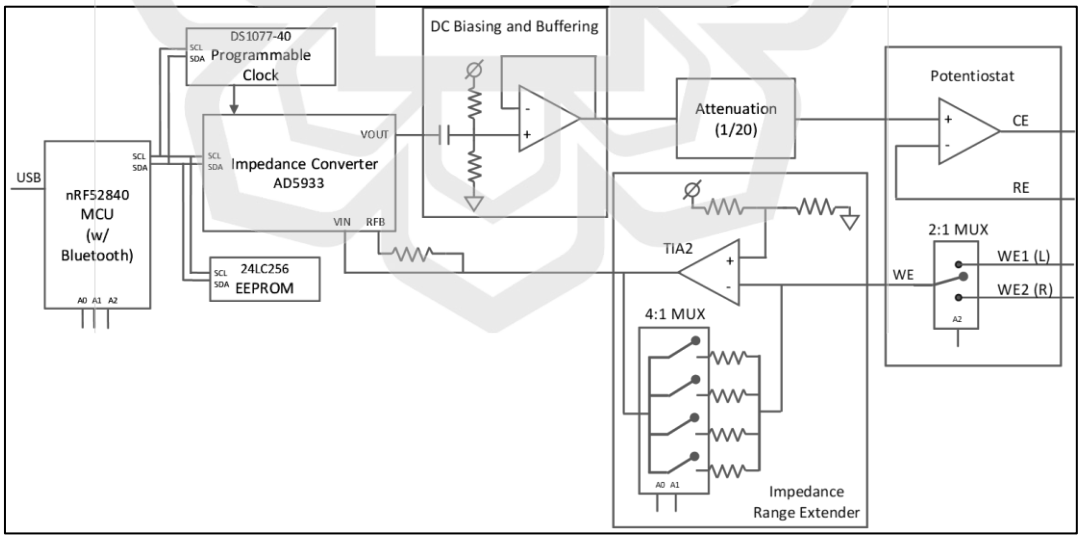


Figure 2.21 Block Diagram of Bi-ECDAQ potentiostat module (Salahandish et al., 2022).

Figure 2.21 shows the block diagram of Bi-ECDAQ potentiostat module. The microcontroller unit, MCU used in this device is the SparkFun Pro nRF52840 Mini with ARM Cortex-M4 32-bit processor (64 MHz, 1 MB flash, 256 kB RAM), and 2.4 GHz

Bluetooth Low-Energy (BLE) radio. The USB interface allows for MCU programming, input voltage, and communication through the UART interface. The device can also be powered by a Lithium-Polymer (LiPo) battery and charged using the same USB interface. The firmware was then developed using Arduino IDE and Adafruit nRF52 Arduino core libraries (Salahandish et al., 2022).

The microcontroller is responsible for receiving commands from the GUI to initialize, calibrate the system, and instruct the impedance converter to produce signals for application to the immuno-biosensors. The signals produced by the Impedance converter undergo conditioning in the analog front-end, involving DC biasing and attenuation (1/20) before being sent through the potentiostat to the counter and reference electrodes (CE, RE).

### 2.5.4 An alternative ready-to-use electrochemical immunosensor for point-of-care COVID-19 diagnosis using graphene screen-printed electrodes coupled with a 3D-printed portable potentiostat (Primpray et al., 2022).

Primpray et al., has produced a custom-designed portable potentiostat to perform the quantitative analysis of COVID-19. This device utilized an amperometry technique for the virus detection. The device is classified as a small medical device with dimensions of 107mm × 143mm × 90mm. The packaging was designed using SolidWorks software, featuring a trapezoid shape with a slanted top surface to accommodate the display for easy reading and a front electrode socket for the insertion of biosensor. The physical device was created through 3D printing which can be seen in Figure 2.22.

The assembled 3D printed device integrate a potentiostat printed circuit board (PCB) for measuring current signals obtained from the detection, a power supply module, and a touchscreen display for device operation. The PCB also housed a programmed microcontroller for interpreting current responses into qualitative and quantitative results within a 5-minute timeframe. The obtained current signal was then converted to the concentration of COVID-19 protein using a calibration curve, and the result was displayed.

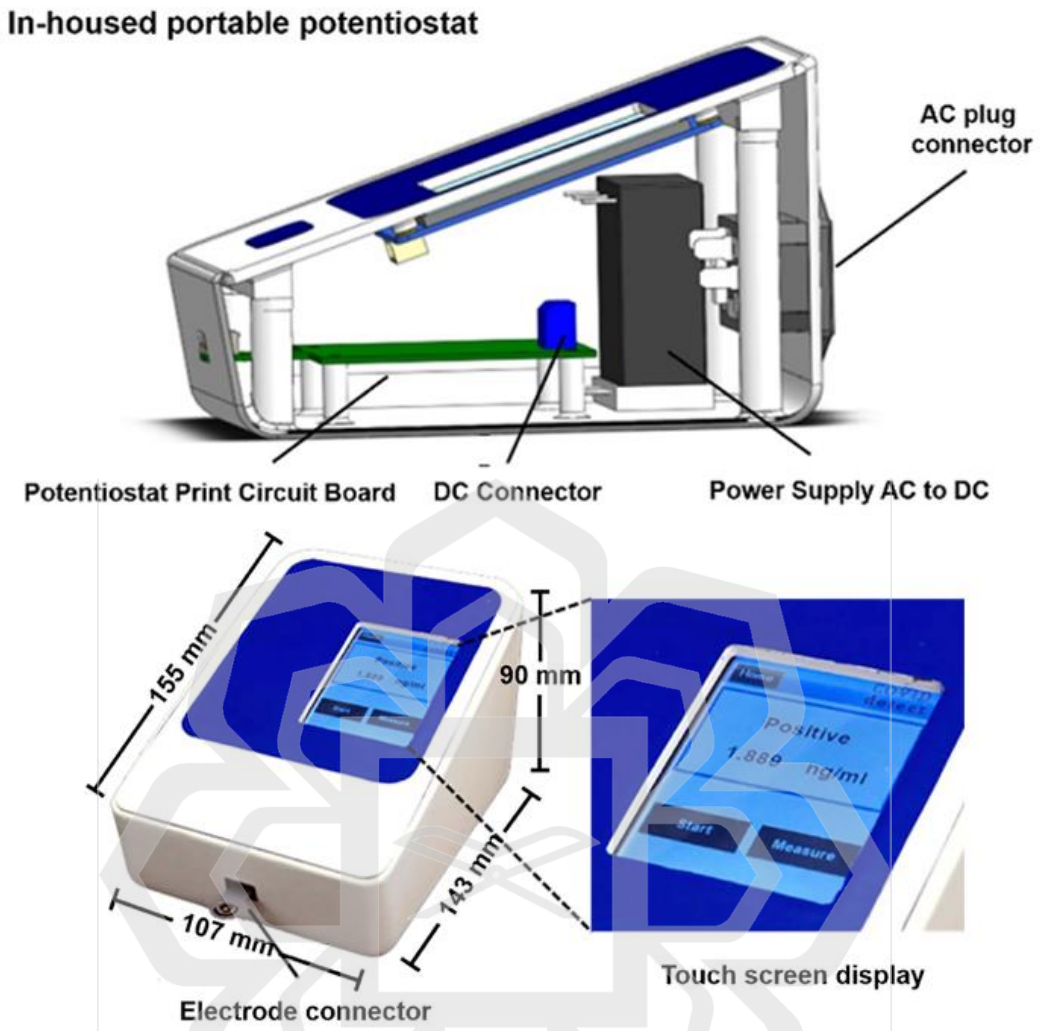


Figure 2.22 In-house designed potentiostat in 3D packaging (Primpray et al., 2022)

Table 2-3 Summary of Comparison of Potentiostats with COVID-19 Detection Capabilities

| Reference | Potentiostat Name | COVID-19 Detection Technique | Detection Time | Platform | Wireless Capability | Display | Limitation |
|---|---|---|---|---|---|---|---|
| (Oliveira et al., 2022) | Portable Potentiostat | CV, DPV | 30 seconds | PC | No | No display | Simple ADC with only 10-bits resolution, compared to other devices which ADCs are usually in the ranges of 12 to 16 bits. |
| (Mahari et al., 2020) | eCovSens | DPV | 1 min | PC and mobile phones | Yes | 16x2 dot matrix display | Simple ADC with only 10-bits resolution, compared to other devices which ADCs are usually in the ranges of 12 to 16 bits. |
| (Salahandish et al., 2022) | Bi-ECDAQ | EIS | 1 min | Stand-alone | Wifi and Bluetooth | LCD with touchscreen capability | EIS results require technical expertise to perform circuit fitting to evaluate the COVID results. |
| (Primpray et al., 2022) | 3D-printed portable potentiostat | Amperometry | 5 min | PC and mobile phones | No information | LCD with touchscreen capability | Amperometry technique have the longest test time which are 5 times longer than other devices. |

## 2.6 Potentiostat Chips

A potentiostat chip is a component used in electrochemical analysis and experiments. It is a device that controls the potential (voltage) between a working electrode and a reference electrode in an electrochemical cell. This control allows researchers to study and manipulate electrochemical reactions.

### 2.6.1 EmStat Pico Core

The EmStat Pico is a miniaturized OEM potentiostat module designed for integration into products requiring electrochemical measurement functionality. The system has two potentiostat circuits which can be used simultaneously in Low-Speed mode (up to 100 Hz) and a High-Speed mode (up to 200 kHz) which can be applied to each channel alternately (PalmSens BV, 2023).

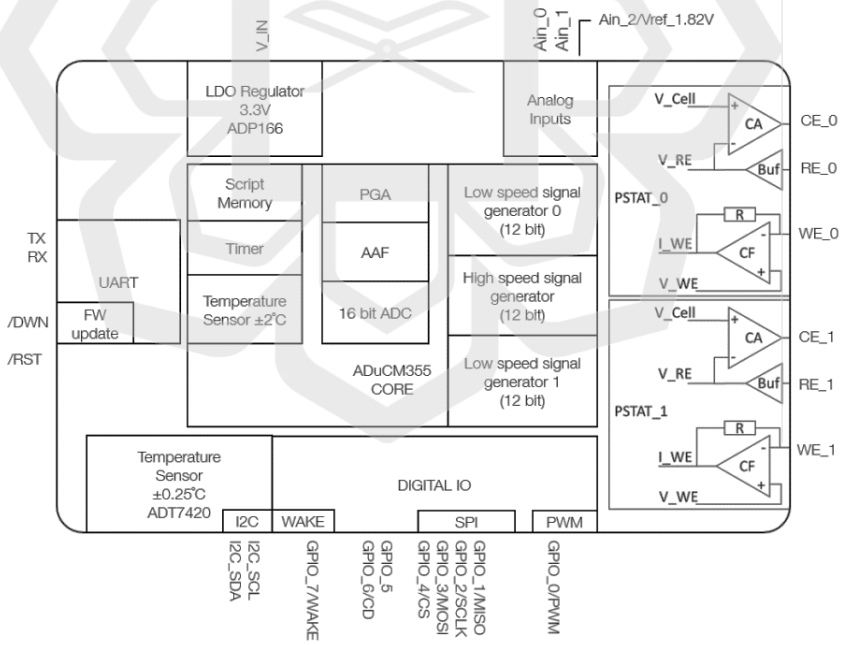


Figure 2.23 Block diagram of EmStat Pico Core (PalmSens BV, 2023)

The EmStat Pico block diagram can be seen in Figure 2.23. The device has an on-board 3.3 V LDO (ADP166) and supply filtering. This provides clean operation from a USB or a 3.5 V to 5.5 V supply. The EmStat Pico has one high-speed Digital to Analog Converters, DAC and two low speed DACs. The low-speed DACs can function

simultaneously at the same time with output range of 0.2 V to 2.4 V. The high-speed DAC has an output range of ±0.607 V. Both high and low speed DACs can be combined to achieve an output range of 0.2 V to 2.8 V(PalmSens BV, 2023).

The EmStat Pico also features an 800 kSPS ,16-bit, successive approximation register (SAR) analog-to digital converter (ADC) with programmable gain amplifier (PGA), built-in anti-aliasing filter (AAF), multiplexer, and input buffers. The input range of 0.2 V to 2.1 V.


Figure 2.24 Packaging of 1.1.1 EmStat Pico Core (PalmSens BV, 2023)

Power-saving settings are available in the system for battery-operated devices. The packaging can be seen in Figure 2.24. It comes with a small footprint with dimensions of 30.5 mm X 18 mm X 2.6 mm.

### 2.6.2 LMP91000

The LMP91000 serves as a customizable analog front-end (AFE) designed for micro-power electrochemical sensing applications. It offers a comprehensive signal path solution connecting a sensor to a microcontroller, generating an output voltage that corresponds to the cell current. Programmable in nature, the LMP91000 accommodates various electrochemical sensors, such as 3-lead toxic gas sensors and 2-lead galvanic cell sensors, within a single design, eliminating the need for multiple discrete solutions. The LMP91000 supports gas sensitivities across a range from 0.5 nA/ppm to 9500 nA/ppm and facilitates the effortless conversion of current ranges from 5 µA to 750 µA full scale (Instruments, 2015).

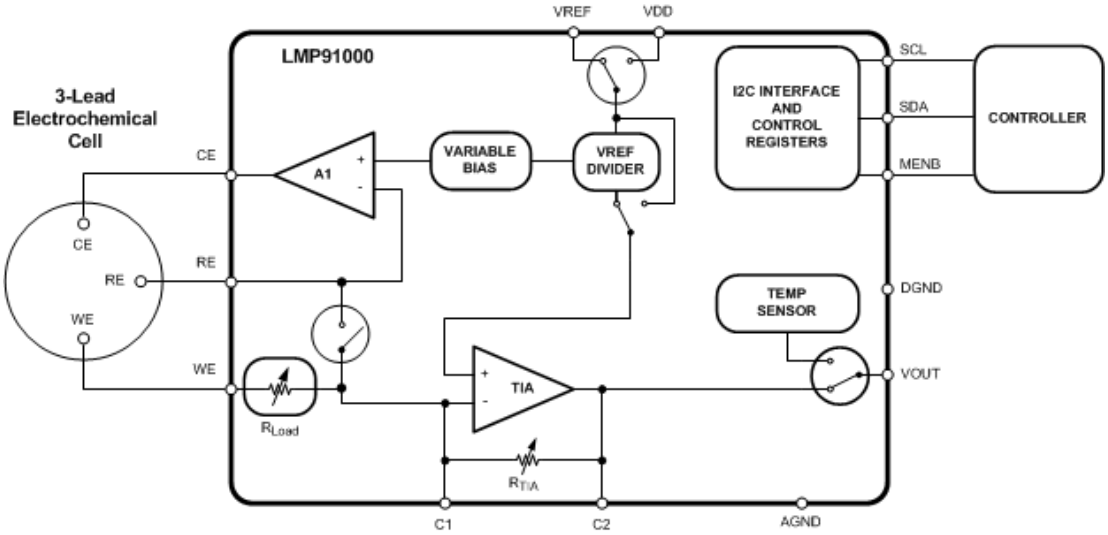


Figure 2.25 LMP91000 Block Diagram (Instruments, 2015)

The LMP91000 allows for the programming of its adjustable cell bias and transimpedance amplifier (TIA) gain using the I2C interface. This interface also serves for sensor diagnostics. Users can read the integrated temperature sensor through the VOUT pin, utilizing the data for additional signal correction in the microcontroller or monitoring to verify temperature conditions at the sensor.

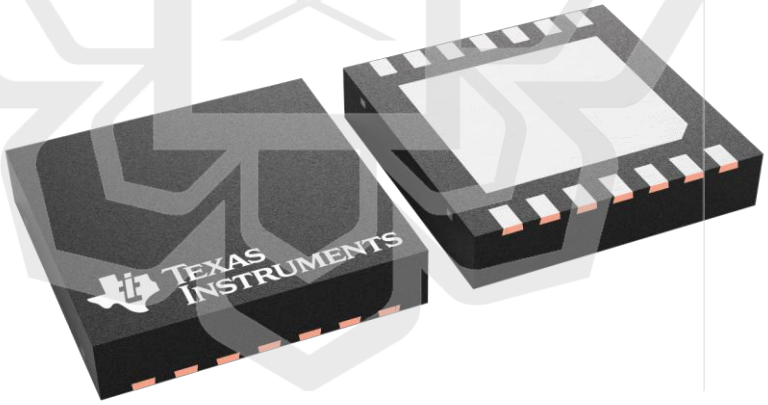


Figure 2.26 LMP91000 packaging (Instruments, 2015).

LMP91000 is designed for micro-power applications which the device functions within a voltage range of 2.7 to 5.25 V, with a total current consumption below 10 µA. Additionally, power conservation can be enhanced by deactivating the TIA amplifier and connecting the reference electrode to the working electrode using an internal switch.

### 2.6.3 ADuCM355

The ADuCM355 or Precision Analog Microcontroller with Chemical Sensor Interface is an on-chip potentiostat system which comes with capabilities to measure and control electrochemical sensors. The ADuCM355 is a mixed-signal microcontroller with ultralow power based on the Arm® Cortex™-M3 processor (Devices, 2023).

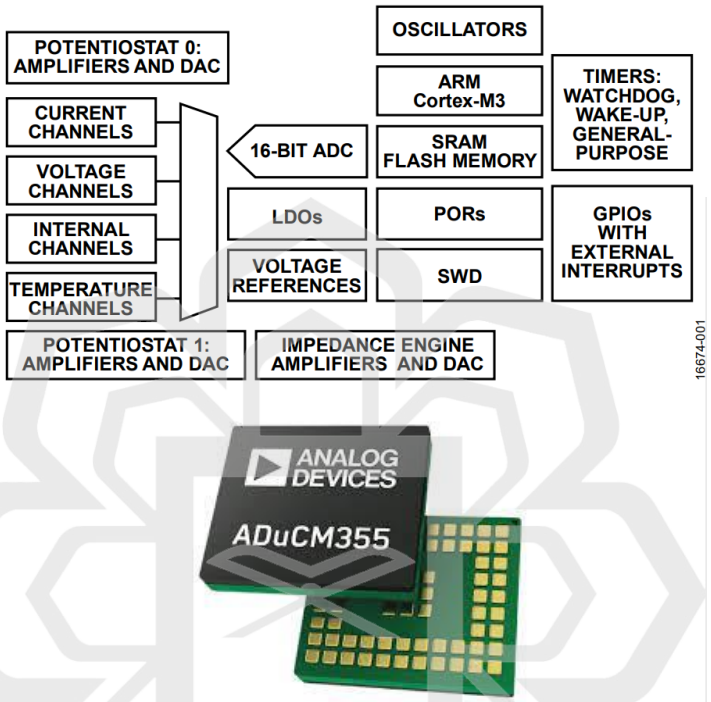


Figure 2.27 ADuCM355 block diagram and packaging (Devices, 2023)

The device is capable of measuring voltage, current, and impedance. The ADuCM355 features a 16-bit analog-to-digital converter (ADC). The device contains two low power amplifiers which are designed to maintain a constant bias voltage to the electrochemical sensor. Dual output digital-to-analog converters (DACs) control the amplifiers.

The ADC operates an input range of −0.9 V to +0.9 V. The user can choose an input channel for measurement using an input mux that comes before the ADC which are current channels, internal channels, and temperature channels.

The ADuCM355 integrates 64 kB of single random-access memory (SRAM), 128 kB of nonvolatile flash memory and an integrated on-chip 26 MHz Arm Cortex-M3

processor. The Arm Cortex-M3 CPU also features an adaptable multichannel direct memory access controller (DMA) that supports two SPI ports independently, as well as I2C communication peripherals, universal asynchronous receiver/transmitter (UART), and SPI ports.

ADuCM355 also features a range of communication peripherals which includes UART, I2C, two SPI ports, and general-purpose input/output (GPIO) ports. The chip is packaged in a 72-lead, with land grid array (LGA) package of size 6 mm × 5 mm (Devices, 2023).

Table 2-4 Potentiostat Chips Comparisons

| | **EmStat Pico** | **ADuCM355** | **LMP91000** |
|---|---|---|---|
| **Amperometry** | YES | YES | YES |
| **Cyclic Voltammetry** | YES | YES | YES |
| **Differential Pulse Voltammetry** | YES | YES | YES |
| **Square Wave Voltammetry** | YES | YES | YES |
| **Chronoamperometry** | YES | YES | YES |
| **Electrochemical Impedance Spectroscopy** | YES | YES | NO |
| **Open Circuit Potential** | YES | YES | NO |
| **Potential DC resolution** | 932 µV | 932 µV | - |
| **Measured Current resolution** | 0.006% of current range | 0.006% of current range | 0.006% of current range |
| **Current ranges** | 100 nA to 5 mA | 100 nA to 5 mA | 5 µA to 750 µA |
| **DAC resolution** | 12 bits | 12 bits | - |
| **ADC resolution** | 16 bits | 16 bits | 16 bits |

## 2.7 Summary

This chapter covered several COVID 19 testing methods such as antigen test, PCR test and serology test. Then, the chapter also reviewed in depth on the electrochemical

techniques that were used throughout the research which included cyclic voltammetry, differential pulse voltammetry and electrochemical impedance spectroscopy. Related works of portable potentiostats had also been reviewed. Six portable potentiostats that were developed by various researchers were reviewed and compared based on measurement capabilities, form factors and resolution.

# CHAPTER 3

# DESIGN AND DEVELOPMENT OF NACOTS POTENTIOSTAT

## 3.1 Overview

Nano system for COVID-19 DNA/Antibody on The Spot Test or known as NACOTS is a rapid molecular in vitro diagnostic tool utilizing an isothermal nucleic acid amplification technology intended for the qualitative detection of nucleic acid from SARS-CoV-2 virus. NACOTS consists of a potentiostat to perform electrochemical measurement and heating chamber to perform LAMP amplification. Electrochemical techniques that are used to detect COVID-19 virus are differential pulse voltammetry. This research are focusing on the electronics portion of the whole system.

To design an electronic device systematically, a design flow has been established. Figure 3.1 shown the fabrication flow of NACOTS. First, components need to be determined. To get an idea of what components need to be used, there are a few things that need to be determined. First, the use case of the components and if the components need other components to function. For example, EmStat Pico Core All needs USB to UART IC to communicate with the computer. Then, need to investigate the availability of the devices in the market. If the devices are not available in the market, then need to look for alternative devices with the same functionality.

Then, design the schematics once all the components needed have been established. Once the schematics have been checked and tested, proceed with the next step, which is design the PCB and send it for fabrication. Once the PCB is fabricated, then solder all the components, and check the continuity tests. If fail, check and fix the PCB design and repeat the flow. When the continuity test is passed, then the device's overall functionalities need to be tested. If fail, then needs to be troubleshot with possibilities of starting the whole flow again.

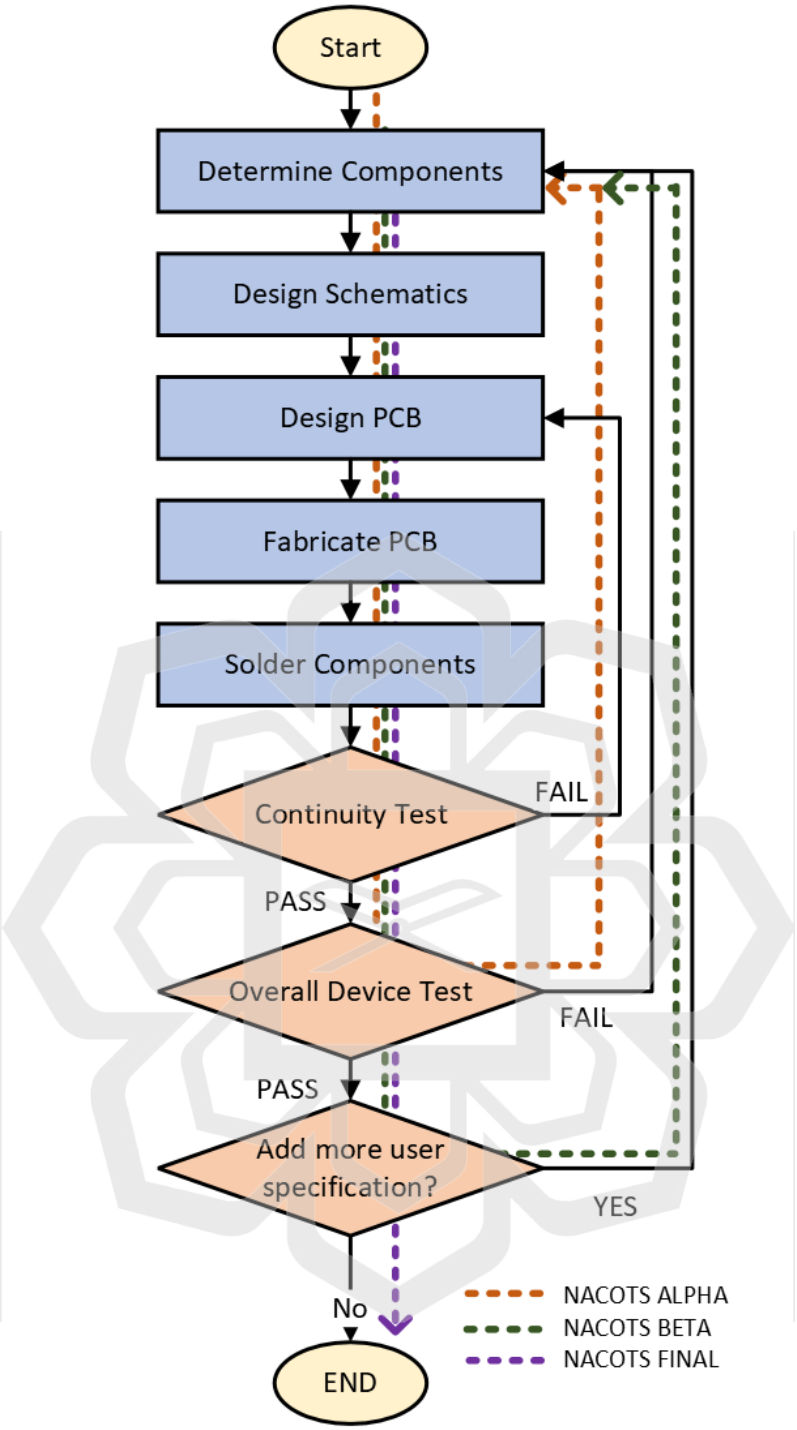


Figure 3.1 NACOTS hardware development flowchart.

### 3.2 NACOTS Potentiostat design specification

NACOTS initial design specification was a streamlined potentiostat which able to connect to a single electrochemical biosensor while being controlled through USB

The design can be further explained in the table below. The initial specification was fulfilled in the Alpha and Beta revision. After getting feedback from user during the testing of Beta revision of the board, more specification was added which includes heater and display capabilities.

Figure 3.2 shows how the user specifications are categorized. NACOTS are built based on four major user specifications, which points to platform, point of care, potentiostat, and incubation chamber. The design characteristics of each user specification and engineering target are further elaborated in Table 3.1.

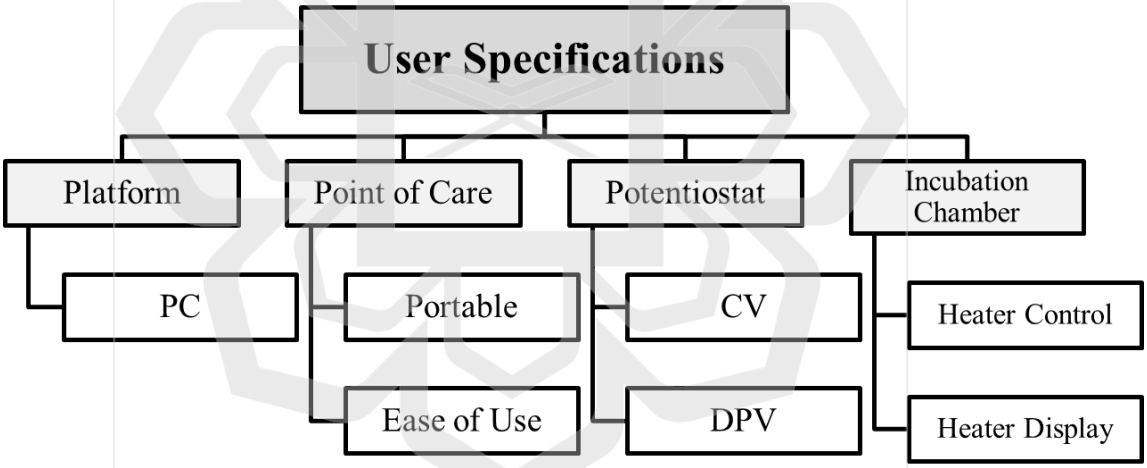


Figure 3.2 NACOTS user specifications overview

Table 3-1 User specification and engineering target on NACOTS device.

| User Specification | Design Characteristics | Engineering target |
|---|---|---|
| **Platform** | PC (Personal Computer) | Designed board needs to have USB connection to connect to PC |
| **Point of Care** | Portable | Designed board must be less than 100 x 100 mm |
| | Ease of Use | Device needs to be easy to use and can be use by anyone. |
| **Potentiostat** | CV | |
| | DPV | |
| **Incubation Chamber** | Heater Control | Heating element needs to be control through touchscreen and microcontroller. |
| | Heater Display | Designed board need to be able to connect to display which shown |

EmStat Pico is the potentiostat chip chosen for this project. EmStat Pico is a miniaturized potentiostat designed for electrochemical applications. It is a product of PalmSens, a company that specializes in instruments for electrochemical research and development. It offers a range of electrochemical techniques, such as cyclic voltammetry, chronoamperometry, and impedance spectroscopy. The chip came with 16 bits Analog to Digital Converter (ADC) and 12 bits signal generators.

### 3.2.1 NACOTS Alpha Revision

NACOTS Alpha revision had been built based on the initial user specification of the board. Block diagram of the design can be seen in the Figure 3.3. Starting from the left side, the port chosen is USB C port, in which are used by various devices. 3.6 voltage regulator is used to power up the potentiostat IC, and 3.3V voltage regulator is used to power up the I2C module. USB to UART controller is an important IC to allow communication in between computer and potentiostat chip. I2C Module functions as interconnection for potentiostat to other experimental modules such as another microcontroller. This module is added to add extra capabilities for experimentation. Based on the block diagram, schematics design for Alpha has been created.

Emstat Pico Core All is chosen as potentiostat chip compared to the other IC on the market because it has the capability to perform high precision electrochemical impedance spectroscopy with lesser noise compared to the other chip. With the 16 bits DAC and ADC capabilities on the chip, the chip able to obtain high resolution result. Besides, Emstat Pico Core All also have the capability to run amperometry, voltammetry and various other techniques.

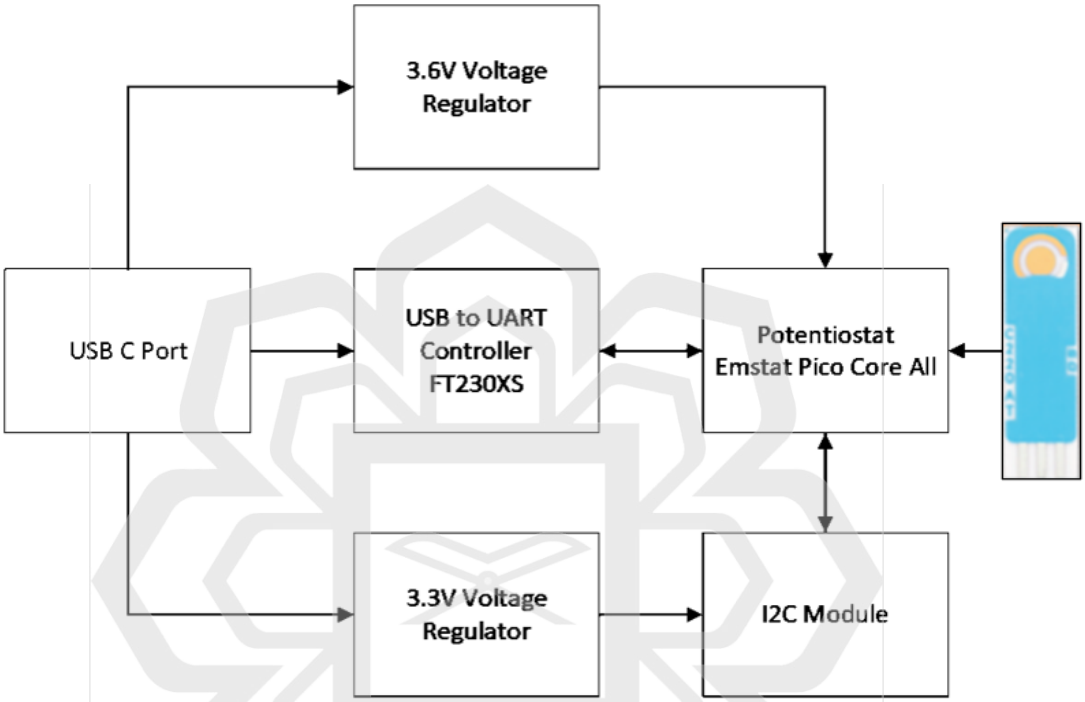


Figure 3.3 NACOTS Alpha revision block diagram

Table 3-2 NACOTS Alpha revision components and functions

| Components | Functions |
|---|---|
| **USB C Port** | Connects the computer and the NACOTS board to transfer data and power from the computer to the components. |
| **3.6V Voltage Regulator** | Lower 5V input from USB C port to 3.6V and voltage source for potentiostat |
| **3.3V Voltage Regulator** | Lower 5V input from USB C port to 3.3V and voltage source I2C module |
| **USB to UART controller FT230XS** | Translate the data from USB format to serial between the computer and potentiostat/microcontroller. This allows a device to send/receive information on one interface to the other. This IC also supports I2C module. |
| **I2C module 24LC32AT** | I2C (Inter-Integrated Circuit) module is a hardware component or integrated circuit that implements the I2C protocol. I2C is a serial communication protocol that allows multiple devices to communicate with each other using a two-wire interface. |
| **AB26TRB** | Crystal Oscillator for I2C module with frequency at 32.7KHz |
| **Potentiostat module (Emstat Pico Core All)** | Potentiostat module which enables the circuit to perform Differential Pulse Voltammetry using the electrochemical sensors. |

Figure 3.4 shows the USB C port connected with USB to UART controller FT230XS. USB to UART controller is used to translate the data from USB format to serial between the computer and potentiostat/microcontroller. FT230XS was chosen for its simplicity and the small size.

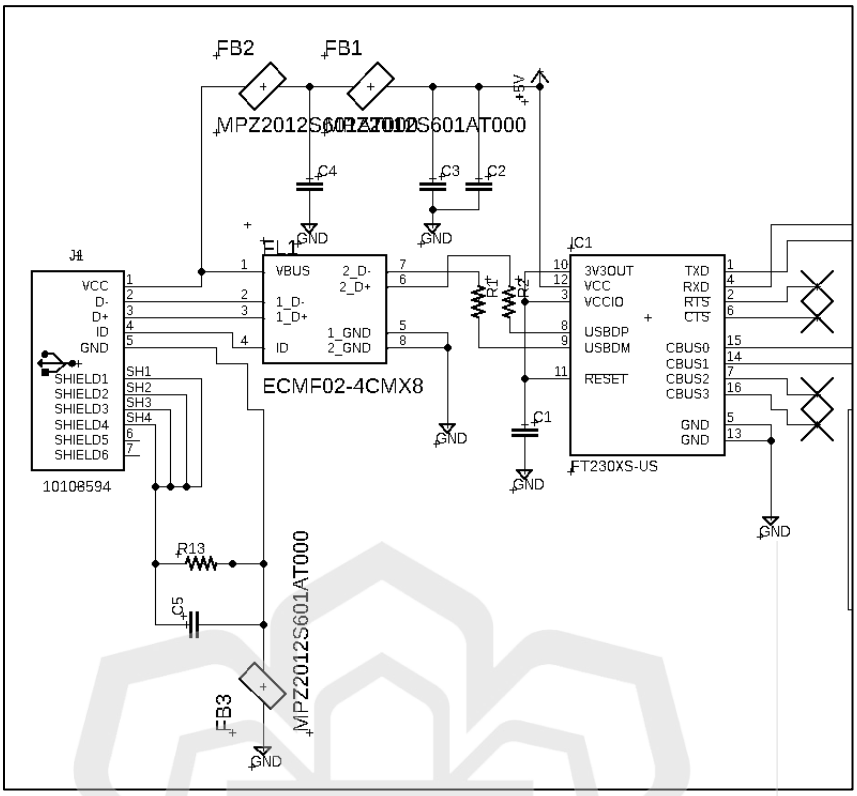


Figure 3.4 USB port and USB to UART controller for NACOTS Alpha

Figure 3.5 shows I2C modules for NACOTS Alpha. I2C, which stands for Inter-Integrated Circuit, is a widely used serial communication protocol that enables communication between electronic devices. The plan was to enable the board to communicate with another micro controller or add Bluetooth chip. However, this feature was removed for the upcoming iterations of the device to further simplify the circuitry.

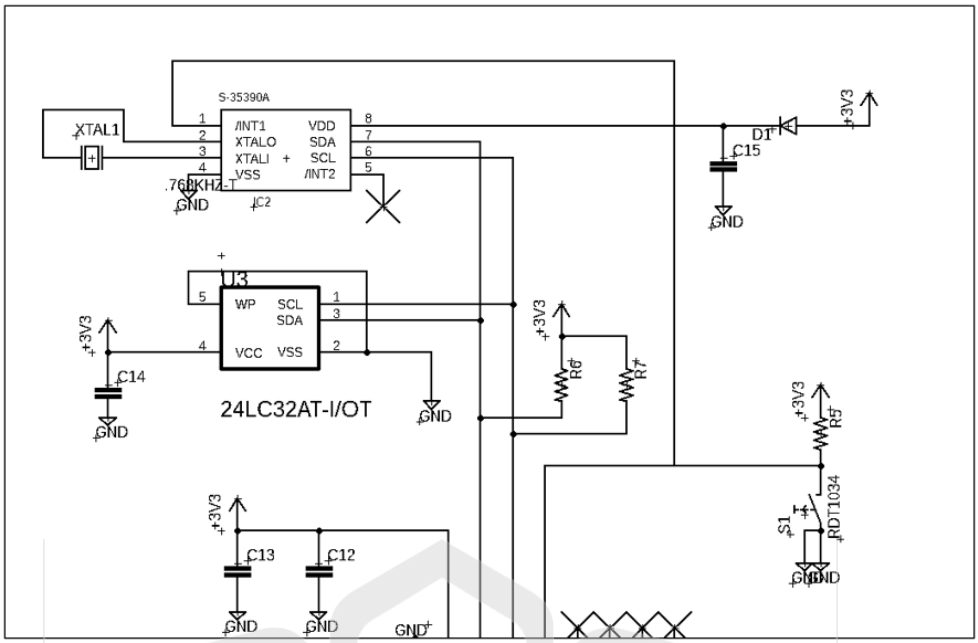


Figure 3.5 I2C modules for NACOTS Alpha

Figure 3.6 shows the voltage regulator for NACOTS Alpha. The function is to lower the 5V input from USB C port to 3.3V. LTC3536 has been chosen due to availability and the flexibility to tune the voltage based on the ratio of resistors. Figure 3.7 shows the potentiostat IC, Emstat Pico. This IC is responsible for the circuit to perform Differential Pulse Voltammetry using electrochemical sensors.

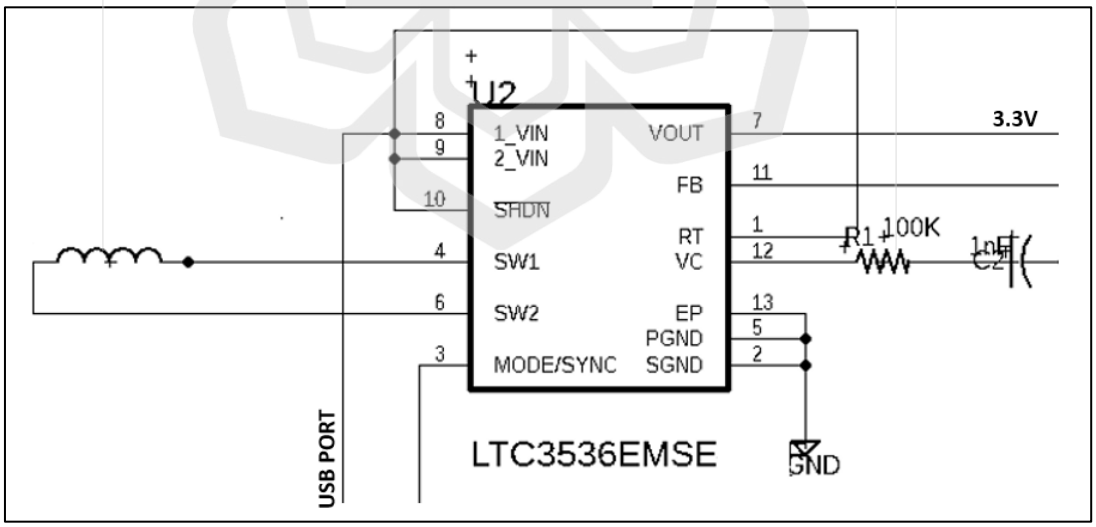


Figure 3.6 Voltage Regulator for NACOTS Alpha

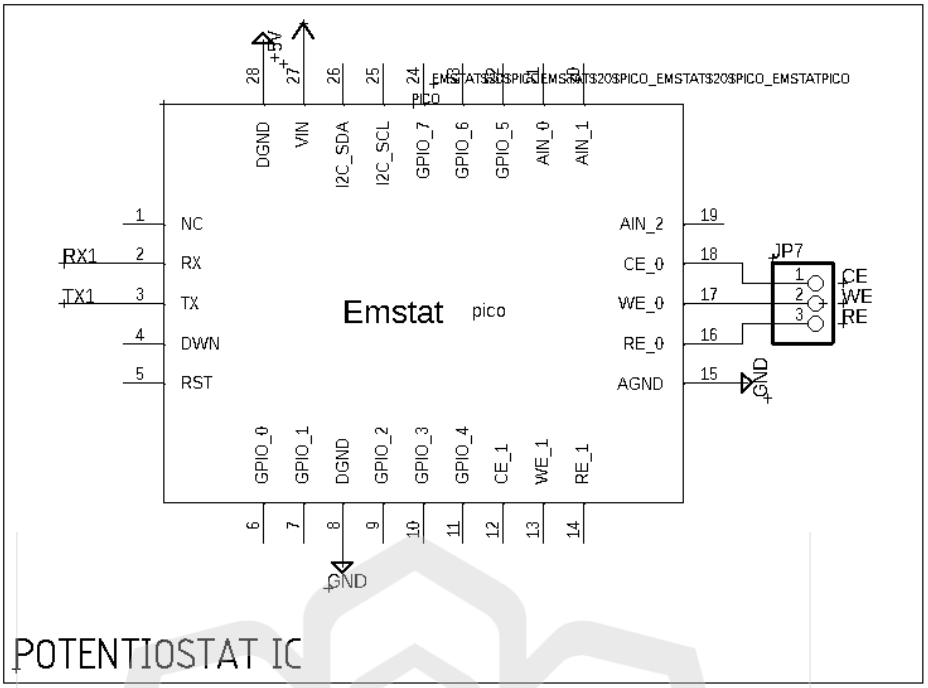


Figure 3.7 Potentiostat IC

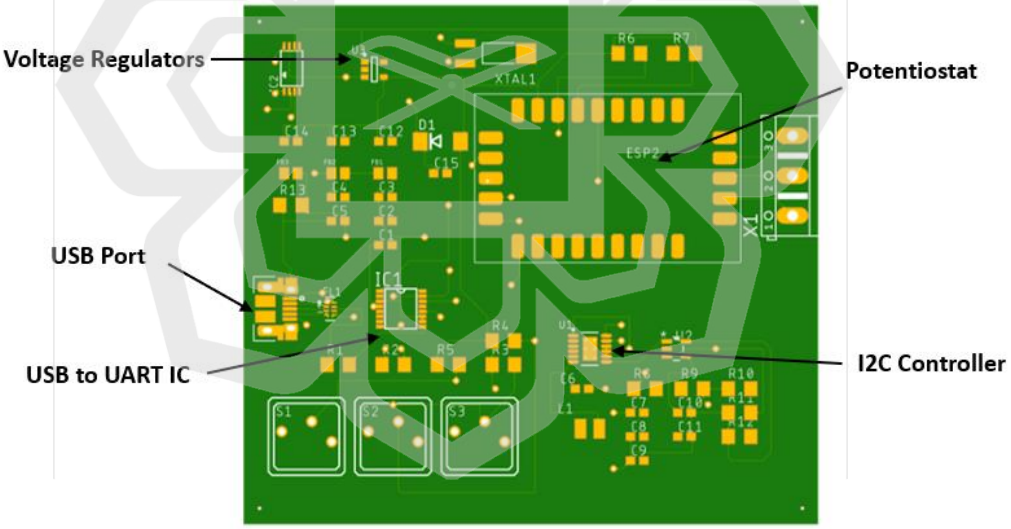


Figure 3.8 NACOTS Alpha Version

The first fabricated printed circuit board, NACOTS Alpha revision can be seen in Figure 3.10. However, the design came with a major flaw in which the grounds were not connected, which caused the board to fail to turn on.

### 3.2.2 NACOTS Beta revision

NACOTS Beta revision is developed with prior issues have been fixed Improved and more compact with the latest and robust version of USB to UART IC, FT234XD. Previous issue on the non-connected ground has been fixed. I2C module also removed to further simplify the design.

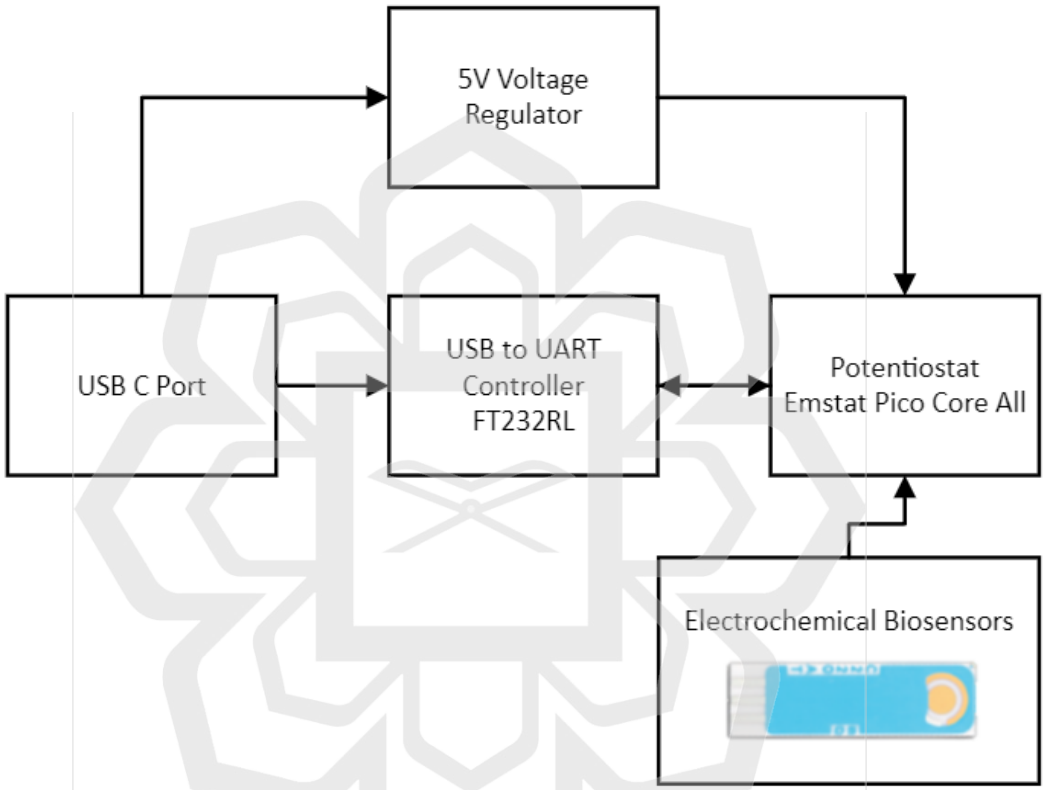


Figure 3.9 NACOTS Beta revision block diagram.

Figure 3.10 shows the NACOTS Beta revision block diagram. Compared to Alpha revision block diagram, the block diagram appears with less blocks which resulted in lesser components and lesser complexity.

Table 3-3 Differences between Alpha and Beta revision of NACOTS

| Features | NACOTS Alpha Revision | NACOTS Beta Revision |
|---|---|---|
| **USB port** | Micro USB | Micro USB |
| **USB to UART IC** | FT230XS | FT234XD |
| **Voltage Regulators** | 5V to 3.6V voltage regulators<br>3.3V voltage regulators | 5V to 3.6V voltage regulators<br>3.3V voltage regulators |
| **Potentiostat** | EmStat Pico Core All | EmStat Pico Core All |
| **I2C module** | 24LC32AT – I2C module for connection with other modules<br>AB26TRB – clock for I2C control | - |

Figure 3.10 shows the USB C port connected with USB to UART controller FT234XD. USB to UART controller is used to translate the data from USB format to serial between the computer and potentiostat/microcontroller. FT234XD was chosen for its simplicity and the small size. The chip had also been chosen due to the FT230XS chips are out of stock.

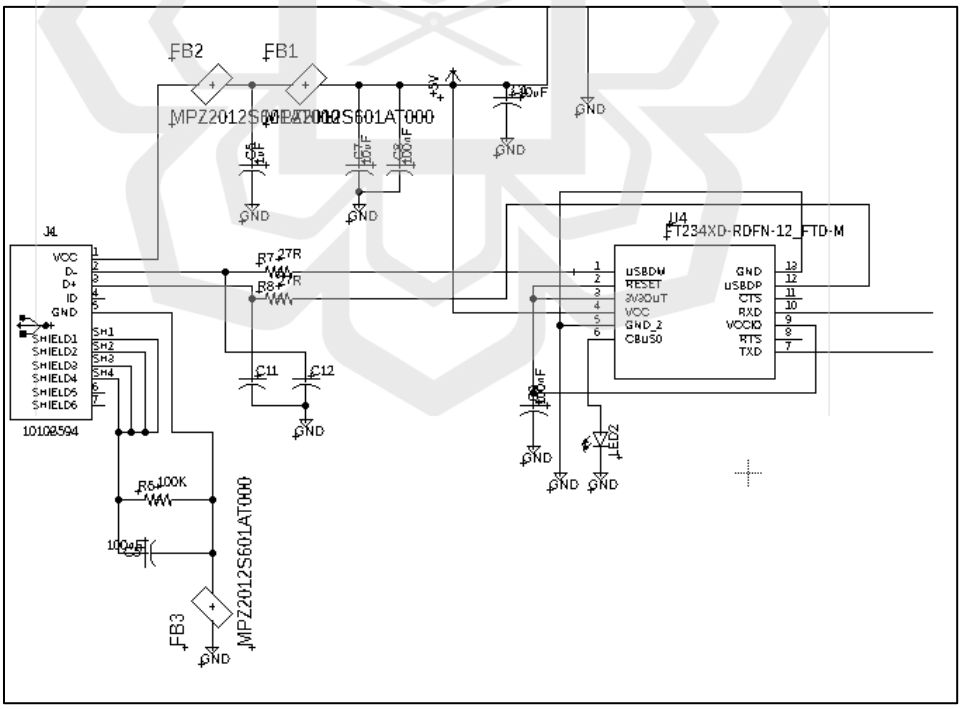


Figure 3.11 USB C port connected with USB to UART controller FT234XD.

Figure 3.11 shows the fabricated board of the NACOTS main board as well as the components are. The board is tested and evaluated through a series of experiments

which compared the board with other potentiostats which will be explained further in the Chapter 4.1.

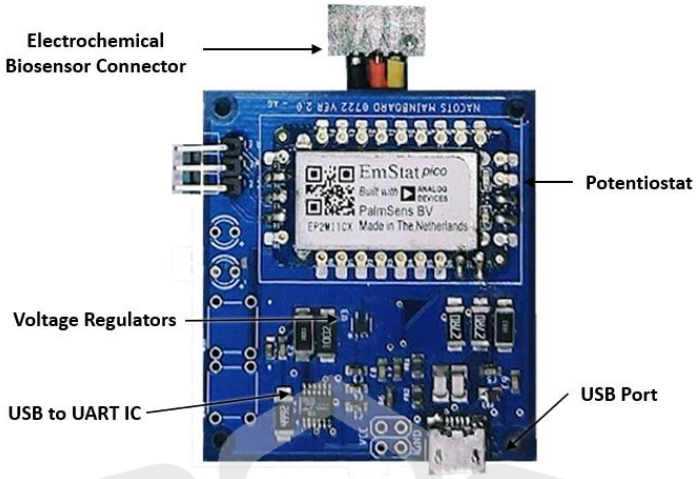


Figure 3.12 NACOTS Beta fabricated printed circuit board.

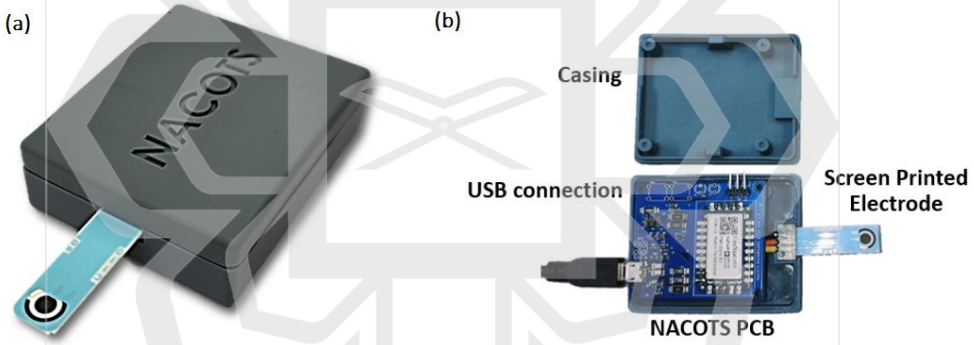


Figure 3.13 (a) NACOTS Beta in 3D printed case (b) Internal view of the device.

Figure 3.12 shown the NACOTS Beta in 3D printed case and in (b) shown the internal view of the device. The device is functional and only contain potentiostat capabilities. The benchmark has been done on this device, in which can be seen in Chapter 4.1.

### 3.2.3 NACOTS Final Revision

NACOTS final revision are being created with new features, which are 2.4-inch TFT display with touchscreen to control heating chamber to heat the COVID sample. Table 3.4 shown all the features that changed in the final revision.

Table 3-4 Differences between Beta and Final revision of NACOTS

| Features | NACOTS Beta Revision | NACOTS Final Revision |
|---|---|---|
| **USB port** | Micro USB | USB C |
| **USB to UART IC** | FT234XD | CH340C |
| **Voltage Regulators** | 5V to 3.6V voltage regulators<br>3.3V voltage regulators | 3.3V voltage regulators |
| **Potentiostat** | EmStat Pico Core All | EmStat Pico Core All |
| **Thermocouple IC** | - | MAX6675ISA+ |
| **Heating Element** | - | 2W 70°C heater |
| **Secondary Microcontroller** | - | ESP32 WROVER E |
| **TFT Display + Touchscreen** | - | ILI9341 |

Figure 3.13 shown the block diagram of the final revision board. The board have more features including heater as well as display and touchscreen module which makes the block diagram larger compared to block diagram for beta revision in Figure 3.9.

To enable these capabilities, a suitable potentiostat chip (Emstat Pico Core All) was chosen to perform these different measurement techniques. The potentiostat should also be able to interact with the heating system, and only perform measurements when the sample is ready. A data selector is connected to the heater's microcontroller system to enable this. When Datapath 'A' is selected, the heating microcontroller is on, and the closed-loop heating system is enabled. Vice versa when data path 'B' is chosen, the results from the potentiostat are transferred to the computer via USB. The overall block diagram of the NACOTS readout and heater circuit is shown in Figure 3.13 below.

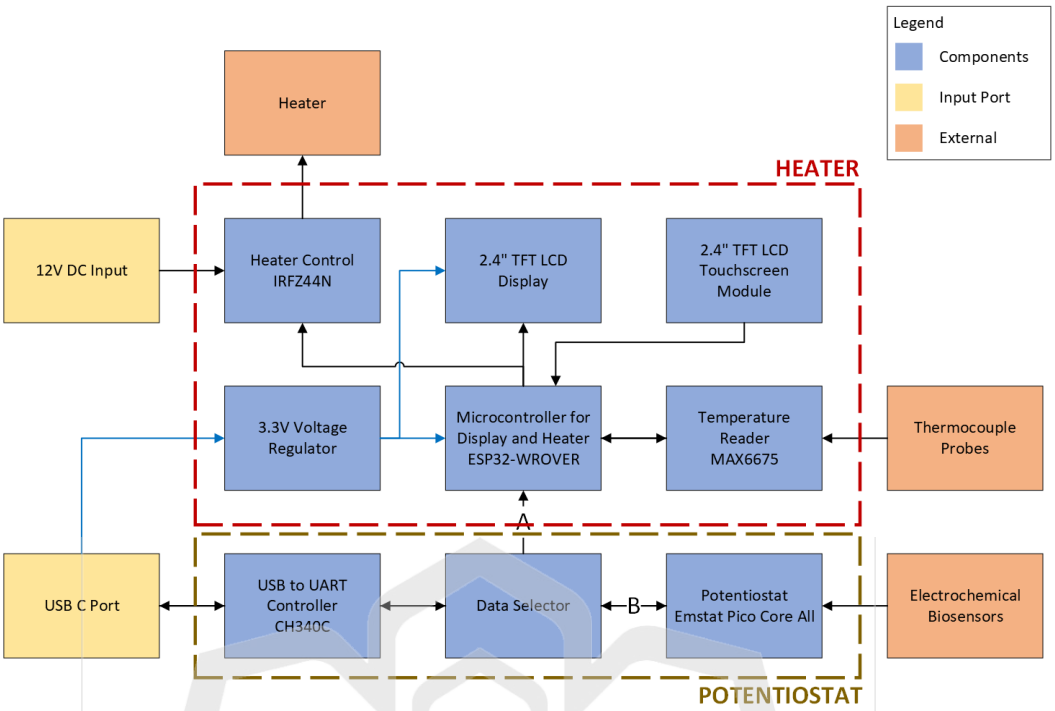


Figure 3.14 NACOTS final revision block diagram

The blocks shown in Figure 3.13 are categorized as follows: Yellow blocks represent input ports, which are a USB C port and a 12V DC input port (PJ-202A). Blue blocks represent the main components on the board while the orange blocks are external inputs and devices (electrochemical sensor, thermocouple probes, and heater). The list in Table 3.4 shows the blocks and a summary of their functionalities starting from top left to right.

To understand how the data flows between each block, the detailed data flow of the system is illustrated in the diagram shown in Figure 3.14 below.

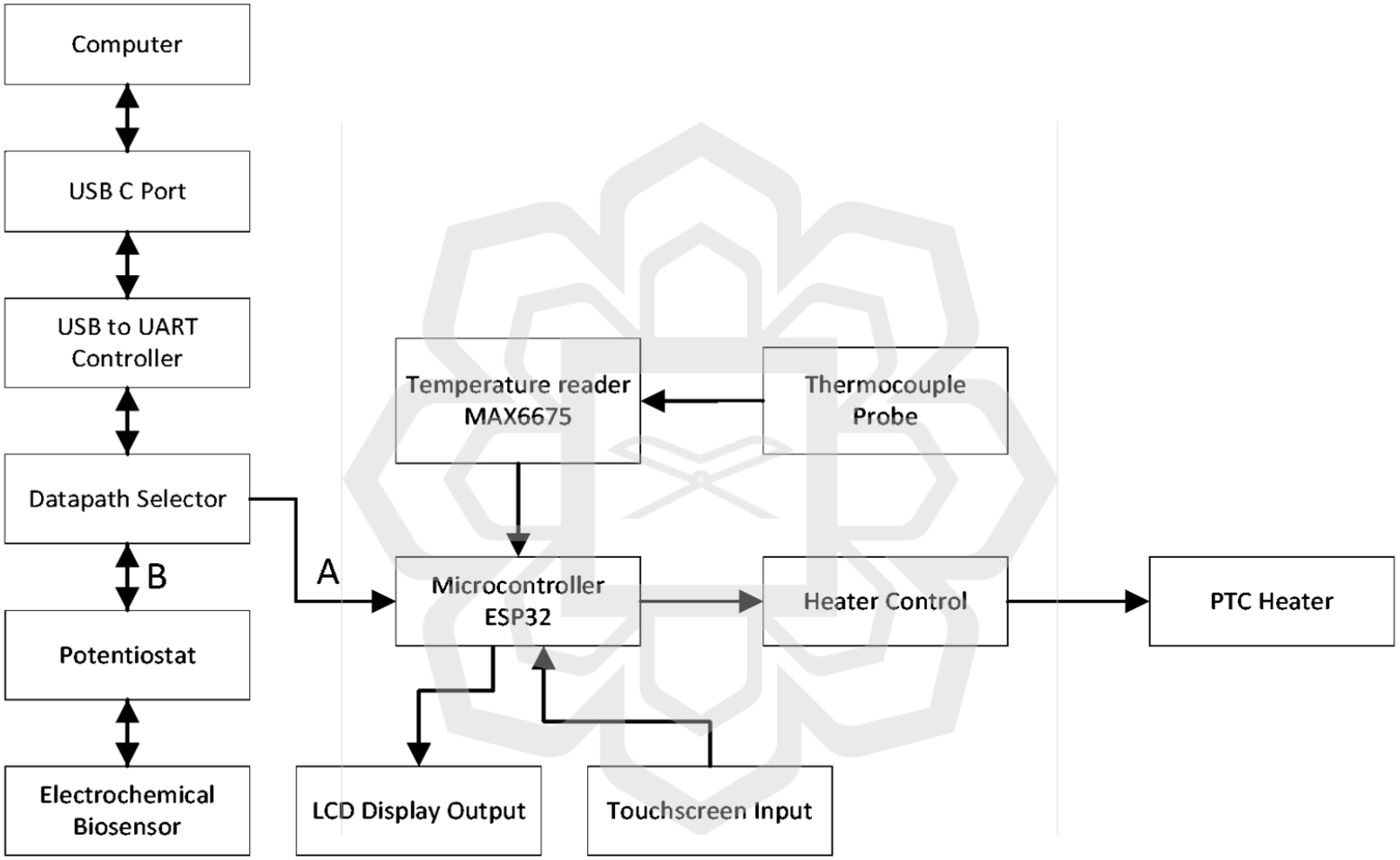


Figure 3.15 The data flow diagram of the NACOTS readout and heater circuit.

The data path of the NACOTS circuit was established when the USB C port was connected to the computer. The device has 4 main pins in USB C connected to the fabricated board which are 5V, GND, D+, and D-. For ESP32 and the potentiostat module to communicate to PC, the data must be in serial format, which requires conversion of USB data (D+, D-) format to serial (TX, RX) format, or vice versa. To perform the data conversion, a USB to UART controller was needed.

NACOTS circuit has two branches of data paths, which were controlled manually through the physical switches to change the TX (transmitter) and RX (receiver) to path A or B. The purpose of the branching of paths A and B was to make it easier for developers to access the microcontroller to reprogram the microcontroller and change the mode back to potentiostat mode for users to operate.

Path A is selected when programming the ESP32 microcontroller, as shown in Figure 3.14, the arrow is only pointing toward ESP32. The PC doesn't have to receive feedback from the microcontroller. On path A (blue), the microcontroller was playing the main role of controlling multiple functions such as reading the temperature, controlling the heater, displaying the output through LCD, and detecting the touchscreen input. Since ESP32 can function stand-alone without being connected to the PC after being programmed, the data path connection was only useful for developers.

Data path B was the path that will be set when the measurement results from the potentiostat were released. This mode enabled the data connection between the potentiostat module and PC to be established. The PC sends specific instructions to the potentiostat module such as voltage levels and scan rates. The potentiostat module had a microcontroller that controlled the input voltage to the electrochemical biosensor based on these settings and measured the output current from the sensor. The potentiostat (EmStat) module also contains an Analog to Digital converter that processes the measured current (I) data. This digital measurement data was sent to PC to be processed by the software.

Table 3-5 NACOTS readout and heater circuit blocks and their functions

| Block | Functions |
|---|---|
| **12V DC Input** | 12V external input to power up the heater. |
| **Heater Control** | nMOS switch mechanism for the heater controlled by the microcontroller. |
| **2.4" TFT LCD Display** | Display the heater's temperature and timer |
| **2.4" TFT LCD Touchscreen Module** | Detecting feedback when a user touches the screen |
| **3.3V Voltage Regulator** | Lower 5V input from USB C port to 3.3V and voltage source for Microcontroller and 2.4" TFT display units. |
| **Microcontroller for display and heater** | Controls the display, heater, and temperature sensor. |
| **Temperature reader (MAX6675)** | Convert analog data read from the temperature probe to a digital value. MAX6675 is a sophisticated thermocouple-to-digital converter with a built-in 12-bit analog-to-digital converter (ADC). |
| **USB C Port** | Connects the computer and the NACOTS readout and heater board to transfer data and power from the computer to the components. |
| **USB to UART controller** | Translate the data from USB format to serial between the computer and potentiostat/microcontroller. This allows a device to send/receive information on one interface to the other. |
| **Data selector** | Manual selector to reroute the data path to either microcontroller or potentiostat. A is the programming mode that will connect the data path to the microcontroller. B is the potentiostat mode which will connect the data path from computer directly to the potentiostat module (Emstat Pico Core All) |
| **Potentiostat module (Emstat Pico Core All)** | Potentiostat module which enables the circuit to perform Differential Pulse Voltammetry using the electrochemical sensors. |

Figure 3.15 shows the routing details (top and bottom) for the designed printed circuit board. The generic width of the routing is 0.254mm except for 12V power rails, in which the width of the routing is 1.027mm to accommodate the larger voltage and current input for the heater.

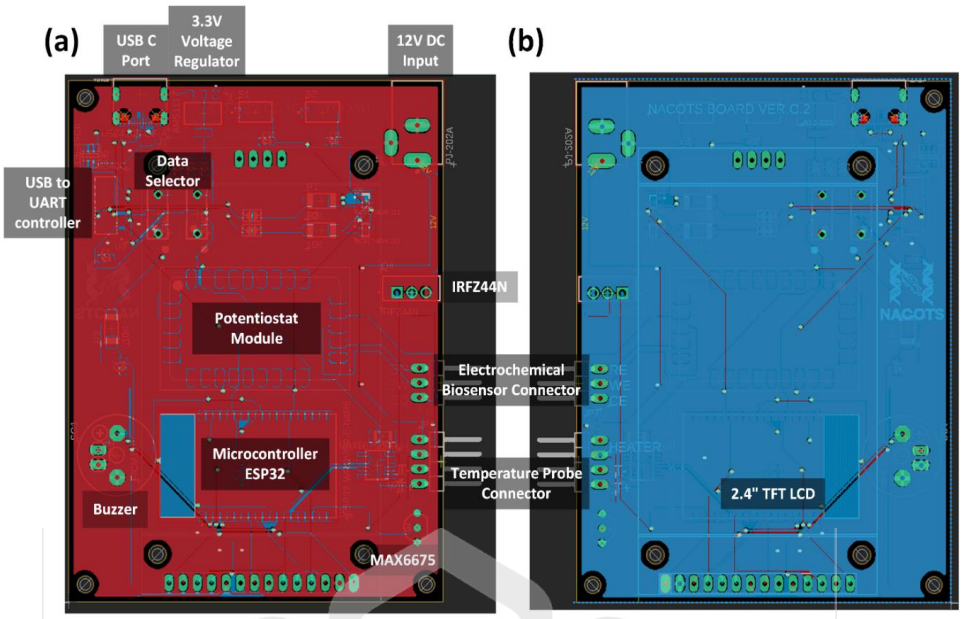


Figure 3.16 NACOTS PCB design (a) Bottom part of the board (b) Top part of the board

Assembled NACOTS potentiostat readout and heater circuit with components can be seen in Figure 3.16. The size of the board is 76.4 x 91.3 mm and has an input slot for a 2.4-inch LCD at the top of the board. The overall device can be seen in enclosed case printed from 3D printer in Figure 3.20.

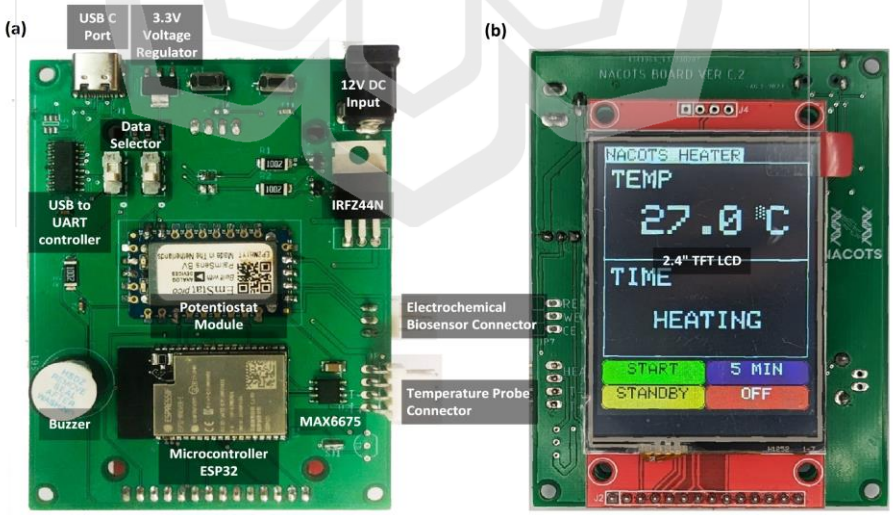


Figure 3.17 NACOTS potentiostat readout and heater circuit with components (a) Bottom view (b) Top view

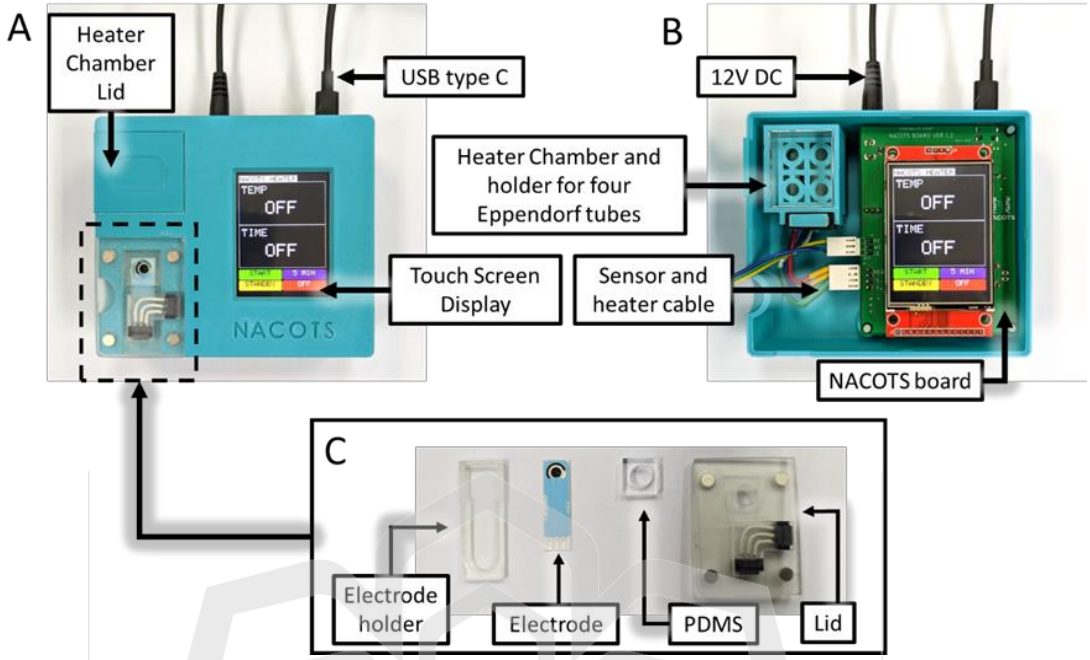


Figure 3.18 (a) Outside view of NACOTS device, (b) Inside view of NACOTS device, and (c) Part of sensor packaging.

Figure 3.21 shows the USB C port, voltage regulator and 12V DC input. Voltage regulator, AMS1117 is used to replace LTC3536 due to the availability of the component and simplicity. AMS1117 is a voltage regulator to lower down input voltage to 3.3V. 12V 1A DC input voltage is used to power up the PTC heater. PTC heater consumes more voltage than other components to the board. To ensure that the device is able to function even with no power adapter, two distinct power rails are added to the device. One exclusively for the heater, another, 5V from USB for the other components on the device.

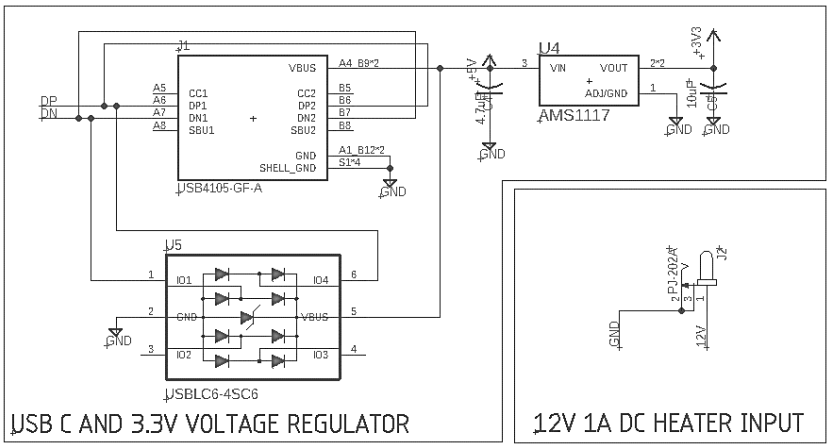


Figure 3.19 USB C port, Voltage Regulator and 12V DC Input

ESP32 WROVER is chosen as microcontroller since the chip has more input output (IO) pins compared to other controllers while also having Bluetooth and Wi-Fi capabilities. These huge number of pins are important due to the number of pins required by the touchscreen displays are 13 pins, and other components also required a lot of pins. ESP32 connections can be seen in Figure 3.22.

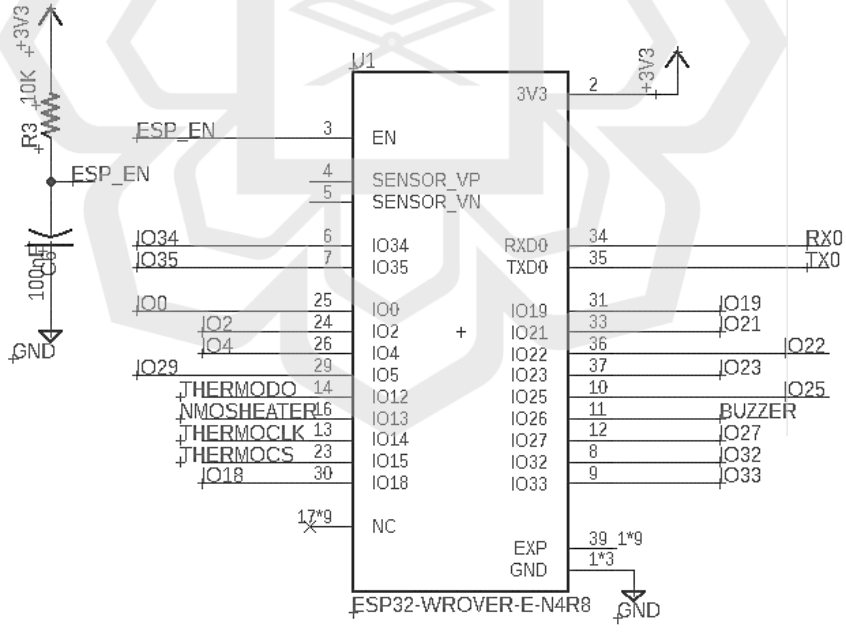


Figure 3.20 Microcontroller to control display and heater.

Figure 3.23 shows the TFT display and touchscreen module. ILI9341 display module was chosen due to the high sensitivity of the touchscreen module as well as it

comes with a 2.4-inch screen. The display is being controlled by the ESP32. ILI9341 was chosen due to the price and availability in the market.

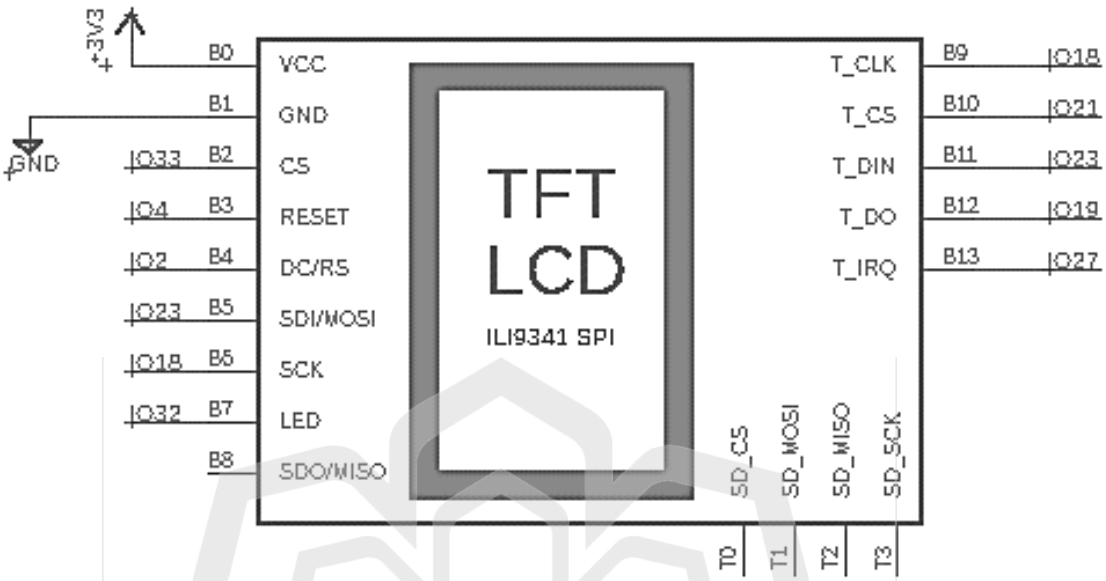


Figure 3.21 TFT display and touchscreen module.

Figure 3.24 shows the heater module and temperature sensor of NACOTS. The heater module is controlled by nMOS mosfet. This mosfet, IRFZ44N functions as a switch for the PTC heater. It also separates the 12V DC input from the 5V input from the USB. The nMOS gate is controlled by the ESP32. MAX6675ISA+ is the temperature reader and can convert analog data read from the temperature probe to a digital value. MAX6675 is a sophisticated thermocouple-to-digital converter with a built-in 12-bit analog-to-digital converter (ADC). The IC is chosen due to the precision of the device and its huge availability in the market.

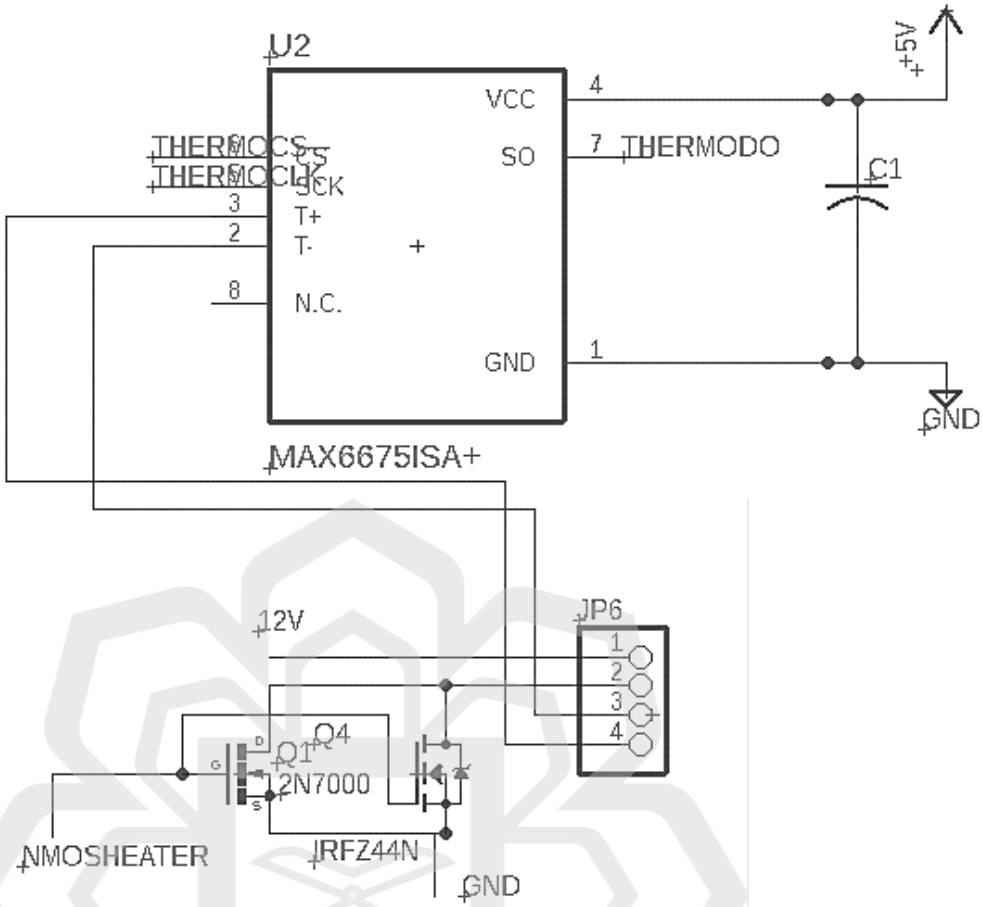


Figure 3.22 Heater module and Temperature sensor.

### 3.3 Summary

Chapter 3 elaborates on the design and development of NACOTS potentiostat. The chapter went through the NACOTS device fabrication flow. After the flow has been established, the design specifications are also explored. Overall board development had also been shown. The improvement from Alpha to Beta and towards Final revision also shown. Table 3.6 shows the technical specification of the NACOTS device.

Table 3-6 NACOTS device technical specification

| TYPE | DESCRIPTION |
|---|---|
| Outputs and Type | 3 - CE, WE, RE |
| Voltage - Output (DAC) | 0.2 to 2.4 V |
| Voltage potential to the sensor | ±2.2 V |
| Current - Output | ±3 mA |
| Current min resolution | 5.5 pA |
| Output Voltage Frequency | 0.016 Hz to 200 kHz |
| Impedance measurement capability | <10Ω to 100MΩ |
| Voltage - Input | 3V ~ 5.5V |
| Current - Input | 1A |
| Heating Element | 2W |
| Utilized IC | AMS1117 3.3V<br>EMSTATPICOALL<br>CH340C<br>MAX6675ISA+<br>ILI9341 |
| Base Product Number | NACOTS BOARD |

# CHAPTER 4

# RESULTS AND DISCUSSION

## 4.1 Overview

To ensure the NACOTS prototypes are working as intended and accurate, several tests have been conducted. Figure 4.1 shows the overall test flow for NACOTS prototypes. The tests can be divided into benchmarking test and reliability test. Benchmarking tests involve a series of electrochemical tests while comparing NACOTS device with commercialized potentiostats. The reliability test involves testing on multiple NACOTS products to check the consistency of the results.

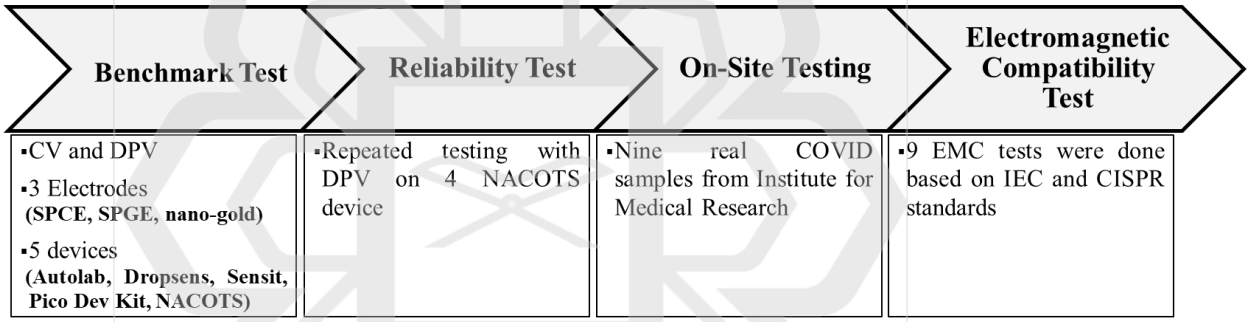


Figure 4.1 Overall Test Flow for NACOTS prototypes.

## 4.2 Benchmark Test

### 4.2.1 Electrochemical Test

The comparison of NACOTS against PGSTAT302N Autolab and µStat-i 400 DropSens has been done to evaluate the reliability and stability of the Pico chip. To have an accurate representation of these three devices in the electrochemical experiments, a few constants need to be established. Experiment constants that are being set are as follows,

- Experiment time. The experiments are conducted on the same date to maintain the constant of the solution as different times of testing might result in some degradation of ferrocyanide solution.
- The solution used for this experiment is 10mmol of Ferrocyanide.
- Electrodes used to evaluate the experiments are SPCE, SPGE and nanogold electrodes.
    - SPCE – Screen printed carbon electrode, C110 electrodes developed by MetroOhm
    - SPGE – Screen printed gold electrode, C220AT developed by MetroOhm
    - Nanogold electrodes - three-dimensional structure of nanoporous gold (NPG) was made by selectively corroding copper (Cu) from gold-copper (Au-Cu) alloys using a two-step electrochemical method developed by EMaS research team (Asyiqin Azman, Mohd, Mohd Zain, & Ying Chin, 2023)

By establishing these constants, only then the variables can be isolated properly, which the variables in this testing are the devices themselves.

The electrochemical experiments are being done by connecting the electrodes to the tested devices, and then, 100 µl of 10mmol Ferrocyanide are dropped on the electrodes before CV and EIS readings are being done. Figure 4.2 shows how the experiments are being done.

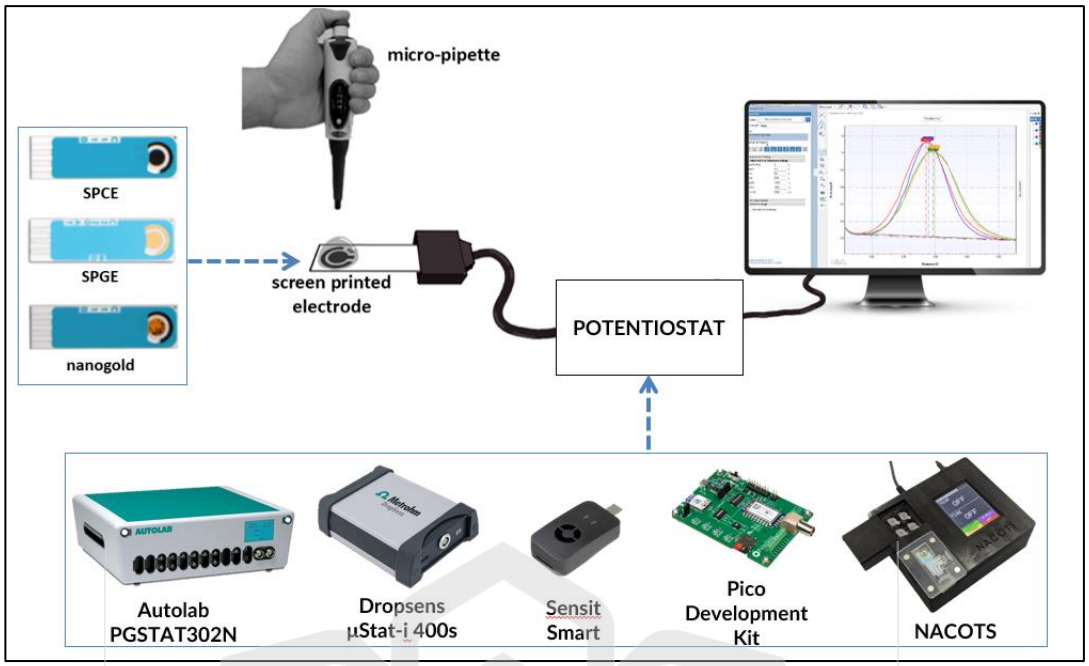


Figure 4.2 Electrochemical experiment setup for the potentiostat

In this dissertation, four different potentiostats were used namely PGSTAT302N Autolab, µStat-i 400 DropSens, Sensit Smart and Pico Development Kit which can be seen in Figure 4.2 are used as a benchmark for the developed system called NACOTS (Nano system for COVID19 DNA/Antibodies on the Spot Test).

Dropsens and developed potentiostat (NACOTS), were used as representatives of portable potentiostats in the experiment. Autolab was used as the main benchmark as it is a commercialized lab-grade potentiostat with demonstrated high accuracies.

Autolab is a potentiostat that has various measurement techniques and features which encompasses voltammetry, polarography spectroscopy, photovoltaic applications as well as temperature control. Autolab is not a portable potentiostat which can be seen from the large dimension of the device which is 52 cm x 160 cm x 420 cm. Due to its precision and reliability, the tool is used as the benchmark for the developed NACOTS.

µStat-i 400 is a portable potentiostat that have various measurement techniques and features which is as diverse Autolab. With smaller dimensions of 13.2 cm x 10.0 cm x

3.6 cm, compared to Autolab and high precision, this tool was also picked as the benchmark against NACOTS.

As mentioned previously, electrochemical techniques that will be used throughout NACOTS development are CV, DPV and EIS, thus the evaluation will only focus on these techniques.

Evaluation techniques that are going to be used are through experimental, in which the circuit design will be experimented, and the data would be collected and analyzed, in which will be compared with the commercialized portable potentiostat and Autolab, which is the high-end commercialized potentiostat.

Performance metrics that will be evaluated are cyclic voltammetry results, electrochemical impedance spectroscopy measurement results and differential pulse voltammetry test on DNA samples.

#### 4.2.1.1 Cyclic Voltammetry

Cyclic voltammetry test parameters are set in the software as shown in Table 4.1. Potential was swept from -0.2V until 0.6V. This is standard parameters to test ferrocyanide oxidation and reduction. Scan rate was set to 0.1V/s, and this value was set after going through multiple tests.

Table 4-1 Cyclic Voltammetry Test Parameters

| **Parameters** | **Settings** |
|---|---|
| T equilibration | 0 s |
| E begin | -0.2V |
| E vertex1 | 0.6V |
| E vertex2 | -0.2 V |
| E step | 0.002 V |
| Scan rate | 0.1 V/s |
| Number of scans | 3 |

#### 4.2.1.2 Electrochemical Impedance Spectroscopy

Electrochemical impedance spectroscopy test parameters are set in the software as shown in Table 4.2. The minimum frequency is set to 1Hz instead of going to an even lower frequency, due to the test time. By setting the minimum frequency to 1Hz, the test time is reduced from 30 minutes to 15 minutes. Number of frequencies also set to 10 per decade of logarithmic frequency to reduce the test time.

Table 4-2 Electrochemical Impedance Spectroscopy Test Parameters

| Parameters | Settings |
|---|---|
| T equilibration | 3 s |
| Scan type | Fixed |
| E dc | 0 V |
| E ac | 0.01 V |
| Frequency Type | Scan |
| n frequencies | 51 = 10/decade |
| Frequency Range | 1Hz - 100 kHz |

#### 4.2.1.3 Differential Pulse Voltammetry

Differential pulse voltammetry test parameters are set in the software as shown in Table 4.3. Potential was swept from -0.2V until 0.6V with the potential increased for 0.004V every 0.1s. Initial of every potential step, a 0.002V potential is pulsed. Scan rate was set to 0.1V/s, and this value was set after going through multiple tests and optimized for COVID-19 detection tests.

Table 4-3 Differential Pulse Voltammetry Test Parameters

| Parameters | Settings |
|---|---|
| T equilibration | 0 s |
| E begin | -0.2V |
| E end | 0.6V |
| E step | 0.004 V |
| E pulse | 0.002 V |
| T pulse | 0.05 s |
| Scan rate | 0.025 V/s |

### 4.2.2 NACOTS Beta Revision Testing Results

Figure 4.3 shows the test flow that were done for NACOTS Beta revision. Cyclic voltammetry, impedance spectroscopy and differential pulse voltammetry tests were done with comparing NACOTS beta revision with Autolab and DropSens.

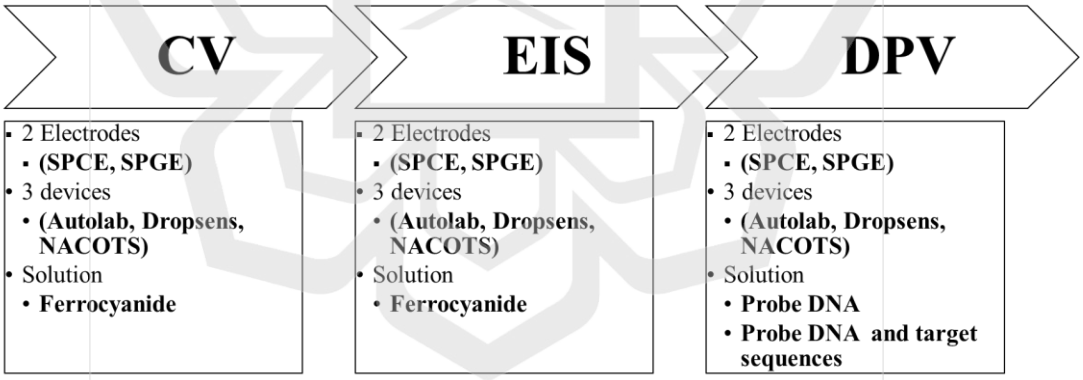


Figure 4.3 NACOTS Beta Revision Test Flow

Table 4.4 shows the comparison of resolution and ranges of NACOTS Beta against commercialized potentiostats. Autolab has the best resolutions for potentials, currents, as well as DAC and ADC. NACOTS Beta potential DC resolution is very similar to Dropsens which is around 1mV. Resolution and ranges of NACOTS are better overall compared to Dropsens. Only current ranges for NACOTS Beta are in the last place compared to the other two potentiostats.

ADC resolution is especially important as this impacts the output resolution for impedance spectroscopy and the current resolution for voltammetry.

Table 4-4 Resolution and ranges of NACOTS and Commercialized Potentiostats

| Parameters | NACOTS Beta | Autolab | µStat-i 400 Dropsens |
|---|---|---|---|
| **Potential DC resolution** | 932 µV | 0.3 µV | 1 mV |
| **Measured Current resolution** | 0.006% of current range | 0.0003% of current range | 0.025 % of current range |
| **Current ranges** | 100 nA to 5 mA | 10 nA to 1 A | 1 nA to 10 mA |
| **DAC resolution** | 12 bits | 16 bits | - |
| **ADC resolution** | 16 bits | 16 bits | 10 bits |

#### 4.2.2.1 Cyclic Voltammetry Measurement Result

For CV experiments, the input potential was swept from -0.2V to 0.6V with 2mV increments, at a scan rate of 0.1V/s. These parameters were set to be the same for all three potentiostats. Table 4.5 shows the result summary for the CV test.

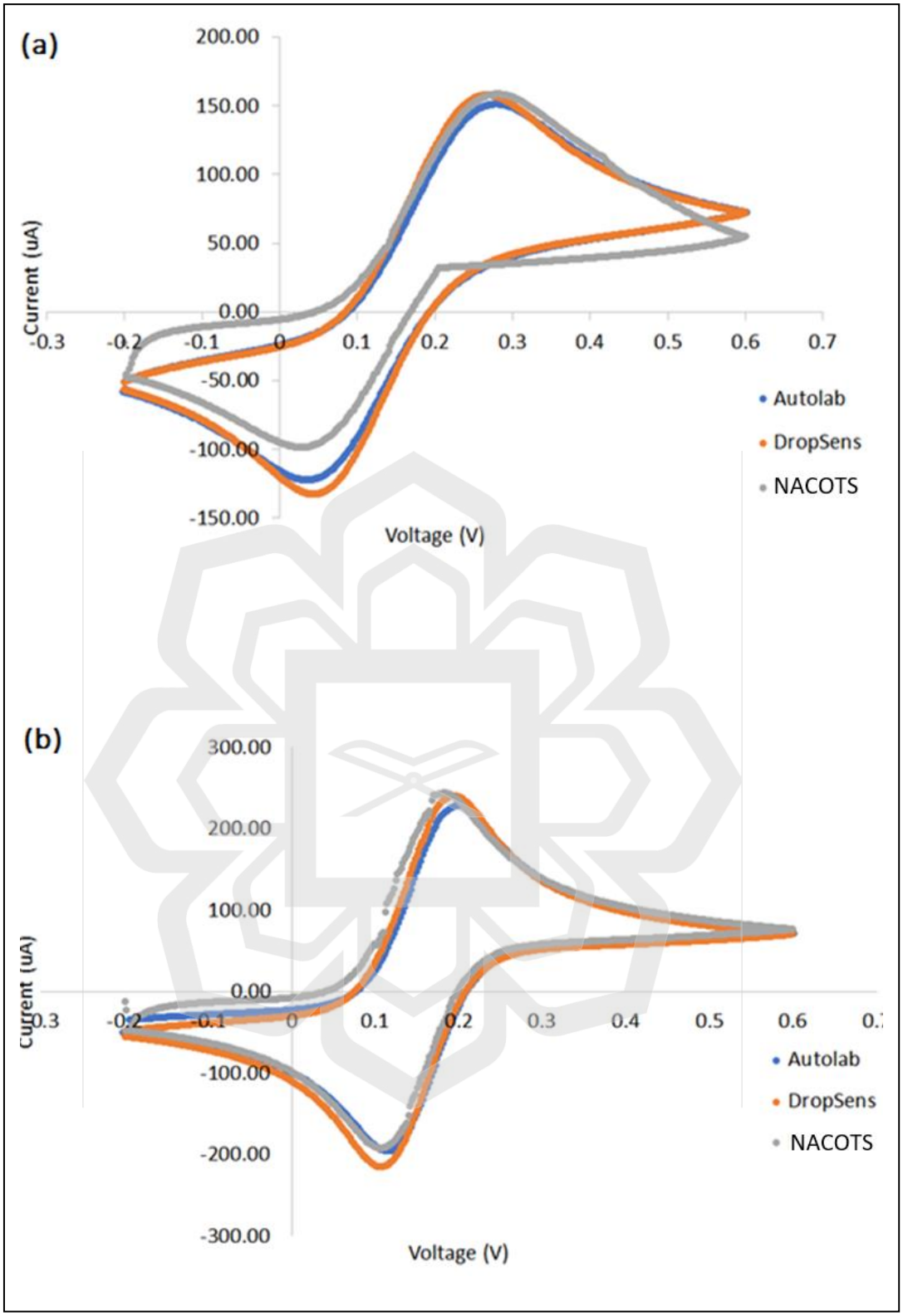


Figure 4.4 Cyclic Voltammetry test comparison on (a) SPCE and (b) SPGE.

Table 4-5 CV Test results summary

| Electrodes | SPCE | | | SPGE | | |
|---|---|---|---|---|---|---|
| **Devices** | **Autolab** | **Dropsens** | **NACOTS** | **Autolab** | **Dropsens** | **NACOTS** |
| **Oxidation Peak (µA)** | 152.5 | 158.05 | 158.6 | 228.89 | 240.1 | 243.7 |
| **Reduction peak (µA)** | -122.2 | -132.6 | -98.3 | -195.0 | -214.4 | -191.8 |
| **Peak Potential Gap (V)** | 0.244 | 0.224 | 0.249 | 0.085 | 0. 088 | 0.074 |

As can be seen from Table 4.5, for SPCE, both the oxidation peaks of the portable potentiostats, DropSens, and Pico development kit are close to each other. This indicates that both portable potentiostats have similar accuracies. The oxidation peak for the lab-grade potentiostat is slightly lower. In terms of the reduction peaks, there are differences in the peak results with the Pico development kit producing the lowest peak of -98.3 µA compared to -122 µA and -132.6 µA for Autolab and Dropsens respectively. Another important parameter for CV is the peak potential gap, which is defined as the difference in voltages between the oxidation and reduction peaks. Ideally, we want the peak potential gap to be small as it shows that the redox system can maintain equilibrium throughout the potential scan. All three potentiostats produced slightly different peak potential gaps, with the largest gap from the Pico development kit at 0.249V.

For SPGE, oxidation peaks are almost similar for both DropSens and Pico development kit at 240.1µA and 243.7 µA with only 3.6µA, while Autolab has the lowest oxidation peak at 228.89µA. Reduction peaks have large differences between Dropsens and the other two potentiostats. Dropsens has the highest oxidation peak at -214.4µA compared to Autolab and Pico development kit which are at -195.0µA and -191.8µA respectively. All three potentiostats produced slightly different peak potential gaps, with the smallest gap from the Pico development kit at 0.074V. The visualization of the data from Table 4.5 can be seen in Figure 4.4 which shows the graph for the three devices, tested on SPCE and SPGE. The CV result for the Pico development kit can be seen with slight differences in Figure 4.4 (a). However, in Figure 4.4 (b), the CV graph for SPGE is almost similar to other potentiostats.

SPGE CV measurements are shown in Figure 4.4(b), all three devices have almost similar results. The differences are lesser in SPGE due to the high conductivity of the gold electrodes compared to the carbon in SPCE. This effect of conductivity can also be seen in the value of the oxidation and reduction peaks. As seen in Table 4.5, SPGE has more than 50μA current for both peaks as compared to the reading from SPCE.

#### 4.2.2.2 Electrochemical Impedance Spectroscopy Measurement Results

For EIS measurements, a 10mV sinusoidal signal was set as the input with frequencies ranging from 1Hz to 100 kHz using all three potentiostats. Ten readings were recorded per decade. Open circuit potential (OCP) testing for the 60s was done prior to EIS measurements to ensure the stability of the results. EIS measurements using SPCE and SPGE are shown in Figure 4.5.

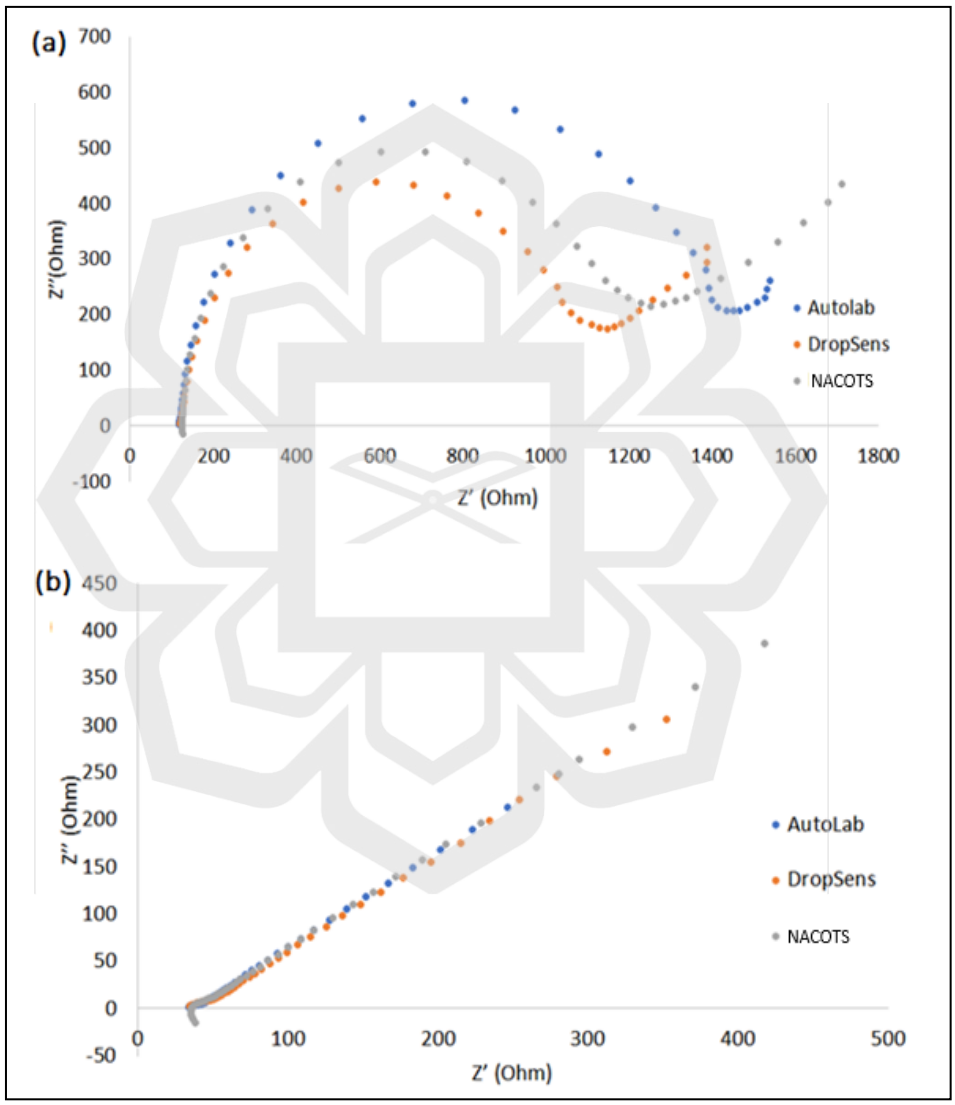


Figure 4.5 Impedance Spectroscopy measurements using Autolab, DropSens, and NACOTS on (a) SPCE and (b) SPGE.

Table 4-6 SPCE EIS Test results summary

| **Electrodes** | **SPCE** | | |
|---|---|---|---|
| **Devices** | **Autolab** | **Dropsens** | **NACOTS** |
| **Solution resistance, $R_s$ (kΩ)** | 0.121 | 0.122 | 0.124 |
| **Charge transfer resistance, $R_{ct}$ (kΩ)** | 1.5 | 0.9 | 1.03 |
| **Double layer capacitance, $C_d$ (µF)** | 1.0 | 1.0 | 1.0 |

Table 4.6 shows the SPCE EIS test result of Figure 4.5(a) after circuit fitting had been done on the Nyquist plot. All three potentiostats have shown similar double layer capacitance, Cd at 1.0µF while the solution resistance, *Rs* is nearly similar at around 121Ω to 124Ω. However, the charge transfer resistance for all potentiostats is different, in which Autolab has shown a higher charge transfer resistance of 1.5kΩ followed by the NACOTS with 1.5kΩ and Dropsens with 0.9kΩ.

The results of SPGE showed nearly similar results for all three potentiostats which can be seen in Figure 4.5(b). All three potentiostats present almost straight lines which demonstrate Warburg impedance. This happened due to the high electron-transfer rate between gold electrodes and ferrocyanide solution.

#### 4.2.2.3 Differential Pulse Voltammetry Test

To illustrate the difference in potentiostat measurements when the SPGE is used as a biosensor, the DPV technique was performed using DNA target sequences. Two experiments were conducted using all three potentiostats.

The first test used only probe DNA and ferrocyanide solution on the SPGE electrode, while the second test involved both the probe DNA and the target sequences in the ferrocyanide solution. DNA probes are single-stranded DNA that is being used to detect complementary nucleic acid sequences, also known as target sequences (Wages, 2005).

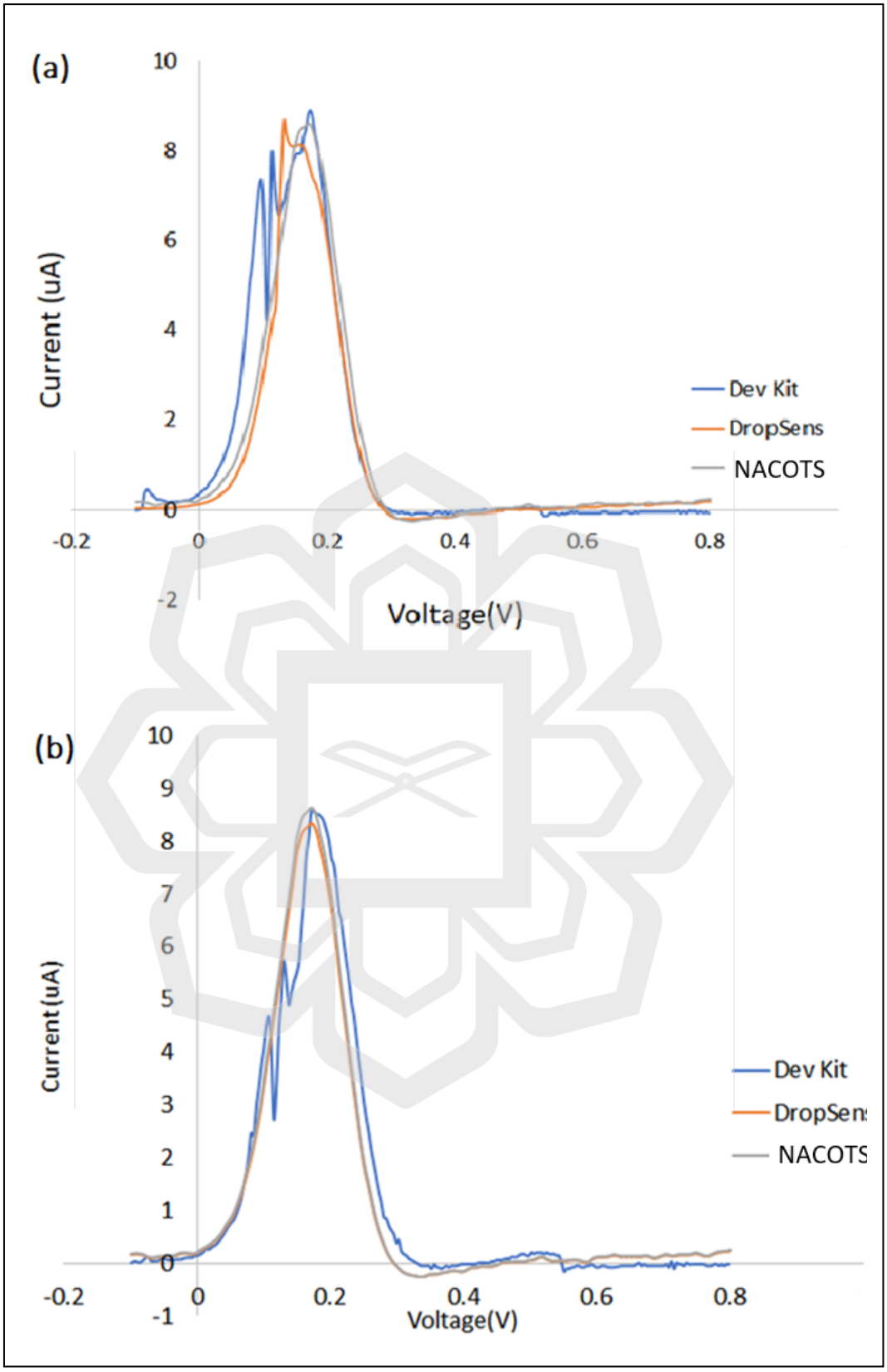


Figure 4.6 Differential pulse voltammetry test comparison with (a) probe DNA deposited on the electrode surface (b) probe DNA and target sequences deposited on the electrode surface.

Table 4-7 DPV Test results summary

| Sample | Probe DNA | | | Probe DNA + Target Sequences | | |
|---|---|---|---|---|---|---|
| **Devices** | **Autolab** | **Dropsens** | **NACOTS** | **Autolab** | **Dropsens** | **NACOTS** |
| **Oxidation Peak (µA)** | 8.55 | 8.64 | 8.88 | 8.61 | 8.34 | 8.55 |

Figure 4.6(a) shows the DPV results of the three potentiostats when the SPGE is exposed to the probe DNA in a 5mM ferrocyanide solution. The oxidation peaks for all three potentiostats are close to each other, which the range being less than 0.3µA. From Table 4-7, Autolab has the lowest oxidation peak at 8.55µA, followed by Dropsens, 8.64µA, and Pico development kit at 8.88µA. The slight differences in DPV peaks are attributed to the fact that the oxidation reactions are repeated on the same electrode for all three potentiostats.

Figure 4.6(b) shows the DPV waveforms for all three potentiostats when the SPGE is tested with both the DNA probe and its target sequences in 5mM ferrocyanide. The oxidation peaks for all three potentiostats are close to each other which can be seen clearly in Table 4-7. The oxidation peaks for the test are almost similar to the first DPV experiments in Figure 4.6(a). This time, Dropsens showed the lowest oxidation peak at 8.34µA, then Pico development kit at 8.55µA, and Autolab at 8.61µA.

Another observation that can be made through graphs in Figure 4.6 is, that noises can be seen happening when readings are taken from Pico development kit. This happened due to the limitation of the potentiostat. Despite the noise, the oxidation peaks that are being collected are nearly the same as the other two potentiostats which are shown in Table 4-7.

Slight discrepancies are happening on some the tests due to the limitation of some of the devices themselves since the current ranges that can be set are quite limited in portable potentiostats compared to Autolab as well as difference in the technologies of different companies.

### 4.2.3 NACOTS Final Revision Test Results

Differential pulse voltammetry test was done with comparing NACOTS (N004) with commercialized potentiostat, Sensit and Pico Development Kit.

#### 4.2.3.1 Differential Pulse Voltammetry Test

The comparison of the NACOTS device against the Sensit and the Pico Development Kit has been done to evaluate the reliability of the board. In this experiment, NACOTS N004 is being picked to be used. Experiments have been done by using 104µL 5mMol Ferrocyanide on 5 different electrodes which are SPCE, SPGE, and 3 nanogold electrodes. This experiment used only 5 electrodes as opposed to the previous experiments, which used 4 different SPCEs and 4 different SPGEs.

Figure 4.7 shows the differential pulse voltammetry comparison for Sensit, Pico Development Kit, and N004 for SPCE and SPGE. In Figure 4.8, differential pulse voltammetry comparison for Sensit, Pico Development Kit, and N004 by using Nanogold electrodes A, B, and C are shown.

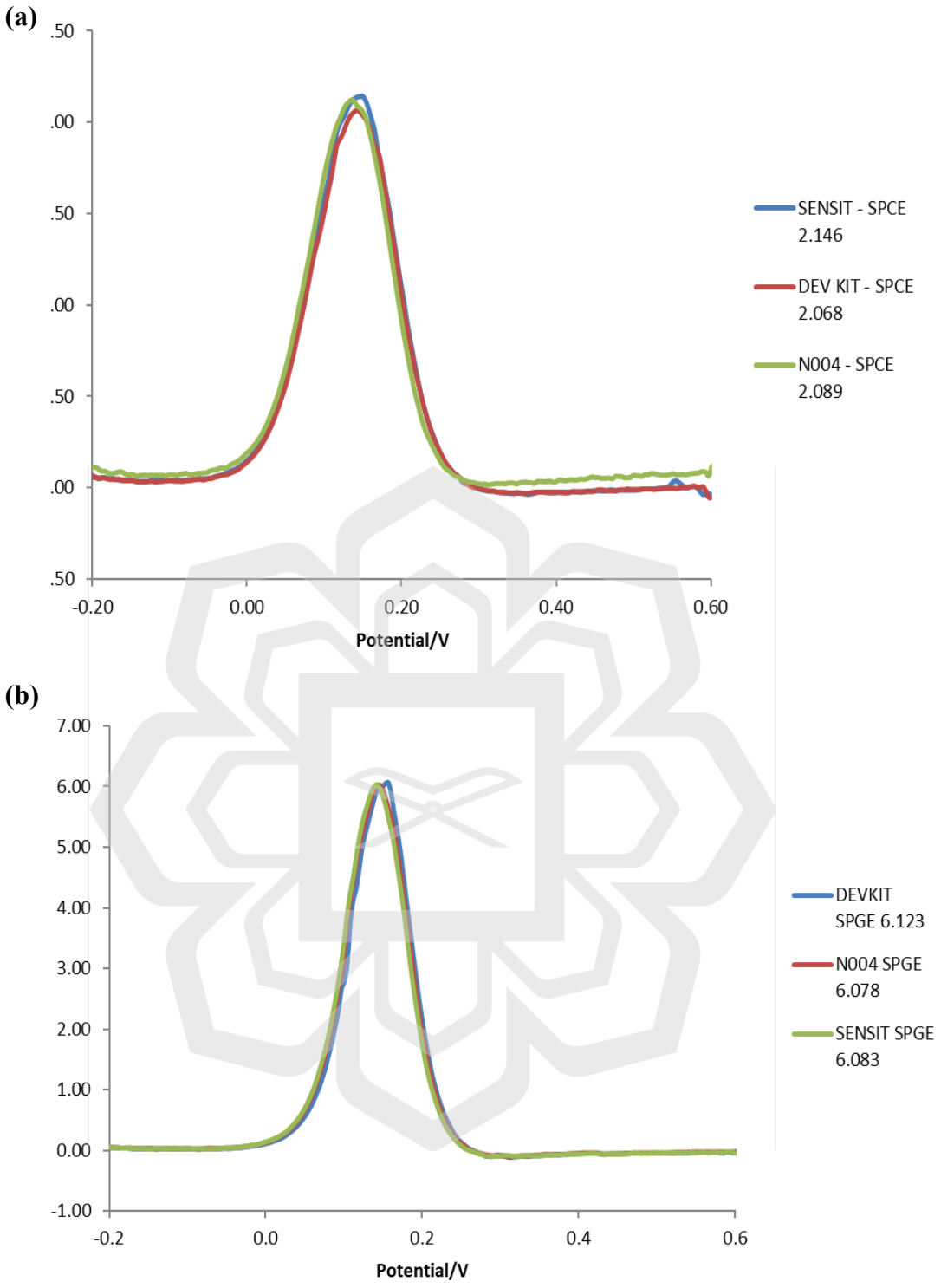


Figure 4.7 Differential Pulse Voltammetry comparison for Sensit, Pico Development Kit, and N004 (a) SPCE (b)SPGE

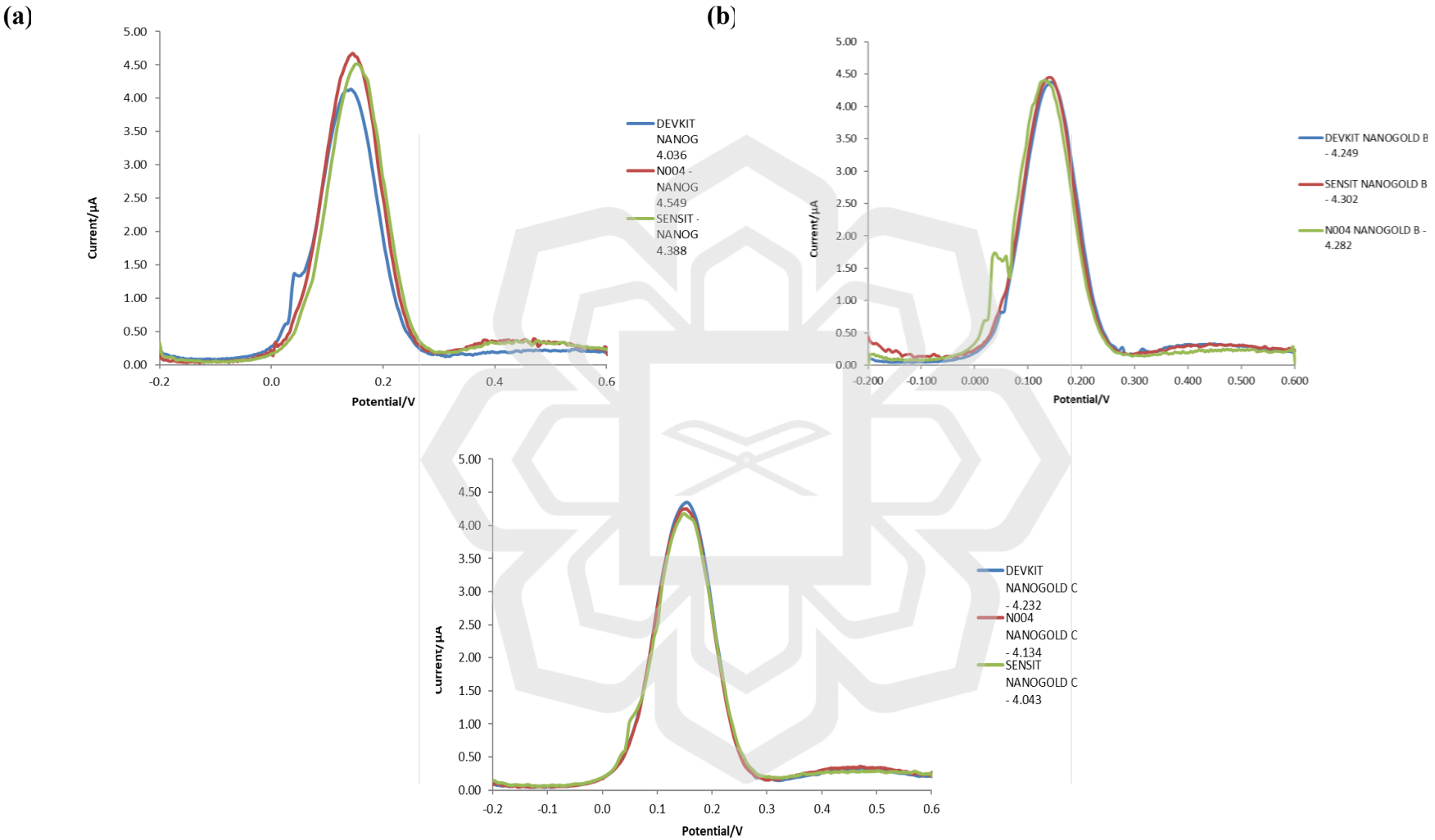


Figure 4.8 Differential Pulse Voltammetry comparison for Sensit, Pico Development Kit, and N004 by using Nanogold electrode (a) Electrode A (b) Electrode B (c) Electrode C

Table 4-8 Benchmarking DPV test results summary.

| Electrode | Devices | Oxidation Peak (µA) | Δ (µA) | Potential (V) of the Peak | Δ (V) |
|---|---|---|---|---|---|
| SPCE | SENSIT | 2.146 | 0 | 0.135 | 0 |
| | DEVKIT | 2.068 | -0.078 | 0.15 | 0.015 |
| | N004 | 2.089 | -0.057 | 0.142 | 0.007 |
| SPGE | SENSIT | 6.083 | 0 | 0.142 | 0 |
| | DEVKIT | 6.123 | 0.04 | 0.157 | 0.015 |
| | N004 | 6.078 | -0.005 | 0.146 | 0.004 |
| NANOGOLD A | SENSIT | 4.388 | 0 | 0.154 | 0 |
| | DEVKIT | 4.036 | -0.352 | 0.142 | -0.012 |
| | N004 | 4.549 | 0.161 | 0.146 | -0.008 |
| NANOGOLD B | SENSIT | 4.302 | 0 | 0.142 | 0 |
| | DEVKIT | 4.249 | -0.053 | 0.142 | 0 |
| | N004 | 4.282 | -0.02 | 0.131 | -0.011 |
| NANOGOLD C | SENSIT | 4.043 | 0 | 0.15 | 0 |
| | DEVKIT | 4.232 | 0.189 | 0.142 | -0.008 |
| | N004 | 4.134 | 0.091 | 0.135 | -0.015 |

Table 4.8 shows the summary of benchmarking DPV test results. Sensit has been chosen as the main device to be compared to Pico Development Kit and device N004. Sensit is one of the world's smallest commercialized potentiostat which was developed by PalmSens with the size of (43 x 25 x 11 mm). Oxidation peak changes and the potential of the peak changes are calculated. The oxidation peak differences are small for SPGE and SPCE and nanogold electrode B, which are less than 0.08µA. For nanogold A and nanogold C, the oxidation peak differences are slightly larger, and the Pico development kit shows the largest differences for both at 0.352µA and 0.189µA.

From the results, the slightly larger differences in nanogold A and C on the oxidation peak especially for the Pico development kit might be due to variances in the structure of the nanogold deposited, since the experiments were repeated by rinsing the electrodes first before collecting data. Other than that, the results have very small differences, in which the prototypes are as reliable as the other portable potentiostats.

### 4.3 Reliability Test

Two more types of tests have been done, which are the consistency test for the built prototypes and another benchmarking test for NACOTS against other portable potentiostats from PalmSens. Consistency tests were done to test the consistencies of the results across similar prototypes that are being built. The second test is benchmarking of a NACOTS device against other commercialized portable potentiostats from PalmSens to test the reliability and accuracy of the results.


Figure 4.9 Four identical NACOTS prototypes (N001, N002, N003, N004) that are fabricated for clinical testing.

Four identical NACOTS prototypes have been built which are labeled as N001, N002, N003, and N004 which can be seen in Figure 4.9. To test the output for these

results and test the reliability of these devices, 4 SPCE and 4 SPGE electrodes are tested on the 4 prototypes. The solution used is 104µL of 5mMol Ferrocyanide.

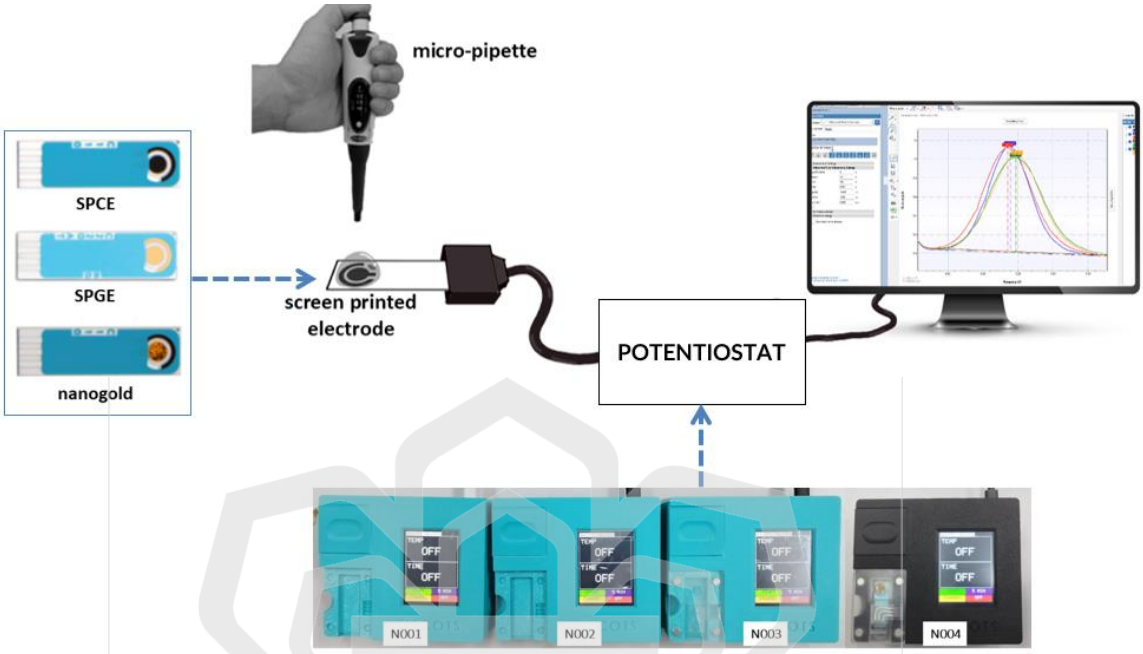


Figure 4.10 Electrochemical experiment setup for the reliability test on NACOTS devices, N001 until N004

Figure 4.11 shows the results of the DPV readings for SPCE, SPGE and nanogold electrodes.

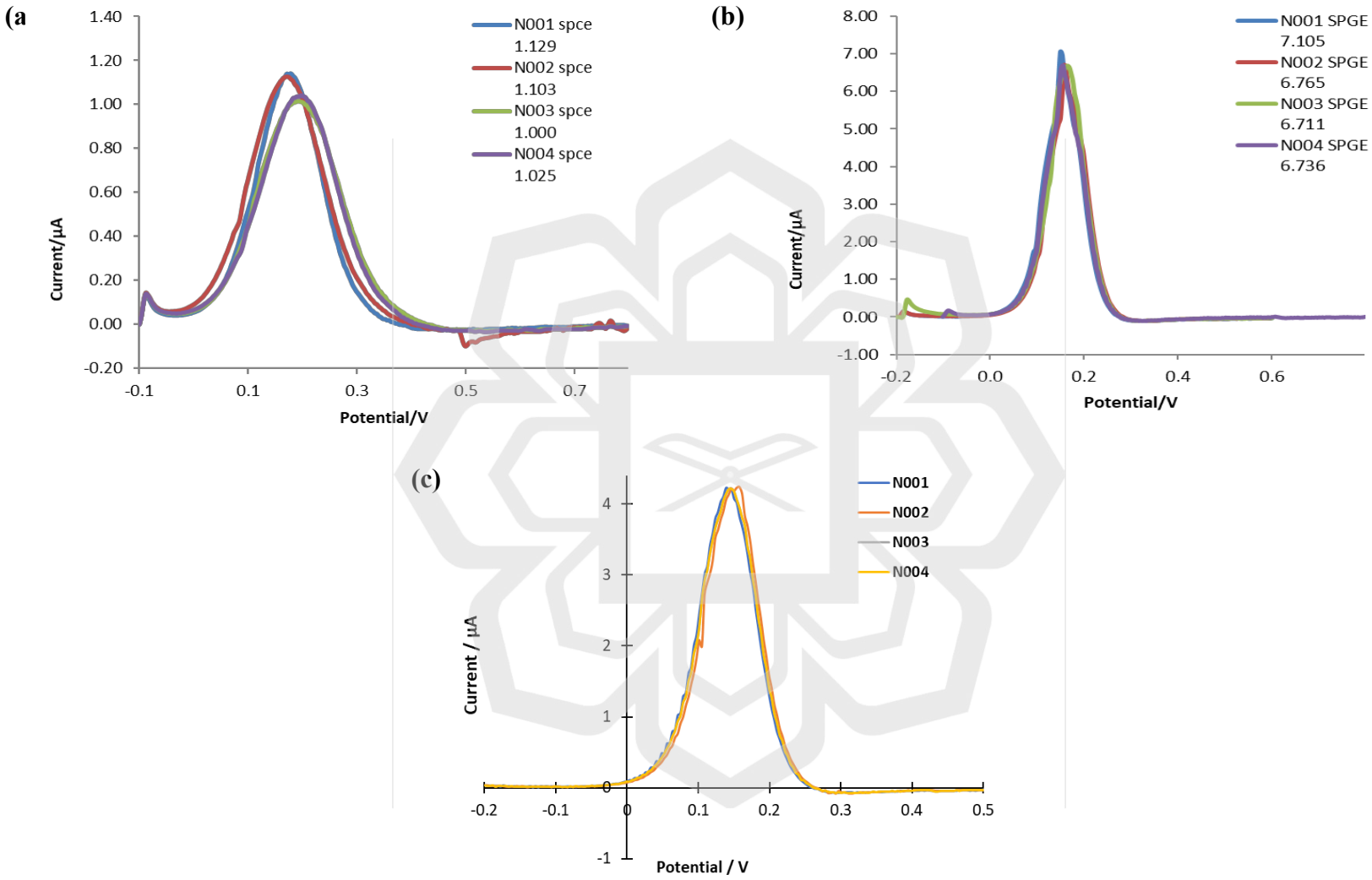


Figure 4.11 DPV for reliability test for NACOTS devices on (a) SPCE (b) SPGE (c) nanogold

Table 4-9 Differential Pulse Voltammetry comparison for NACOTS prototypes test results summary

| Electrode | Devices | Oxidation Peak (µA) | Δ (µA) | Potential (V) of the Peak | Δ (V) |
|---|---|---|---|---|---|
| SPCE | N001 | 1.129 | 0.129 | 0.178 | -0.015 |
| | N002 | 1.103 | 0.103 | 0.171 | -0.022 |
| | N003 | 1.000 | 0 | 0.193 | 0 |
| | N004 | 1.025 | 0.025 | 0.197 | 0.004 |
| SPGE | N001 | 7.105 | 0.394 | 0.150 | -0.015 |
| | N002 | 6.765 | 0.054 | 0.157 | -0.008 |
| | N003 | 6.711 | 0 | 0.165 | 0 |
| | N004 | 6.736 | 0.025 | 0.156 | -0.009 |
| Nanogold | N001 | 4.223 | 0 | 0.138 | 0 |
| | N002 | 4.243 | 0.020 | 0.157 | 0.019 |
| | N003 | 4.213 | 0.010 | 0.142 | 0.004 |
| | N004 | 4.218 | 0.005 | 0.146 | 0.008 |

Table 4.9 shows the summary of the comparisons of the Differential Pulse Voltammetry results for the NACOTS prototypes. Prototype N003 has been chosen as the reference prototype. Oxidation peak changes and the potential of the peak changes are calculated. The oxidation peak differences are not big for SPGE except for device N001 the difference is at 0.394µA. However, for SPCE, the peak differences are below 0.15µA. The differences for the potential of the oxidation peak are quite low, which are below 0.25 for SPCE and 0.01 for SPGE.

From the results, all the devices have oxidation peaks formed at near similar potential, however, the slight difference in the oxidation peak might be due to the test being done on 4 different SPCEs and 4 different SPGEs. All devices have consistent results with slight oxidation peak differences.

### 4.4 On-site Testing

On-site testing was conducted on COVID-19 samples by using NACOTS Final revision devices. Samples were obtained from Institute for Medical Research Malaysia. Figure 4.12 shows the testing flow for COVID 19 using NACOTS. First, the sample will be heated to 65 degrees for 35 minutes, after that, sample will be dropped on the sensor before running the DPV and obtain the positive/negative result.

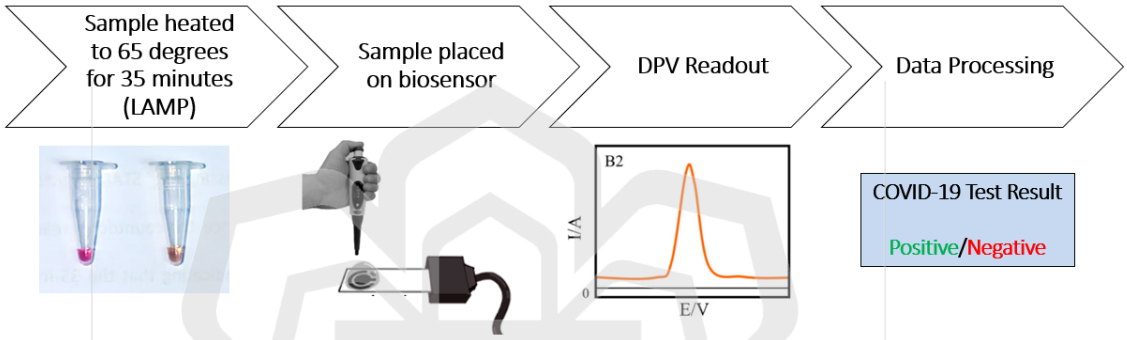


Figure 4.12 COVID-19 Testing flow using NACOTS.

The peak potential for the DPV results indicates the positive and negative test result. To determine whether the sample is positive, or negative is based on the equation below. The main parameters for the equation are the threshold value and the blank value.

Δ are differences of peak current between blank (ferrocyanide) and samples. Negative test is when Δ is less than 0.94. Positive test is when Δ is larger than or equal to 0.94. The threshold value of 0.94 is obtained through experimentation from research partners in UITM. (Zulhairee et al., 2023)

- Negative $\Delta < 0.94$
- Positive $\Delta \geq 0.94$

Two on-site testing had been conducted at the Institute of Medical Research (IMR) on the following date, test 1 on 22nd February 2023 and test 2 on 21st March 2023. Both tests were done using NACOTS Final revision devices. The objective of these tests is to verify the functionality of NACOTS devices.

The experimental setup for a system on all the tests comprises a unit of NACOTS Final Revision device, a unit of adapter, a unit of USB type cable, and a unit of a laptop with NACOTS software as shown in Figure 4.13.

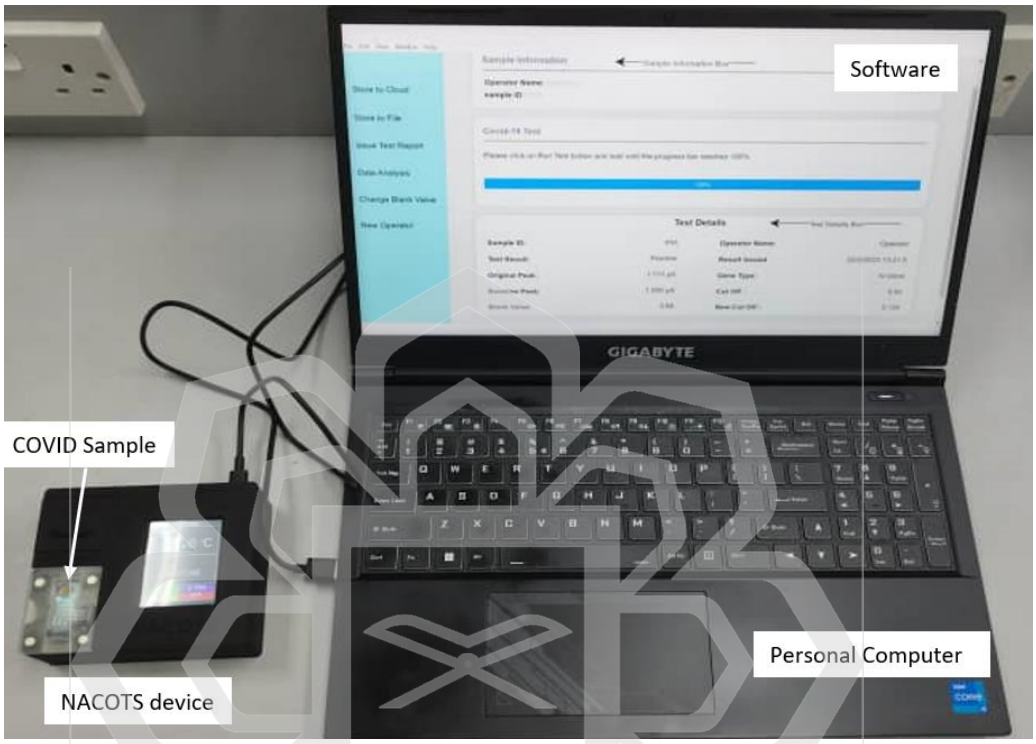


Figure 4.13 The experiment setup for On-Site Test 1

### 4.4.1 On-Site Test 1

On-site Test 1 was conducted to verify and validate the hea’er's capabilities in heating samples for LAMP amplification in the NACOTS device. The test details can be seen in Table 4.10. Three samples were used during the test, which comprised a negative and two positive samples.

Table 4-10 Experiment details for On-site test 1

| Parameters | Values |
|---|---|
| **Negative samples** | 1 |
| **Positive samples** | 2 |
| **Blank value** | 3.651 µA |
| **Threshold value** | 0.94 |
| **Number of systems** | 1 |

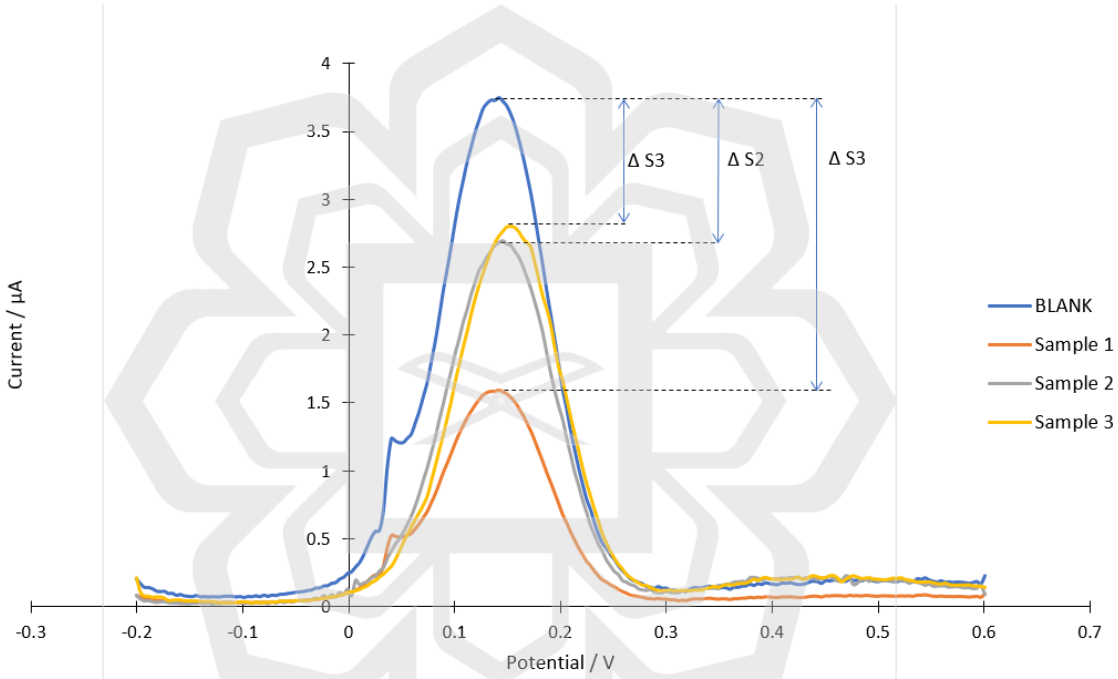


Figure 4.14 On-site Testing Result for Sample–1 - 3

A standalone incubator was used to heat all samples to 65°C for 35 minutes to proceed with the test. Then, data was collected using DPV; the result can be seen in Table 4.11. NACOTS system result was similar to RT-PCR. However, the sample size on this test round is too small to draw any conclusions. The detail observation of the result can be seen in Table 4.11.

Table 4-11 NACOTS Final revision on-site test 1 result

| Sample Name | NACOTS System | Actual Results (RT-PCR) | Blank value | Peak Value | Delta Value |
|---|---|---|---|---|---|
| **1** | Positive | Positive | 3.651 µA | 1.550 µA | 2.101 |
| **2** | Positive | Positive | 3.651 µA | 2.625 µA | 1.026 |
| **3** | Negative | Negative | 3.651 µA | 2.721 µA | 0.93 |

### 4.4.2 On-Site Test 2

Six samples were tested in this experiment, with the test details outlined in Table 4.12, and the test results in Table 4.13 and Table 4.14. In the experiment two computers were used and named as system A and system B. 6 COVID-19 human samples were used, 3 positives and 3 negatives. Each sample is duplicated into 2 samples to be used for system A and system B. For example, sample 1 can be split into sample 1A and sample 1B.

Table 4-12 Experiment details for On-site test 1

| Parameters | Values |
|---|---|
| **Negative samples** | 3 |
| **Positive samples** | 3 |
| **Blank value** | 5.215 |
| **Threshold value** | 0.94 |
| **Number of systems** | 2 (A and B) |

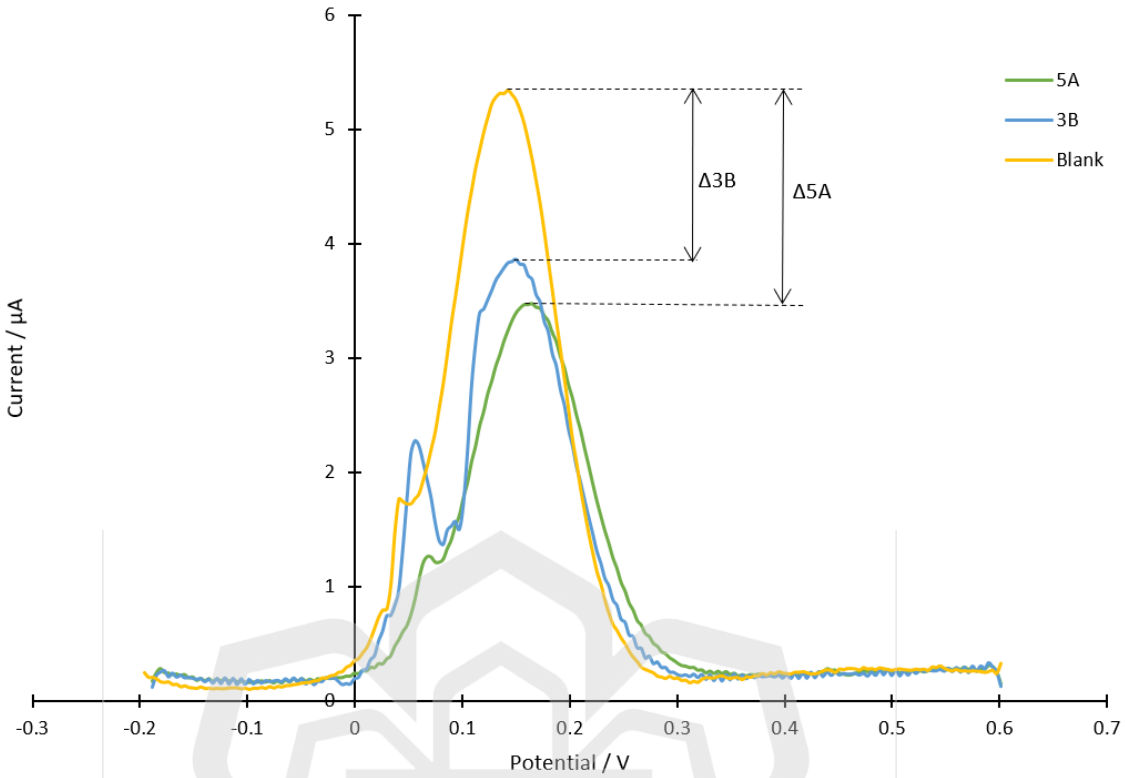


Figure 4.15 On-site Testing Result for Sample 5A and 3B

Figure 4.15 shows the differential pulse voltammetry results from on-site testing for samples 5A and 3B. The overall test results can be seen in Table 4.13 and Table 4.14. Table 4.13 compares the results of the NACOTS system and RT-PCR results of COVID-19. The NACOTS system comprises NACOTS potentiostat, NACOTS electrode, and LAMP solution. The blank value mentioned in the Table 4.13 and Table 4.14 is the potential peak of 104 µL of Ferrocyanide.

The negative samples were not predicted correctly, while each positive sample was correctly predicted as positive. The negative samples peak values were approximately 2.9 µA to 3.7 µA, which is the same range as the peak values of the positive samples.

Table 4-13 On-site testing result for NACOTS system A

| Sample Name | NACOTS System | Actual Results (RT-PCR) | Blank value | Peak Value | Delta Value |
|---|---|---|---|---|---|
| **1A** | Positive | Positive | 5.215 µA | 3.731 µA | 1.484 |
| **2A** | Positive | Positive | 5.215 µA | 3.366 µA | 1.849 |
| **3A** | Positive | Positive | 5.215 µA | 3.482 µA | 1.733 |
| **4A** | Positive | Negative | 5.215 µA | 3.586 µA | 1.629 |
| **5A** | Positive | Negative | 5.215 µA | 3.319 µA | 1.896 |
| **6A** | Positive | Negative | 4.174 µA | 3.034 µA | 1.140 |

Table 4-14 NACOTS Final revision on-site testing result for system B

| Sample Name | NACOTS System | Actual Results (RT-PCR) | Blank value | Peak Value | Delta Value |
|---|---|---|---|---|---|
| **1B** | No Reading | Positive | 5.215 µA | Unable to collect data | - |
| **2B** | Positive | Positive | 5.215 µA | 3.162 µA | 2.053 |
| **3B** | Positive | Positive | 5.215 µA | 4.104 µA | 1.111 |
| **4B** | Positive | Negative | 5.215 µA | 2.426 µA | 2.789 |
| **5B** | No Reading | Negative | 5.215 µA | Unable to collect data | - |

Based on the presented data in the table, it can be concluded that the positive samples were predicted perfectly. However, some negative samples were predicted as positive due to the similarity in peak values between the negative and positive samples. After investigating the issue by testing the nanogold sensors, it was discovered that the nanogold sensors are not reliable due to variation of nano porous structure of gold deposited on the electrode (Asyiqin Azman et al., 2023). The NACOTS devices are working as intended when tested with commercial SPCE and SPGE based on the results in Table 4.6.

### 4.4.3 Clinical Testing by UITM

UITM team has performed clinical testing on 148 COVID-19 samples on RT-PCR and NACOTS. From the data obtained, 74 samples were identified as positive samples, and another 74 samples were negative samples. Mean differences for both delta I (ΔI) of positive and negative samples have been validated by student t-test as shown in the bar graph from Figure 4.16. Hence, there are significant differences between positive and negative samples due to p-values of less than 0.05 ($p<0.0001$)(Zulhairee et al., 2023).

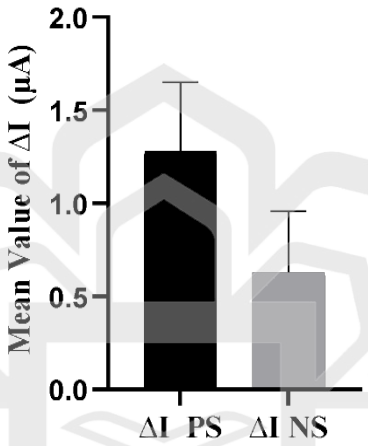


Figure 4.16 The mean difference with standard deviation between ΔI (μA) of positive and negative samples. (Zulhairee et al., 2023)

## 4.5 Electromagnetic Compatibility Certification (EMC) for the NACOTs electronics system

Paperwork for the Electromagnetic Compatibility Certification (EMC) for the NACOTs electronics system had been done and submitted. RF EMC Centre Malaysia Sdn Bhd had been chosen as the tester for the EMC certification.

RF EMC Centre Malaysia Sdn Bhd uses the facilities of UTHM Commercial Laboratories (UCL), Universiti Tun Hussein Onn Malaysia, Batu Pahat. The laboratories are accredited and approved according to ISO/IEC 17025 and ILAC Mutual Recognition Arrangement (ILAC MRA). Figures 4.17 and 4.18 are a few experimental setups that are used during the EMC certification test.

Figure 4.17 Radiated emission and radio-frequency electromagnetic field setup.

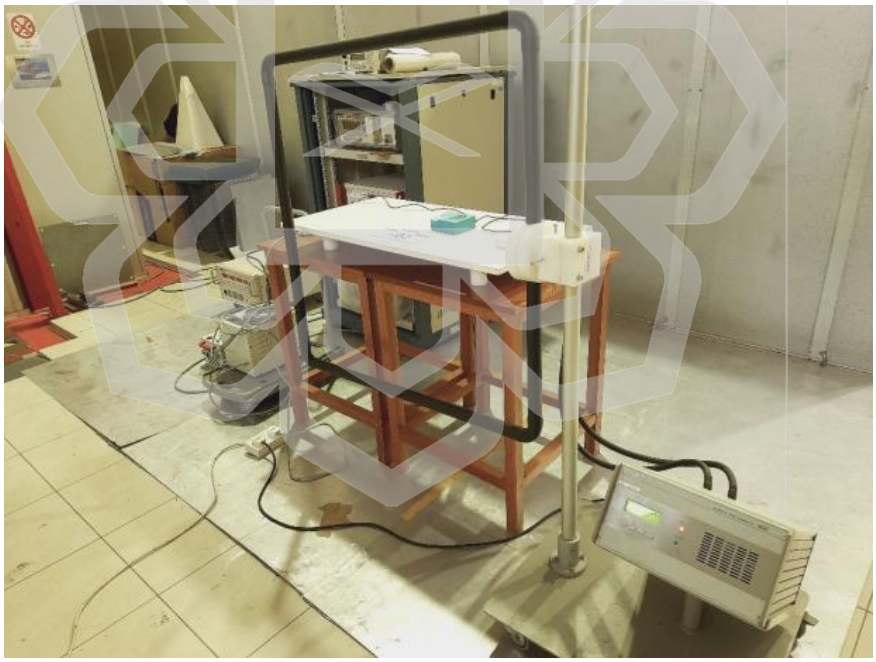

Figure 4.18 Power-frequency magnetic field-testing setup

Out of the 9 EMC tests, 7 of the tests are passing the criterion. The EMC test results summary can be seen Table 4.15. Conducted emission test was found below the limit for emission tests. Fast transients test, surges test, radio-frequency common mode test, power-frequency magnetic field test (setup in Figure 4.17), voltage dips and interruptions test, and radio-frequency electromagnetic test results all pass with A

ratings. Radiated emission (setup in Figure 4.18) was found above the allowed limit and the electrostatic discharge test was rated C which is below the performance criteria at B.

Table 4-15 EMC Test Results Summary

| EMISSION (CISPR11: 201 5 +AMD1:2016+AMD2:2019) | | | | |
|---|---|---|---|---|
| No | Methods | Test Type | Result | Performance criterion |
| 1 | CISPR 16-2-1:2014+A1+2017 | Conducted emission | **BELOW** | Below Limit |
| **2** | **CISPR 16-2-3:2016+A1+2019.** | **Radiated emission** | **ABOVE** | **Below Limit** |
| IMMUNITY (IEC 61000-6-1:2016) | | | | |
| No | Methods | Test Type | Result | Performance criterion |
| **3** | **IEC 61000-4-2:2009** | **Electrostatic discharge** | **C** | **B** |
| 4 | IEC 61000-4-4:2012 | Fast transients | **A** | B |
| 5 | IEC 61000-4-5:2014+A1:2017 | Surges | **A** | B |
| 6 | IEC 61000-4-6:2013 | Radio-frequency common mode | **A** | A |
| 7 | IEC 61000-4-8:2010 | Power-frequency magnetic field | **A** | A |
| 8 | IEC 61000-4-11:2020, | Voltage dips and interruptions | **A** | B / C |
| 9 | IEC 61000-4-3:2020 | Radio-frequency electromagnetic field | **A** | A |

## 4.6 Summary

The designed potentiostat was benchmarked against multiple commercialized potentiostats. For the first round of benchmarking, the designed NACOTS Beta was compared against PGSTAT302N Autolab and µStat-i 400 DropSens produced by MetroOhm for cyclic voltammetry, differential pulse voltammetry, and electrochemical impedance spectroscopy. Table 4.13 shows the comparison of all potentiostats that were tested throughout the research period. Pico Development Kit, Sensit Smart and NACOTS have similar resolutions and ranges due to all three using the same potentiostat chip, which is EmStat Pico Core.

Table 4-16 Resolution and ranges for various potentiostat.

| **Parameters** | **PGSTAT302n** | **µStat-i 400** | **Pico Dev Kit** | **Sensit Smart** | **NACOTS** |
|---|---|---|---|---|---|
| | **(MetroOhm, 2023)** | | **(PalmSens, 2023)** | | |
| **Potential resolution** | 0.3 µV | 1000 µV | 932 µV | 932 µV | 932 µV |
| **Current resolution** | 0.0003% of current range | 0.025 % of current range | 0.006% of current range | 0.006% of current range | 0.006% of current range |
| **Current ranges** | 10 nA to 1 A | 1 nA to 10 mA | 100 nA to 5 mA | 100 nA to 5 mA | 100 nA to 5 mA |
| **DAC resolution** | 16 bits | - | 12 bits | 12 bits | 12 bits |
| **ADC resolution** | 16 bits | 10 bits | 16 bits | 16 bits | 16 bits |

Table 4.17 shows the comparison of developed potentiostats with COVID-19 detection capabilities against NACOTS device. NACOTS have the edges in terms of NACOTS came with incubation chamber for LAMP process, detection time, which is less than a minute, as well as the number of samples that being tested through the clinical test. NACOTS have been tested on 148 samples compared to the benchmarked papers which are tested only on 7 and 14 samples. As for eCovSens, there are no mention on sample sizes in the published paper. However, NACOTS lacks in terms of portability. The device still needs a PC to work compared to Bi-ECDAQ which can run stand-alone.

Table 4-17 Comparison of Potentiostats with COVID-19 Detection Capabilities against NACOTS

| Potentiostat | COVID-19 Detection Technique | Detection Time | Platform | Wireless Capability | Display | Incubation Chamber | Clinical Test |
|---|---|---|---|---|---|---|---|
| **eCovSens** (Mahari et al., 2020) | DPV | 1 min | PC and mobile phones | Yes | 16x2 dot matrix display | No | No mention on sample sizes |
| **Bi-ECDAQ** (Salahandish et al., 2022) | EIS | 1 min | Stand-alone | Wifi and Bluetooth | LCD with touchscreen capability | No | 14 samples. 7 positive and 7 negative samples |
| **3D-printed portable potentiostat** (Primpray et al., 2022) | Amperometry | 5 min | PC and mobile phones | No information | LCD with touchscreen capability | No | 7 samples |
| **NACOTS** | DPV | Less than a minute | PC | Yes, for heater control | LCD with touchscreen capability | Yes | 148 samples; 74 positive and 74 negative samples |

# CHAPTER 5

# CONCLUSIONS

## 5.1 Conclusions

We have successfully designed a circuit of portable potentiostat with cyclic voltammetry, differential pulse voltammetry, and electrochemical impedance spectroscopy capabilities. The potentiostat chip used is EmStat Pico Module, capable of performing multiple electrochemical techniques. The circuit was designed using Autodesk Eagle. The circuit.

The designed potentiostat was benchmarked against multiple commercialized potentiostats. For the first round of benchmarking, the designed NACOTS Beta was compared against PGSTAT302N Autolab and μStat-i 400 DropSens produced by MetroOhm for cyclic voltammetry, differential pulse voltammetry, and electrochemical impedance spectroscopy. The findings from CV and EIS were only marginally different, SPCE and SPGE results from EIS and DPV were hardly different among the potentiostats. The experiments indicate that the little measurement variations won't have a significant influence on the outcomes of the biosensing. The second round of benchmarking involves DPV test of NACOTS Final revision against another two portable potentiostat from PalmSens which is Sensit Smart and Pico Development Kit. All three portable potentiostats results have very small differences, in which the NACOTS Final revision are as reliable as the other portable potentiostats.

On-site diagnosis of COVID-19 was done using NACOTS Final revision. The incubation chamber and potentiostats are working fine. However, the data collected is inconsistent. The first test results are almost similar to PCR, but the second test is unable to give similar results, in which negative samples are shown as positive. It was discovered that the nanogold sensors are not reliable due to variation of nano porous structure of gold deposited on the electrode.

## 5.2 Significance to the field

The project is hoped to improve the accessibility of comprehensive virus detection especially COVID-19 to rural area. With electrochemical techniques being explored and proven to be able to give sensitive results, this can be a new standard for detection of viruses alongside PCR and LAMP.

The research also aims to develop hardware that can be used on-site to screen and diagnose COVID-19 cases and for other viruses. With the development of this point-of-care device, and the simplicity to operate the hardware, even the medical officer can use the device as a rapid point-of-care testing in the face of unexpected outbreak.

## 5.3 Limitations and future work

This project comes with few limitations which can improved further in the future. One of the aspects that we can improve for the device is the resolution and ranges to achieve performance like Autolab. Table 23 shows the potential and current resolutions and ranges for various potentiostats used during the research. Higher resolution for the DC potential, will enables a higher scan-rate to the electrochemical techniques especially for voltammetry techniques. Therefore, the improvement from the current NACOTS device should be higher resolution for DC potential and higher ranges for the current measurement.

The limitation of the NACOTS device is the portability. Current NACOTS devices are portable, but the portability can still be improved. There are two strategies to improve portability. One, by adding Bluetooth or wireless module which allows the device to support computer-based systems and smartphone. ABE-Stat is an example of a potentiostat that can be run on smartphone (Jenkins, Lee, Jun, Reyes-De-Corcuera, & McLamore, 2019). The second strategy that can be used to improve the portability of the device is to make the device run standalone and upload the results directly to the

server. This can be accomplished by adding a more powerful microcontroller that can handle the data processing on the device.

Another improvement that can be made is in terms of cost. In this research, the NACOTS device was developed to perform various electrochemistry techniques such as cyclic voltammetry, differential pulse voltammetry, and electrochemical impedance spectroscopy. To be able to execute these techniques with great precision, EmStat Pico Module was chosen. However, this comes with a cost that the chip cost around $500 each. Nearing the end of the development, we found that only a single technique, DPV, is needed. Multiple ICs can be used to perform DPV without EIS support cost much cheaper, such as LMP91000, which costs around $5, or ADUCM350, which costs around $25. The overall production cost can be cut to almost 80% with the alternative potentiostat ICs.

The device's current limitation is that it lacks parallel testing. It can only test a single sample at a time. In future works, parallel testing can be integrated into the device system to enable multiple samples to be tested simultaneously. Thus, would improve the overall test time for virus detection especially when facing a lot of samples.

Another limitation that was observed throughout the research, the DPV results reading from the electrodes sometimes produced a lot of noise. To tackle this issue, experimentation on scan rate needs to be performed with many details.

Another limitation that needs to be addressed is the Electromagnetic Compatibility Certification. To pass the certification, especially on the electrostatic discharge test and radiation test, the case needs to be created with ESD-safe filaments to block the radiation from the circuit to leak from the case to user. Other than that, ESD protection circuitry and IC can be improved to comply with standards.

# PUBLICATIONS AND AWARDS

Ghani, A., Nordin, M. A.;, Zulhairee, A. N. ;, Che, M. ;, Nor, M., Shihabuddin, A. ;, … Zain, Z. M. (2022). Portable Electrochemical Biosensors Based on Microcontrollers for Detection of Viruses: A Review. *Biosensors 2022, Vol. 12, Page 666*, *12*(8), 666.

Ghani, M. A. A., Nordin, A. N., Rahim, R. A., Gunawan, T. S., & Zain, Z. M. (2022). Evaluation of Portable Potentiostats for Electrochemical Measurements: Voltammetry and Impedance Spectroscopy. *8th IEEE International Conference on Smart Instrumentation, Measurement and Applications, ICSIMA 2022*, 132–137.

# REFERENCES


Adams, S. D., Doeven, E. H., Quayle, K., & Kouzani, A. Z. (2019). MiniStat: Development and Evaluation of a Mini-Potentiostat for Electrochemical Measurements. *IEEE Access*, *7*, 31903–31912.

Adamson, B., Sikka, R., Wyllie, A. L., & Premsrirut, P. (2022). Discordant SARS-CoV-2 PCR and Rapid Antigen Test Results When Infectious: A December 2021 Occupational Case Series. *MedRxiv*, 2022.01.04.22268770.

Albert, E., Torres, I., Bueno, F., Huntley, D., Molla, E., Fernández-Fuentes, M. Á., … Navarro, D. (2021). Field evaluation of a rapid antigen test (Panbio$^{TM}$ COVID-19 Ag Rapid Test Device) for COVID-19 diagnosis in primary healthcare centres. *Clinical Microbiology and Infection*, *27*(3), 472.e7-472.e10.

Asyiqin Azman, N., Mohd, Y., Mohd Zain, Z., & Ying Chin, L. (2023). Modification of a screen-printed carbon electrode with nanoporous gold by electrodeposition and dealloying of a gold-copper alloy. *International Journal of Nanoelectronics and Materials*, *16*(4).

Batchelor-Mcauley, C., Kätelhçn, E., Barnes, E. O., Compton, R. G., Aborda, E., & Molina, A. (2015). *Recent Advances in Voltammetry*. Retrieved from www.chemistryopen.org

Brandal, L. T., MacDonald, E., Veneti, L., Ravlo, T., Lange, H., Naseer, U., … Elisabeth, M. H. (2021). Rapid communication Outbreak caused by the SARS-CoV-2 Omicron variant in Norway, November to December 2021. *Euro Surveill*, 5.

Brazaca, L. C., Ribovski, L., Janegitz, B. C., & Zucolotto, V. (2017). Nanostructured materials and nanoparticles for point of care (POC) medical biosensors. *Medical Biosensors for Point of Care (POC) Applications*, 229–254.

Chaibun, T., Puenpa, J., Ngamdee, T., Boonapatcharoen, N., Athamanolap, P., O'Mullane, A. P., … Lertanantawong, B. (2021). Rapid electrochemical detection of coronavirus SARS-CoV-2. *Nature Communications*, *12*(1).

Chau, C. H., Strope, J. D., & Figg, W. D. (2020). COVID-19 Clinical Diagnostics and Testing Technology. *Pharmacotherapy*, *40*(8), 857–868.

Chaudhary, N., & Khanuja, M. (2022). Electrochemistry—Concepts and methodologies. *Electrochemical Sensors: From Working Electrodes to Functionalization and Miniaturized Devices*, 31–50.

Cook, J. (2020). *SIMstat: Hardware Design Considerations for Implementing a Low-Cost, Portable Potentiostat* (Honors College Thesis). Oregon State University , Oregon.

COVID-19 IgM/IgG Rapid Test – BioMedomics Inc. (n.d.). Retrieved December 26, 2023, from https://www.biomedomics.com/products/infectious-disease/covid-19-rt/

Devices, A. (2023). Reference Manual ADuCM355 ADuCM355 Hardware Reference Manual. *Analog Devices, Inc*. Retrieved from https://www.analog.com/media/en/technical-documentation/user-guides/ADuCM355-Hardware-Reference-Manual-UG-1262.pdf

Elgrishi, N., Rountree, K. J., McCarthy, B. D., Rountree, E. S., Eisenhart, T. T., & Dempsey, J. L. (2018). A Practical Beginner's Guide to Cyclic Voltammetry. *Journal of Chemical Education*, *95*(2), 197–206.

Forrister, T. (2018, July 3). Analyzing Cyclic Voltammetry at a Microdisk Electrode with Simulation | COMSOL Blog. Retrieved September 7, 2022, from COMSOL website: https://www.comsol.com/blogs/analyzing-cyclic-voltammetry-at-a-microdisk-electrode-with-simulation/

Harvey, D. (2013, July 31). Effect of Scan Rate in Cyclic Voltammetry . Retrieved January 7, 2022, from Image and Video Exchange Forum website: https://community.asdlib.org/imageandvideoexchangeforum/2013/07/31/effect-of-scan-rate-in-cyclic-voltammetry/

Hoilett, O. S., Walker, J. F., Balash, B. M., Jaras, N. J., Boppana, S., & Linnes, J. C. (2020). Kickstat: A coin-sized potentiostat for high-resolution electrochemical analysis. *Sensors (Switzerland)*, *20*(8).

Huang, C.-Y., Huang, H.-T., & Yuan, R.-T. (2017). *Design of a Portable Mini Potentiostat for Electrochemical Biosensors*. Chongqing: IEEE.

Instruments, T. (2015). LMP91002 Sensor AFE System : Configurable AFE Potentiostat for Low-Power Chemical. *Device Information*.

Jenkins, D. M., Lee, B. E., Jun, S., Reyes-De-Corcuera, J., & McLamore, E. S. (2019a). ABE-Stat, a Fully Open-Source and Versatile Wireless Potentiostat Project Including Electrochemical Impedance Spectroscopy. *Journal of The Electrochemical Society*, *166*(9), B3056–B3065.

Jenkins, D. M., Lee, B. E., Jun, S., Reyes-De-Corcuera, J., & McLamore, E. S. (2019b). ABE-Stat, a Fully Open-Source and Versatile Wireless Potentiostat Project Including Electrochemical Impedance Spectroscopy. *Journal of The Electrochemical Society*, *166*(9), B3056–B3065.

Kissinger, P. T., & Heineman, W. R. (1996). *Laboratory techniques in electroanalytical chemistry*. Marcel Dekker, Inc.

Laborda, E., González, J., & Molina, Á. (2014). Recent advances on the theory of pulse techniques: A mini review. *Electrochemistry Communications*, *43*, 25–30.

Lalkhen, A. G., & McCluskey, A. (2008). Clinical tests: Sensitivity and specificity. *Continuing Education in Anaesthesia, Critical Care and Pain*, *8*(6), 221–223.

Lanese, N. (2022, January 6). Rapid tests may not detect omicron early in infection | Live Science. Retrieved January 7, 2022, from LiveScience website: https://www.livescience.com/rapid-test-accuracy-omicron-coronavirus-infections

Li, X., Qin, Z., Fu, H., Li, T., Peng, R., Li, Z., … Liu, X. (2021). Enhancing the performance of paper-based electrochemical impedance spectroscopy nanobiosensors: An experimental approach. *Biosensors and Bioelectronics*, *177*, 112672.

Lippi, G., Simundic, A. M., & Plebani, M. (2020). Potential preanalytical and analytical vulnerabilities in the laboratory diagnosis of coronavirus disease 2019 (COVID-19). *Clinical Chemistry and Laboratory Medicine*, *58*(7), 1070–1076.

Liu, J., Xu, Y., Liu, S., Yu, S., Yu, Z., & Low, S. S. (2022). Application and Progress of Chemometrics in Voltammetric Biosensing. *Biosensors 2022, Vol. 12, Page 494*, *12*(7), 494.

Macdonald, J. R., & Johnson, W. B. (2018). *Fundamentals of Impedance Spectroscopy*.

Mahari, S., Roberts, A., Shahdeo, D., & Gandhi, S. (2020a). Ecovsens-ultrasensitive novel in-house built printed circuit board based electrochemical device for rapid detection of nCovid-19 antigen, a spike protein domain 1 of SARS-CoV-2. *BioRxiv*.

Mahari, S., Roberts, A., Shahdeo, D., & Gandhi, S. (2020b). eCovSens-Ultrasensitive Novel In-House Built Printed Circuit Board Based Electrochemical Device for Rapid Detection of nCovid-19 antigen, a spike protein domain 1 of SARS-CoV-2. *BioRxiv*, 2020.04.24.059204.

Miller, T. E., Garcia Beltran, W. F., Bard, A. Z., Gogakos, T., Anahtar, M. N., Astudillo, M. G., … Lennerz, J. K. (2020). Clinical sensitivity and interpretation of PCR and serological COVID-19 diagnostics for patients presenting to the hospital. *FASEB Journal*, *34*(10), 13877–13884.

Nossol, E., Muñoz, R. A. A., Richter, E. M., de Souza Borges, P. H., Silva, S. C., & Rocha, D. P. (2021). Sensing Materials: Graphene. *Reference Module in Biomedical Sciences*.

Oliveira, M. E. ;, Lopes, B. V. ;, Rossato, J. H. H. ;, Maron, G. K. ;, Gallo, L., Rosa, A. B. ;, … Carreño, V. (2022). Electrochemical Biosensor Based on Laser-Induced Graphene for COVID-19 Diagnosing: Rapid and Low-Cost Detection of SARS-CoV-2 Biomarker Antibodies. *Surfaces 2022, Vol. 5, Pages 187-201*, *5*(1), 187–201.

PalmSens BV. (2023). EmStat Pico - Electrochemical interface module. *EmStat Pico Module*.

Pavia, C. S., & Plummer, M. M. (2021). The evolution of rapid antigen detection systems and their application for COVID-19 and other serious respiratory infectious diseases. *Immunology and Infection*, *54*, 776–786.

Pilarowski, G., Lebel, P., Sunshine, S., Liu, J., Crawford, E., Marquez, C., … Derisi, J. (2021). Performance Characteristics of a Rapid Severe Acute Respiratory Syndrome Coronavirus 2 Antigen Detection Assay at a Public Plaza Testing Site in San Francisco. *Journal of Infectious Diseases*, *223*(7), 1139–1144.

Platto, S., Xue, T., & Carafoli, E. (2020, September 1). COVID19: an announced pandemic. *Cell Death and Disease*, Vol. 11. Springer Nature.

Primpray, V., Kamsong, W., Pakapongpan, S., Phochakum, K., Kaewchaem, A., Sappat, A., … Karuwan, C. (2022). An alternative ready-to-use electrochemical immunosensor for point-of-care COVID-19 diagnosis using graphene screen-printed electrodes coupled with a 3D-printed portable potentiostat. *Talanta Open*, *6*.

Pruna, R., Palacio, F., Baraket, A., Zine, N., Streklas, A., Bausells, J., … López, M. (2018). A low-cost and miniaturized potentiostat for sensing of biomolecular species such as TNF-α by electrochemical impedance spectroscopy. *Biosensors and Bioelectronics*, *100*, 533–540.

Ramdas, K., Darzi, A., & Jain, S. (2020, June 1). 'Test, re-test, re-test': using inaccurate tests to greatly increase the accuracy of COVID-19 testing. *Nature Medicine*, Vol. 26, pp. 810–811. Nature Research.

Roy, B., Dhillon, J., Habib, N., & Pugazhandhi, B. (2021). Global variants of COVID-19: Current understanding. *Journal of Biomedical Sciences*, *8*(1), 8–11.

Salahandish, R., Haghayegh, F., Ayala-Charca, G., Hyun, J. E., Khalghollah, M., Zare, A., … Sanati-Nezhad, A. (2022). Bi-ECDAQ: An electrochemical dual-immuno-biosensor accompanied by a customized bi-potentiostat for clinical detection of SARS-CoV-2 Nucleocapsid proteins. *Biosensors and Bioelectronics*, *203*, 114018.

Schuit, E., Veldhuijzen, I. K., Venekamp, R. P., Van Den Bijllaardt, W., Pas, S. D., Lodder, E. B., … Moons, K. G. M. (2021). Diagnostic accuracy of rapid antigen tests in asymptomatic and presymptomatic close contacts of individuals with confirmed SARS-CoV-2 infection: cross sectional study. *BMJ*, *374*, 1676.

Simões, F. R., & Xavier, M. G. (2017). Electrochemical Sensors. *Nanoscience and Its Applications*, 155–178.

Smith, R. L., Gibson, L. L., Martinez, P. P., Ke, R., Mirza, A., Conte, M., … Brooke, C. B. (2021). Longitudinal Assessment of Diagnostic Test Performance over the Course of Acute SARS-CoV-2 Infection. *Journal of Infectious Diseases*, *224*(6), 976–982.

Smyrlaki, I., Ekman, M., Lentini, A., Rufino De Sousa, N., Papanicolaou, N., Vondracek, M., … Reinius, B. (n.d.). *Massive and rapid COVID-19 testing is feasible by extraction-free SARS-CoV-2 RT-PCR*.

Venton, B. J., & DiScenza, D. J. (2020). Voltammetry. *Electrochemistry for Bioanalysis*, 27–50.

Wages, J. M. (2005). NUCLEIC ACIDS | Immunoassays. *Encyclopedia of Analytical Science: Second Edition*, 408–417.

Zia, R., Taj, A., Younis, S., Bukhari, S. Z., Latif, F., Feroz, Y., … Bajwa, S. Z. (2022). Application of nanosensors for pesticide detection. *Nanosensors for Smart Agriculture*, 259–302.

Zulhairee, M., Mohd Zain, R., Che Mohamad Nor, A., Fadhilah Jafar, N., Fairulnizal Md Noh, M., Shihabuddin Ahmad Noorden, M., … Mohd Zain, Z. (2023). Clinical Performance of Reverse Transcription Loop-mediated Isothermal Amplification COVID-19 Assay on Gold-nanoparticle-modified Screen-printed Carbon Electrode Using Differential Pulse Voltammetry. *Sensors and Materials*, *35*(10), 4731–4750.

# APPENDIX

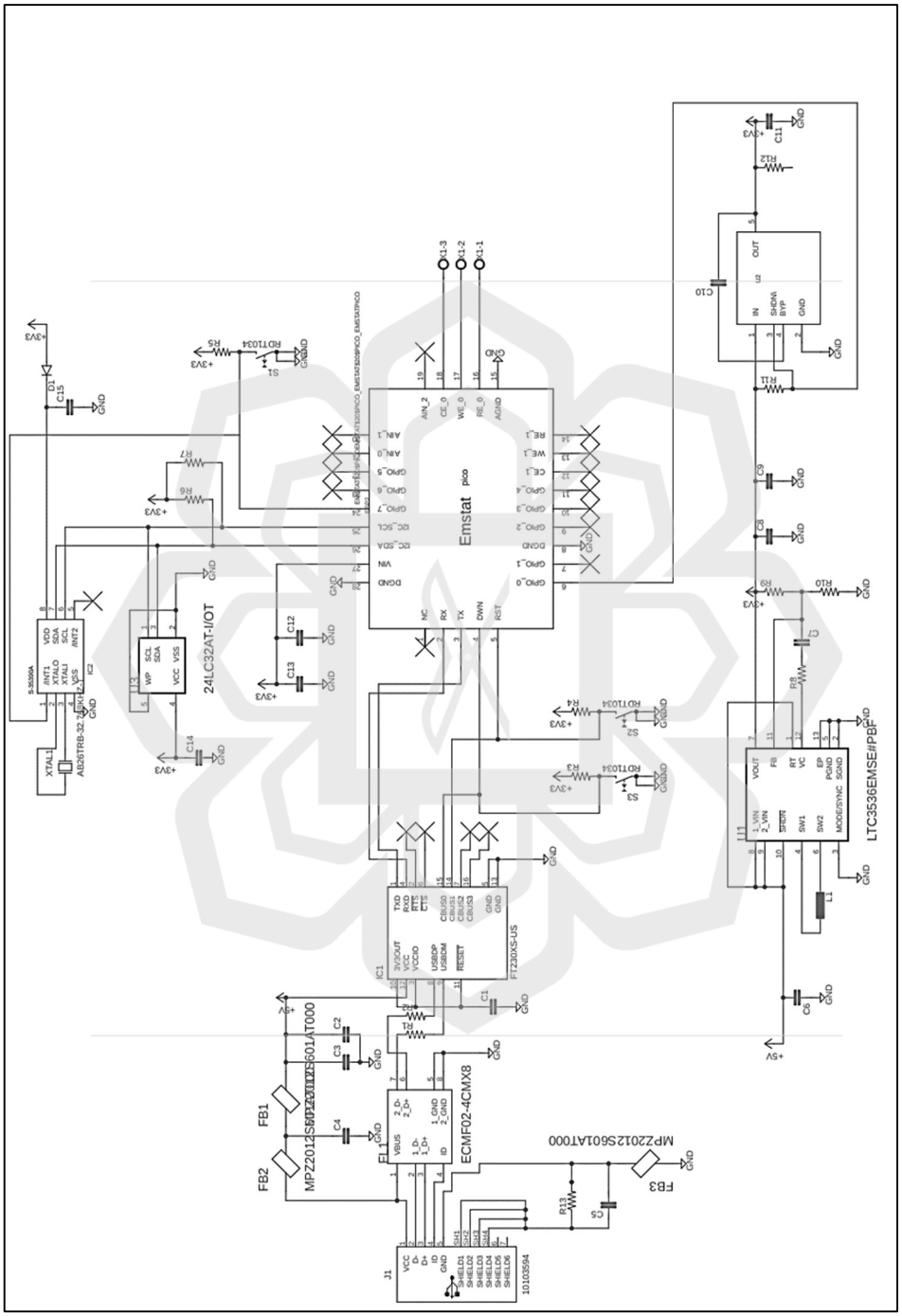


A. NACOTS Alpha schematic design

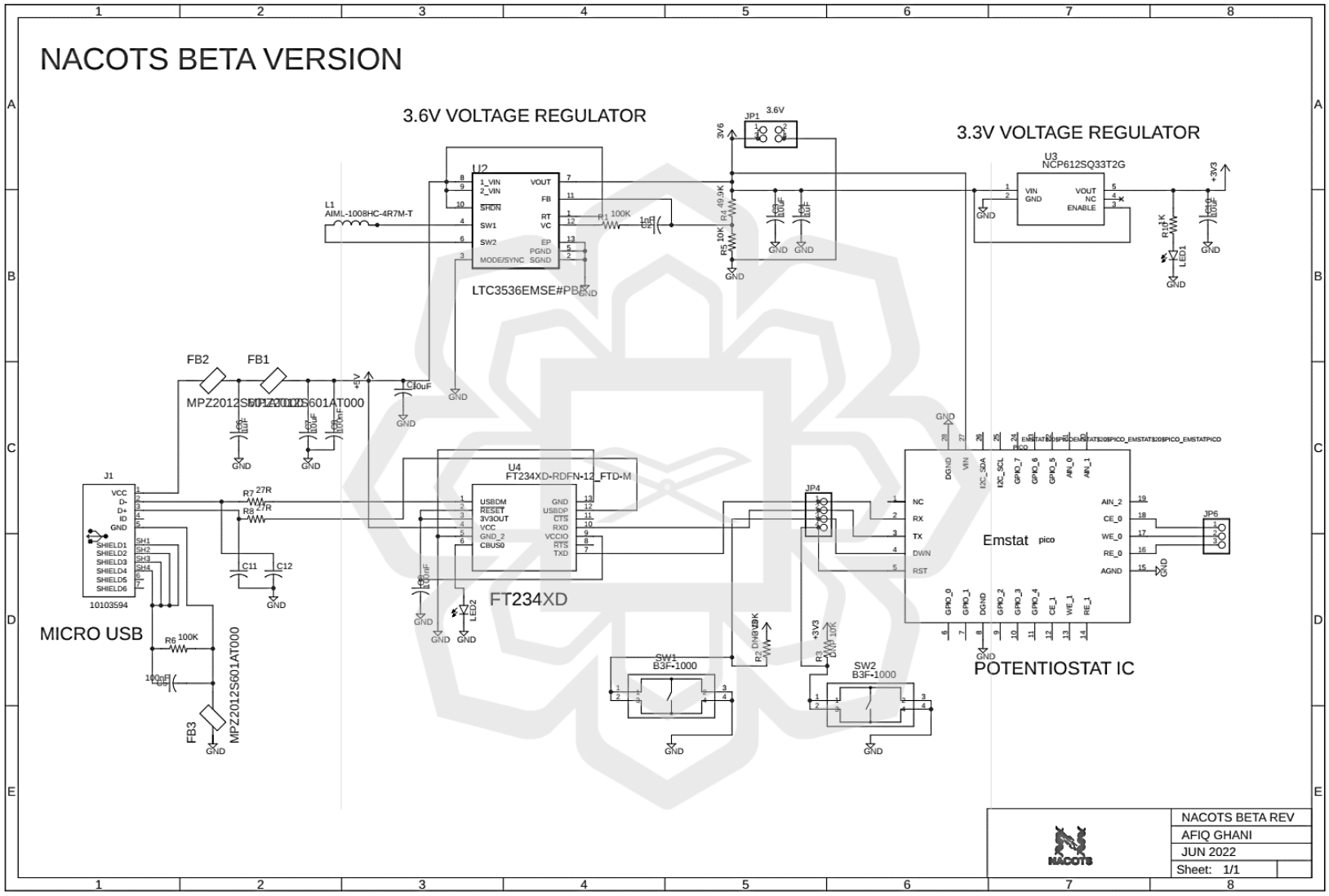


B. NACOTS Beta schematic design

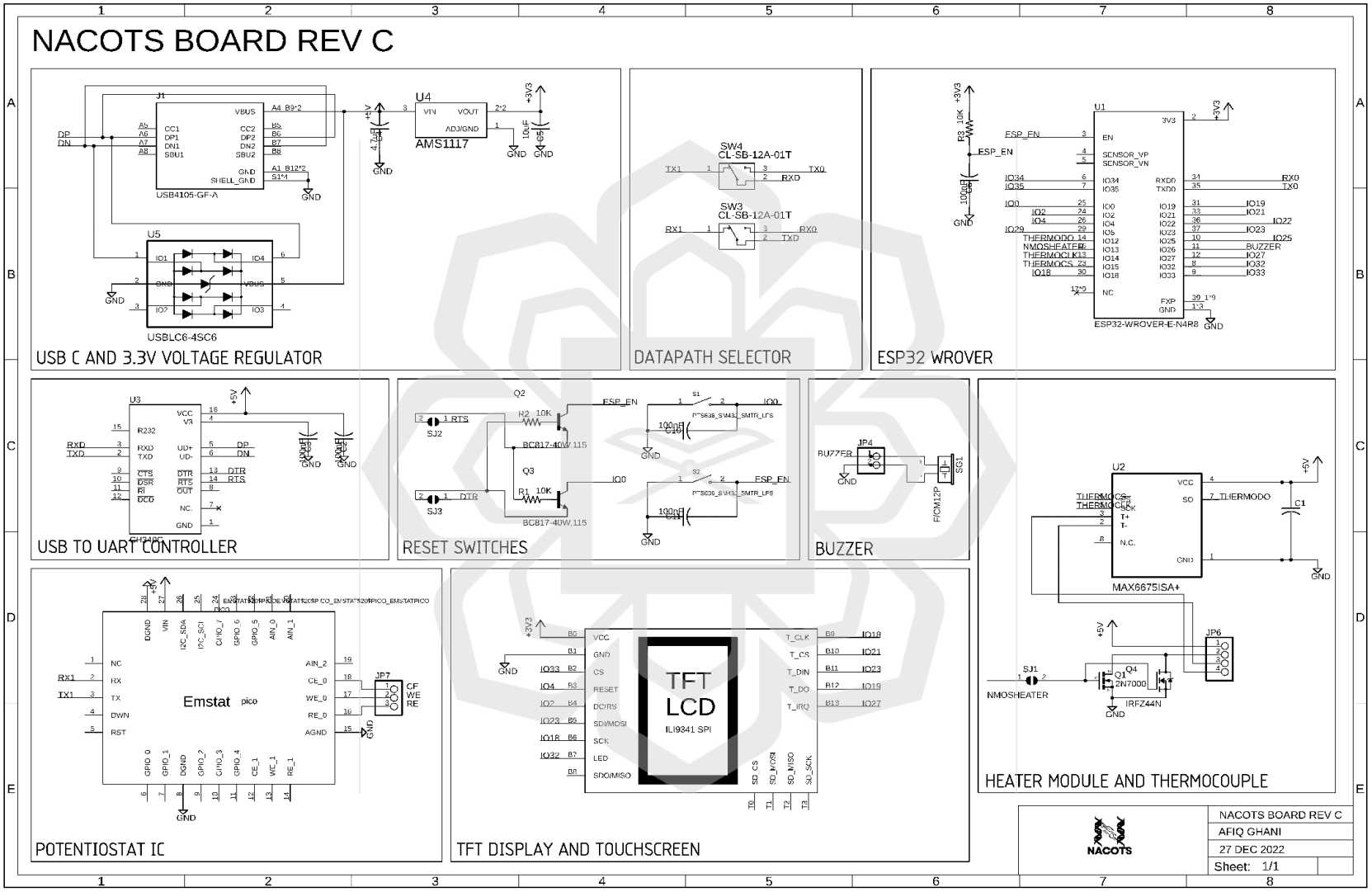


C. NACOTS Final schematic design